UNIVERSITY OF LATVIA
FACULTY OF CHEMISTRY

APPLICATION OF HIGH RESOLUTION MASS SPECTROMETRY AND MULTI-ENZYMATIC BIOSENSORS FOR NON-TARGETED SCREENING OF CHEMICAL ENVIRONMENTAL AND FOOD CONTAMINANTS

DOCTORAL THESIS

AUGSTAS IZŠĶIRTSPĒJAS MASSPEKTROMETRIJAS UN MULTI-ENZIMĀTISKU BIOSENSORU PIELIETOJUMS ĶĪMISKO VIDES UN PĀRTIKAS PIESĀRŅOTĀJU NEMĒRĶĒTAM (NON-TARGETED) SKRĪNINGAM

PROMOCIJAS DARBS

JĀNIS RUŠKO

Scientific supervisors:
Prof., Dr. chem. Vadims Bartkevičs
Prof., Dr. chem. Arturs Vīksna

Rīga
2021

The doctoral thesis was carried out at the Institute of Food Safety, Animal Health and Environment "BIOR" from 2017 to 2020 and National Research Council of Italy – Institute of Protein Biochemistry from 2017 to 2018.

UNIVERSITY OF LATVIA

The thesis contains the introduction, 3 chapters, conclusions, reference list, 9 annexes.

Form of the thesis: dissertation in chemistry, analytical chemistry.

Supervisors: Prof., Dr. chem. Vadims Bartkevičs
Prof., Dr. chem. Arturs Vīksna

Reviewers: 1) Prof., Dr. habil. chem. Māris Kļaviņš, University of Latvia;
2) Dr. Kristaps Kļaviņš, Riga Technical University;
3) Prof., Habil. Dr. Arunas Ramanavicius, Vilnius University, Lithuania.

The thesis will be defended at the public session of the Doctoral Committee of Chemistry, University of Latvia, at the Faculty of Chemistry of the University of Latvia (Jelgavas Str. 1, Riga, Latvia) on June 18th, 2021 at 14:00.

The thesis is available at the Library of the University of Latvia, Raiņa Blvd. 19, Riga, Latvia.

Chairman of the Doctoral Committee _____/ Prof., Dr. chem. Edgars Sūna/

Secretary of the Doctoral Committee _____/ Dr. chem. Vita Rudoviča/

CONTENTS

ABBREVIATIONS

4-MU or MU	4-Methylumberlliferone
4-MUBu	4-Methylumbelliferyl butyrate
AChE	Acetylcholinesterase
AGC	Automatic gain control
AIF	All ion fragmentation method
ANOVA	Analysis of variance
APL	Amprolium
Arb. or a.u.	Arbitrary units
BBD	Box-Behnken response surface design model
BChE	Butyrylcholinesterase
CASRN or CAS	Chemical abstracts service registry number
CIR	Chemical Identifier resolver KNIME extention
CLOP	Clopidol
COC	Chemicals of concern
DCZ	Diclazuril
DEC	Decoquinate
DMSO	Dimethyl sulfoxide
DNC	Nicarbazin
EC	European Commission
EFSA	European Food Safety Authority
ELISA	Enzyme-linked immunosorbent assay
EST2	Esterase-2
EU	European Union
EURL	European Union Reference Laboratory
FCM	Food contact materials
FS-ddMS^2	Full scan – data dependent tandem mass spectrometry method
FWHM	Full width half maximum
GC	Gas chromatography
GOx	Glucose oxidase
HAL	Halofuginone
HEPES	Hydroxyethyl piperazineethanesulfonic acid
H-ESI	Heated electrospray ionization
HILIC	Hydrophilic interaction chromatography

HRMS	High resolution mass spectrometry
HRMS/MS	High resolution – tandem mass spectrometry
IAS	Intentionally added substances
IT	Ion injection time
KNIME	Konstanz Information Miner – an open-source data analytics platform
LAS	Lasalocid
LC	Liquid chromatography
LOD	Limit of detection
LOQ	Limit of quantification
MAD	Maduramacin
ML	Maximum level
MON	Monensin
MRL	Maximum residue level
MS	Mass spectrometry or mass spectra
MS/MS or MS^n	Tandem mass spectrometry or fragmentation spectra
m/z	Mass-to-charge ratio
NAR	Narasin
NBS	*N*-Bromo succinimide
NCE	Normalized collision energy
NCI	U.S. National Cancer Institute
NEQ	Nequinate
NIAS	Non-intentionally added substances
NIG	Nigericin
NIH	U.S. National Institutes of Health
OECD	Organization for Economic Co-operation and Development
OFAT	One factor at a time model
OP	Organophosphate pesticides
OPAA	Organophosphorus acid anhydrolase
OPH	Organophosphorus acid hydrolase
PCA	Principal component analysis
PP	Polypropylene
QSAR	Quantitative structure activity relationship models
QSRR	Quantitative structure retention relationship models
QA	Quality assurance
QC	Quality control

QqQ	Triple quadrupole mass spectrometer
QuEChERS	Solid phase extraction method
ROB	Robenidine
RSD	Relative standard deviation
RT	Retention time
SAL	Salinomycin
SD	Standard deviation
SDF	Structure-data file
SDS-PAGE	Sodium dodecyl sulfate–polyacrylamide gel electrophoresis
SEM	Semduramicin
SML	Specific migration limit
SRM	Single reaction monitoring method
SST	System suitability samples
TEST	Toxicity Estimation Software Tool by USEPA
TIC	Total ion current
TOF	Time of flight mass spectrometer/-y
TOL/-S/-X	Toltrazuril /- sulfone /- sulfoxide
UHPLC	Ultra high-pressure liquid chromatography
USEPA	U.S. Environmental Protection Agency
USFDA	U.S. Food and Drug Administration
VBA	Visual basic
vDIA	Variable data-independent analysis

ABSTRACT

Application of high resolution mass spectrometry and multi-enzymatic biosensors for non-targeted screening of chemical environmental and food contaminants. Ruško, J., supervisors Dr. Chem., Prof. Bartkevičs, V. and Dr. Chem., Prof. Vīksna, A. Doctoral thesis in analytical chemistry, 127 pages, 33 figures, 8 tables, 127 literature references, 9 appendices. In English.

A variety of studies were performed in the course of this thesis, contributing to the advancement of non-target mass spectrometry and the development of enzymatic bioassays. Novel analytical methodologies were developed using ultra high-performance liquid chromatography combined with high resolution mass spectrometry (UHPLC-HRMS) to ensure high analysis specificity and sensitivity.

A targeted-suspect methodology was developed for the determination of veterinary drugs of anticoccidial class in poultry and eggs. Instrumental parameters were optimized by the means of statistical experimental designs to improve the sensitivity, precision, and repeatability of the method. High selectivity was achieved via full scan – data dependent tandem mass spectrometry (FS-ddMS^2) detection method, allowing to broaden the scope of analysis with further suspect lists.

A non-target screening strategy was developed for the safety evaluation of potentially hazardous chemicals in paper food contact materials (FCMs). A tentative list of suspect analytes was generated using publicly available FCM substance inventories. A workflow for mass spectrometric data analysis was developed for unambiguous identification of suspects. The workflow allowed for the identification of 74 suspect compounds, of which 40 were assigned a high confidence level of detection. Special attention in the study was drawn to the hazard identification and risk prioritization strategy using quantitative structure-activity relationship (QSAR) models to indicate which compounds have mutagenic or carcinogenic potential.

Esterase-2 (EST2) from *Alicyclobacillus acidocaldarius* based biorecognition elements were used for the development of biosensor assays for the determination of organophosphate pesticides (OPs) and thio-OPs. In a combination with automated robotic system with fluorescence detection and fluorescent substrate, low detection levels were achieved of OP residues. Differences in the shape of the EST2 residual activity during the inhibition led to pseudo-fingerprinting of substances.

NON-TARGET ANALYSIS, SUSPECT SCREENING, HIGH RESOLUTION MASS SPECTROMETRY, BIOSENSOR, ESTERASE, *ALICYCLOBACILLUS ACIDOCALDARIUS*, RISK ASSESSMENT

ANOTĀCIJA

Augstas izšķirtspējas masspektrometrijas un multi-enzimātisku biosensoru pielietojums ķīmisko vides un pārtikas piesārņotāju nemērķētam (*non-targeted*) skrīningam. Ruško, J., zinātniskie vadītāji Dr. ķīm., prof. Bartkevičs, V. and Dr. ķīm., prof. Vīksna, A. Promocijas darbs, 127 lappuses, 33 attēli, 8 tabulas, 127 literatūras avoti, 9 pielikumi. Angļu valodā.

Šī darba ietvaros veikti vairāki pētījumi, kas ir sekmējuši nemērķētās masspektrometrijas nozares attīstību un enzimātisko biosensoru izstrādi. Analīzes specifiskuma (selektivitātes) un jutības nodrošināšanai, izstrādātas jaunas analītiskās metodoloģijas, izmantojot ultra augsti efektīvo šķidruma hromatogrāfiju apvienojumā ar augstas izšķirtspējas masspektrometriju (UHPLC-HRMS).

Izstrādāta mērķa savienojumu metode veterināro zāļu kokcidiostatu noteikšanai mājputnu gaļā un olās. Lai uzlabotu metodes jutību, precizitāti un atkārtojamību, pētījuma gaitā, izmantojot statistikas eksperimentālos modeļus, optimizēti instrumentālie parametri. Augsta selektivitāte iegūta, izmantojot pilna masas skenēšanas diapazona – no datiem atkarīgas fragmentācijas (FS-ddMS^2) noteikšanas instrumentālo metodi, kas ļauj paplašināt analizējamo kandidātsavienojumu (kandidātvielu) sarakstu.

Pētījumu ietvaros izstrādāta nemērķētā skrīninga metode potenciāli bīstamu vielu noteikšanai pārtikas kontaktmateriālos (FCM). Tika izveidots kandidātsavienojumu saraksts, apkopojot publiski pieejamas FCM datubāzes. Darba procesā izstrādāta datu analīzes darbplūsma, lai identificētu kandidātu savienojumus. Darbplūsma ļāva identificēt 74 aizdomīgus savienojumus, no kuriem 40 raksturo augsts identificēšanas ticamības līmenis. Īpaša uzmanība pētījumā pievērsta apdraudējuma faktoru identificēšanai un risku prioritizēšanai, izmantojot kvantitatīvās struktūras un aktivitātes (QSAR) modeļus, lai paredzētu, kuriem savienojumiem piemīt mutagēns vai kancerogēns potenciāls.

No *Alicyclobacillus acidocaldarius* iegūti esterāzes-2 (EST2) enzīmi jeb bioatpazīšanas elementi tikai izmantoti, lai izstrādātu biosensorus organofosfātu pesticīdu (OP) un tio-OP noteikšanai. Apvienojot iegūtos EST2 proteīnus ar automatizētu robotizētu sistēmu ar fluoroscences noteikšanu un fluorescējošu substrātu, sasniegti zemi OP noteikšanas līmeņi. Atšķirības pēcinhibīcijas EST2 aktivitātē ļāva identificēt individuālās vielas.

NEMĒRĶĒTĀ ANALĪZE, KANDIDĀTVIELU SKRĪNINGS, AUGSTAS IZŠĶIRSTPĒJAS MASSPEKTROMETRIJA, BIOSENSORI, ESTERĀZE, *Alicyclobacillus acidocaldarius*, RISKA NOVĒRTĒJUMS

INTRODUCTION

The development of modern analytical techniques has driven the progress in the exploration of the chemical space around us. The advancements and increasing availability of high-resolution mass spectrometry (HRMS) equipment has allowed to pave the way for advanced instrumental methods used for chemical discovery. One of the catalysts in the discovery process is the development of non-target mass spectrometry methods. Non-target screening methodologies can now permit to simultaneously detect thousands of chemical compounds and identify the emerging unknown hazards. This thesis is a contribution to the continuing investigation of man-made chemicals via a novel approach.

The practical relevance of the problem.

There is a constant need for faster, cheaper, more sensitive, and more robust analytical methods, that can cover broader spectrum of chemical compounds of interest. A substantial part of this thesis, additionally to non-targeted experiments, was based on the targeted screening approach, where the goal was to develop as robust and reliable as possible analytical method for the determination of veterinary drugs with an option to increase the number of suspects analyzed, thus enabling non-target screening capabilities. It was important to develop a HRMS/MS method as it has been previously shown in literature [1] that full scan measurements using HRMS and tandem QqQ systems are not sufficiently selective and robust for the analysis of difficult matrices, such as liver, muscle, and urine. The developed FS-ddMS^2 method allows for better confirmatory abilities over single reaction monitoring (SRM) or all ion fragmentation (AIF) detection methods [2] and enables us to attach the suspect lists of choice for confirmatory capabilities. Additionally, it is rare to see operators assess the influence of the instrumental parameter settings on the overall system sensitivity. The variables and factors of MS systems are interdependent and produce combined effects [3], and the optimization of these settings can yield an increase in the quality of analysis. The data generated using this method is relevant even after gathering occurrence data, as it allows for non-targeted retrospective screening [4]. After thoroughly assessing the methods quality assurance, the same instrumental LC-MS method would be later adapted for non-target experiments in the follow up paper.

The work on food contact materials (FCMs) highlights the issues in the regulatory landscape of FCM testing and safety evaluation, especially in the context of upcoming changes as a part of European Union (EU) green strategy. Food contact materials as a source of chemical compounds in food are not a new phenomenon. There are regulations set in place that try to ensure the consumer safety, such as Regulation (EC) 1935/2004 [5]. The regulation prohibits for constituents of materials and articles manufactured and consumed in EU to endanger human health, which is an ambiguous definition. Besides the general safety requirement, some materials are well regulated, such as plastics

and recycled plastics by Regulations (EC) 10/2011, and 282/2008 [6,7]. First one is based on a positive list of authorized substances, which may be intentionally used in the manufacture of plastic layers in plastic materials. Specific manufacturing articles, related restrictions, and specific migration limits (SMLs) for individual compounds are listed.

Analysis of the available legislative and inventory documents shows that over 6000 unique substances, including solvents, binders, dyes, pigments and photoinitiators can be used in the manufacture of printed paper and cardboard FCMs. Most of the substances have not been fully evaluated and have the potential to migrate into the food or drink and become bioavailable [8]. Many knowledge gaps exist which pose several questions about the occurrence of unwanted chemicals and potential adverse effects on human health. Quantitative structure-activity relationship (QSAR) screening and inventory comparison studies have previously identified many health effect endpoints for compounds present in the FCM substance inventories, which has exemplified that most of paper and cardboard FCMs sold on the market can potentially harm human health [9–12].

Material choice (paper straws) was largely in line with the current European Union green strategy to reduce the environmental pollution by banning single-use plastics, such as cutlery, cotton buds, straws, and stirrers. The regulation, first proposed in May 2018, has been valid and agreed on by EU ambassadors of the member states since 18th January 2019. The single-use plastics directive builds on the EU's existing waste legislation, but goes further by setting stricter rules for those types of products and packaging, which are among the top ten most frequently found items polluting European beaches [13].

Regarding the use of biosensors for pesticide detection. Pesticides are one of the most known wide-spread persistent organic pollutants with undesirable health effects [14,15]. Pesticides and their transformation products have been found present in a wide variety of environmental samples [14,16]. These substances are usually found in water at low concentration levels, from traces at ppb levels to low ppm levels, but since they normally occur as complex mixtures, they have potential adverse effects on environment and human health [14]. One of the most widely used are organophosphate pesticides (OP). OP compounds are widely used for agriculture, horticulture, pest control, industrial, vector control and domestic purposes. Acute or chronic exposure to OPs can produce varying levels of toxicity in humans, animals, plants, and insects [17].

Most research on OP occurrence has been based on mass spectrometry methods. Though these methods provide excellent sensitivity and accuracy for the measurements, the routine analysis process is quite expensive and slow, and requires sample preparation. Enzyme-based techniques are gaining interest, due to lower cost per analysis. Several types of enzymes have been utilized for biosensor construction – acetylcholinesterase (AChE), butyrylcholinesterase (BChE), glucose oxidase (GOx), urease, organophosphorus acid anhydrolase and hydrolase (OPAA and OPH), among others [18].

In our research, we have investigated the use of esterase-2 from *Alicyclobacillus acidocaldarius* (EST2) as efficient alternative in terms of stability (resistance to temperature, organic solvents, detergents, etc.) and specificity towards OPs. To increase the sensitivity threshold of OP detection by using EST2, our studies include the use of a fluorogenic substrate – 4-methylumbelliferyl butyrate (4-MUBu) [19] to determine the residual enzymatic activity.

The aim of the work. Two main aims were proposed during this work:

i. Development of new non-target and suspect HRMS-based methodologies and their application for the analysis of various types of contaminants;
ii. Development of biosensor-based methodologies for the screening of phosphorothionate and organophosphate pesticides.

The approach used. To achieve the aims of the work, several tasks were proposed:

i. Development and validation of a robust and efficient sample preparation method for the analysis of veterinary drugs in poultry meat and egg matrices;
ii. Development of new UHPLC-HRMS analysis methods that are sufficiently robust for high sample throughput and analyte coverage;
iii. Development of HRMS data analysis workflows intended for non-target data processing;
iv. Hazard assessment and prioritization based on non-target results;
v. Expression and purification of esterase-2 from *E. coli* strain BL21(DR3), and further use in fluorescence-based bioassays with 4-methylumbelliferone butyrate as a substrate.

Scientific novelty:

i. First published method for the analysis of anticoccidials using Orbitrap-HRMS system with improved results over other conventional systems using a simpler analysis protocol;
ii. One of the first studies that has investigated the influence on individual ion generation (source conditions) and Orbitrap detection parameters on the sensitivity and stability of the analysis;
iii. The study of non-target screening of FCMs highlights a prominent regulatory issue regarding the analysis of paper and board materials;
iv. The developed workflow for FCM testing can be implemented for rapid bottom-up priority-based identification of hazards and be implemented in rapid risk assessment process;
v. For the first time, prosphorothionate pesticide oxidation using *N*-bromosuccinimide has been used in combination with enzymatic assay;
vi. An automated analysis process has been developed for the analysis of phosphorothionate and organophosphate pesticides using esterase-2 bioassay.

Practical application of the work. The developed suspect-target screening method of anticoccidial class veterinary drugs is used for continuous routine monitoring programs in poultry and egg samples. The non-target suspect screening method is highly adaptable and versatile, and is further applied in other studies of environmental and food analysis context. The work on biosensors is fundamental for the development of further applications, fine-tuning of methods and real-time detection in industry applications.

Scientific publications.

1. **Rusko, J.**; Febbraio F. Development of an automated multienzymatic biosensor for risk assessment of pesticide contamination water and food. *EFSA Journal*[1] **2018**, *16*, e16084.
2. Cetrangolo, G. P., Gori, C., **Rusko, J.**, Terreri, S., Manco, G., Cimmino, A., Febbraio, F. Determination of Picomolar Concentrations of Paraoxon in Human Urine by Fluorescence-Based Enzymatic Assay. *Sensors*[2] **2019**, *19*(22), 4852.
3. **Rusko, J.**, Jansons, M., Pugajeva, I., Zacs, D., Bartkevics, V. Development and optimization of confirmatory liquid chromatography—Orbitrap mass spectrometry method for the determination of 17 anticoccidials in poultry and eggs. *Journal of pharmaceutical and biomedical analysis*[3] **2019**, *164*, 402-412.
4. Cetrangolo, G. P. †, **Rusko, J.** †, Gori, C., Carullo, P., Manco, G., Chino, M. †, & Febbraio, F. † Highly Sensitive Detection of Chemically Modified Thio-Organophosphates by an Enzymatic Biosensing Device: An Automated Robotic Approach. *Sensors*[2] **2020**, *20*(5), 1365.
5. **Rusko, J.**, Perkons, I., Rasinger, J. D., & Bartkevics, V. Non-target and suspected-target screening for potentially hazardous chemicals in food contact materials: investigation of paper straws. *Food Additives & Contaminants: Part A*[4] **2020**, *37*(4), 649-664.

List of conferences.

1. Risk Assessment Research Assembly (RARA), Utrecht, Netherlands, 2018. **Rusko, J.**; Febbraio, F. Biosensing devices as a tool to refine the routine analysis of organophosphate pesticides (poster and oral presentation);
2. 77th University of Latvia conference, Riga, Latvia, 2019. **Rusko, J.**, Perkons, I., Rasinger, J., Bartkevics, V. Non-targeted screening and identification of compounds in paper food contact materials (in book of abstracts, oral presentation);
3. 78th University of Latvia conference, Riga, Latvia, 2020. **Rusko, J.**, Vainovska, P., Bartkevics, V., Investigating the authentical fingerprint of regional honeys: a non-target metabolomics approach (in book of abstracts, oral presentation);
4. International scientific symposium "Science to strengthen sustainable and safe food systems", Riga, Latvia, 2020. **Rusko, J.**, Perkons, I., Rasinger, J., Bartkevics, V. Non-targeted screening and identification of compounds in paper food contact materials (poster).

† *These authors contributed equally to this manuscript.*
[1] *Peer reviewed journal, imprint of John Wiley & Sons (IF=2.74 (2019)), eISSN: 1831-4732*
[2] *Peer reviewed journal, imprint of MDPI (IF=3.275 (2019)), eISSN: 1424-8220*
[3] *Peer reviewed journal, imprint of Elsevier (IF=3.209 (2019)), ISSN: 0731-7085*
[4] *Peer reviewed journal, imprint of Taylor & Francis (IF= 2.340(2019)), ISSN: 1944-0049*

1. LITERATURE REVIEW

1.1. Principles of non-target methodologies

Identification of chemical compounds in the environmental analytical chemistry is split in three main approaches, that are target analysis, suspect screening, and unknown screening, the latter two being non-target analysis methods.

For target screening, a reference standard should be available for each investigated compound and it should be determined using the exact same analysis setting for enable confirmation of the identity. Subsequently, high resolution mass spectrometry (HRMS) allows suspect screening. Those are the compounds that are *expected* in samples, but the reference standards for these compounds are not available. We *know* that these compounds might be present in samples based on various *suspect lists*, relevant to the scope of the investigation. Since the identity of accurate mass match is known, it is possible to confirm the theoretical suspected compound molecular formula with the one observed in samples by the isotope pattern. This and other evidence (later discussed in the compound identification chapter) can be used for a tentative confirmation of accurate identification. Target and suspect methods are complimented by the screening of unknowns. Unknown screening methods allow to observe all detectable substances in one measurement. Overviews in in environmental fields reveal that thousands of masses can be observed in a single sample and are reported in most non-targeted studies with available datasets. In most cases, that is multiple orders of magnitude higher of observed features than common targeted methods, which is a significant challenge for elucidation that requires careful detection and prioritization of relevant features [20,21].

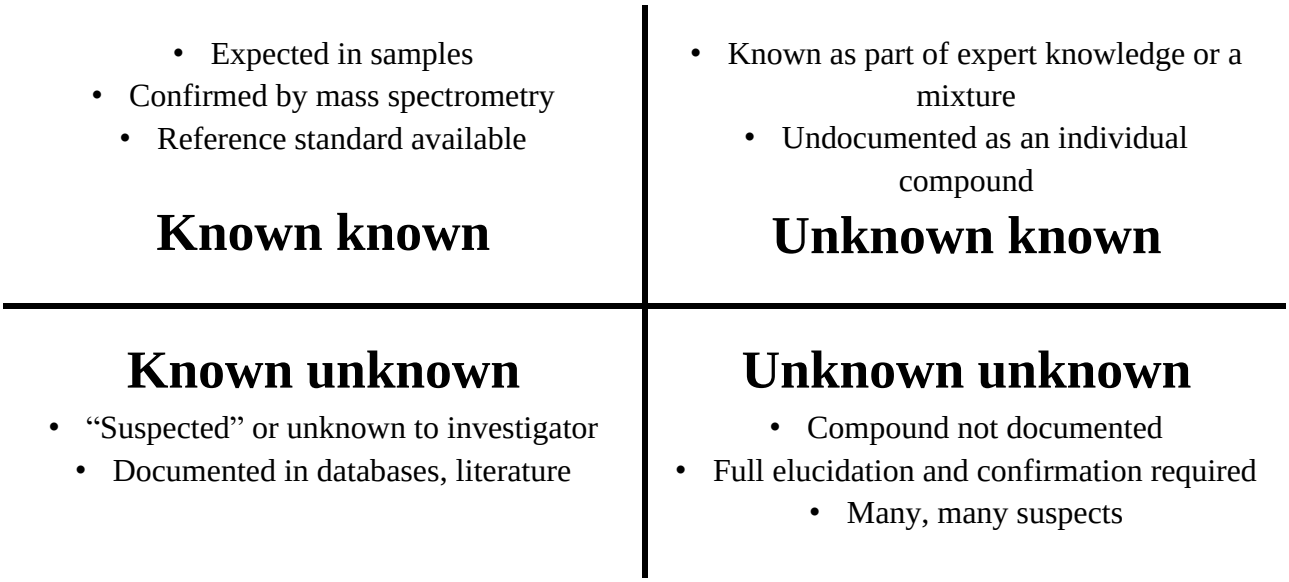

Figure 1.1. **Types of suspects in analytical methods** [22,23]

The increasing possibilities to elucidate unknowns and the ability to enable priority-based screening for the discovery of the unknown chemical space in human exposome is one of the reasons these methods are an increasingly important asset in modern analytical chemistry. Subsequently, the final step of all non-target analysis workflows is the true confirmation of the compound requiring a reference standard, thus, in a way, "upgrading" the suspects and unknowns to quantifiable target compounds [20,23].

Figure 1.1 illustrates the difference between the several categories of known and unknown substances [22,23]. *Known knowns* are substances that are expected to be in samples and whose identity is confirmed by mass spectrometry. Those are typical targeted method analytes. A *known unknown* is a compound that is unknown to the investigator, but the information of the compound is present in scientific literature or databases, hence these are the typical suspects in suspect screening methodologies. *Unknown unknowns* are compounds that have not yet been found or documented and are the major constituents of the gray area of the exposome and targets of unknown screening. *Unknown knowns* are substances that are known to be parts of complex mixtures, but are not yet documented as individual substances, e.g. homologue series consisting of discrete building blocks, such as perfluorinated compounds or lipids.

For the mass spectrometry-based work performed in this thesis, the object of analyses has been the search of suspects or *known unknowns* in a definite subset of samples.

1.1.1. Sample preparation methods

Since the goal of non-targeted methods is to maximize the scope of the analytes investigated, generic sample preparation methods are needed. At the same time, the prepared sample extracts still must be relatively "clean" in order to decrease the contamination of the analysis system. Commonly used methods in environmental and food analysis include "dilute-and-shoot" methods and variations of liquid-liquid extraction, such as QuEChERS or generic extraction protocols using acidified methanol or acetonitrile, due to their compatibility with LC analysis. QuEChERS is advantageous because it is routinely used for pesticides and other compounds of concern in a variety of sample matrices [24]. Various sorbents are available for QuEChERS to reduce interfering compounds and further clean up the samples; however, investigators should be aware that the use of these sorbents may compromise the non-targeted method by removing suspects of interest [25]. Also, syringe or other membrane filters, used for sample extract cleanup prior LC-MS analysis, can account for potential heavy analyte loss. In a recent study [26], Aichinger et al. uncovered the fact that major losses of various *Alternaria* toxins occur when extracts are filtered. This resulted in a necessity to re-evaluate a lot of previous food occurrence data in the light of new results as *Alternaria* toxins are one of the biggest foodborne disease and cancer causes in the world [27].

For any unknown or suspect screening application to be successful, methods need to be tested with appropriate standards and relevant sample types to demonstrate that they are fit for purpose. Repeat measurements of a pool of all samples of the same sample type can be beneficial in measuring the reproducibility of features common to that matrix, especially for routine screening of the same sample type. Due to the wide diversity and variety of sample matrices and potential compounds that may be present for food safety applications, the non-targeted field would benefit greatly from a validated QC standard that could be spiked into sample matrices [25]. It would need to be a stable mixture of compounds that covers a wide retention time and m/z range, molecular formula would need to contain elements that may be expected or should be monitored, and compounds should be included that ionize in positive and/or negative ion modes. These strategies would enable standardization and validation of developed sample preparation, instrumental analysis protocols and would help unknown and suspect screening methods to become routine [25].

1.1.2. Instrumental analysis methods

Chromatography is a fine tool for the separation of difficult mixtures of environmental or food origin, however, the procedures to finely tune the chromatographic conditions to fit the purpose of the methods are quite time-consuming. Because of the continuous development of modern mass spectrometry equipment, the chromatographic requirements have become more flexible, allowing for faster method development. It is still very important to separate most of the analytes to prevent the effects of major ion suppression, which can result in poor quality signal or even missed peaks [28]. Even though ion suppression should be reduced by optimizing the analysis method, it is unavoidable and one of the reasons why robust quality control (QC) is necessary.

For the types of chemical analysis performed in non-target screening, full-scan instruments are a requirement. Several types of instruments are used, most frequently tandem-HRMS, such as time of flight (TOF) and Orbitrap detectors equipped with quadrupoles and/or ion traps that allow for data-dependent MS/MS or MS^2 spectra acquisition (an example of $ddMS^2$ experiment is illustrated in Figures 3.8., 3.9 and 3.10). $ddMS^2$ events are triggered by the occurrence of either predefined ion lists (i.e. suspect lists) or by semi-random chance based on the most intensive precursor signals present in the full scan spectrum. The fragmentation events can also set to occur based on observed neutral losses in the full scan spectrum. The $ddMS^2$ method is best used on TOF instruments, because the scan rate is much higher compared to Orbitrap detectors, which sacrifice the overall cycle time of measurements with an increase of MS^2 scans. Higher cycle time can result in chromatographic peaks of poor shape or even missed peaks. The resolving power of full scan and MS/MS must be reduced as a tradeoff [29].

1.1.3. Building blocks of non-target analysis

Non-target analysis consists of the same building blocks as target analysis: sample preparation, instrumental and data analysis. However, the data analysis part is much more elaborate in non-target applications. Figure 1.2 illustrates the main differences between the workflows of target analysis, suspect and unknown screening and Figure 1.3 illustrates the steps and levels of the data analysis in non-target screening.

Feature extraction and filtering

For a successful non-target screening method, peak detection, and the merge of various adduct masses belonging to the same compound (ion deconvolution), the combination of both further referenced as feature extraction, plays an important role. Feature extraction and further filtering provides the best compromise between keeping most of the relevant mass spectral information and discarding a maximum of irrelevant data [30].

The feature extraction settings must be adjusted depending on the quality of the acquired chromatographic and mass spectrometric data. Peak width and shape, the frequency of scans and mass accuracy are the most important aspects of automated peak picking. In order to make the data reproducible both from a data analysis and generation perspective, most researchers use standard data processing protocols and analysis methods. For example, chromatographic separation is typically done on C18 columns using acidic water and methanol or acetonitrile mobile phase gradient. Further detection is performed using electrospray ionization in in positive and negative ion mode in separate analysis runs and full scan acquisition is performed [29].

Feature extraction software preprocesses raw LC-MS (or GC-) data and generates feature (or peak) lists, depending on the type of software. Then the data is smoothed and baseline is subtracted either using blank samples or various algorithms. An intensity threshold is specified to determine what can be considered peaks above the noise level. This is a crucial step as small differences in the cut-off value can yield orders of magnitude different amount of filtered features. Not only that, but when setting the threshold too high, critical components of mixtures can be overlooked. Afterwards, the retention times of common features are compared and aligned between samples of the same analysis sequence. Lastly, the individual peaks and the mass differences between peaks, considering the expected adducts and neutral losses, are grouped in the same features. In the end, each extracted chemical feature is a unique combination of *m/z* values, RT and sometimes MS/MS scans.

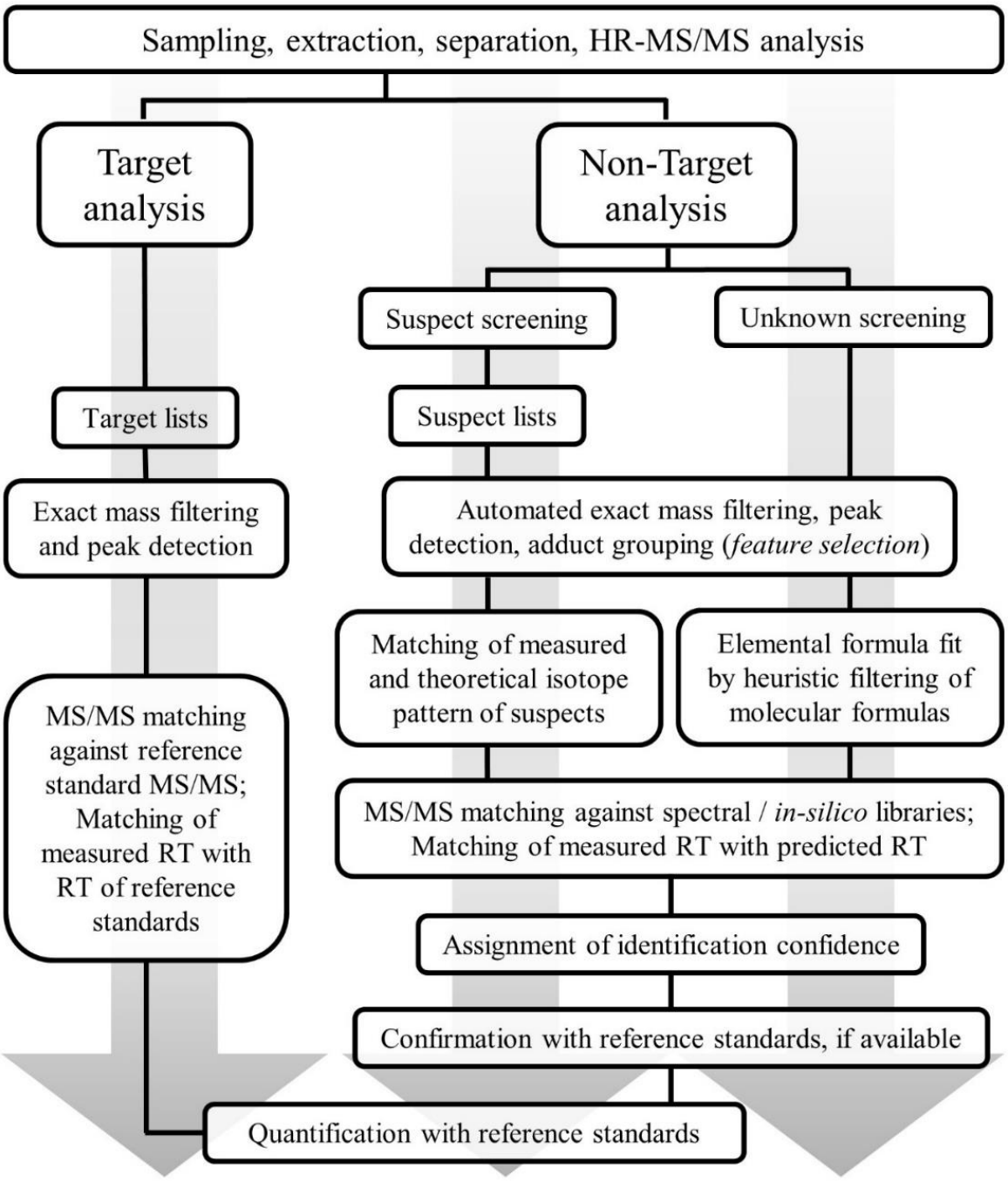

Figure 1.2. **The main workflow differences between target and non-target analysis**

Most widely used open source software packages for feature extraction and further processing of LC-HRMS data are MZmine 2 [31] and XCMS [32] among others. Commercial, vendor specific software such as Compound Discoverer (Thermo), Progenesis QI (Waters), Masshunter software suite (Agilent) is also available for non-target analysis needs.

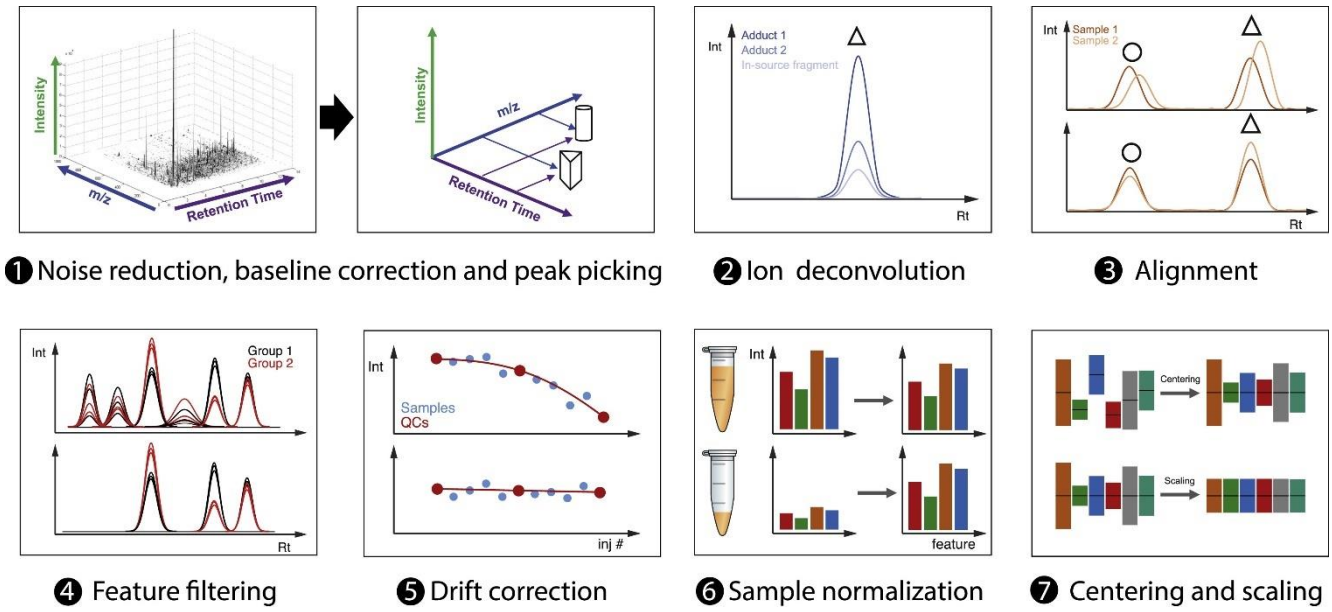

Figure 1.3. **Steps comprised into the Data Processing part of the workflow** [30]

Following feature filtering, data often are accounted for drift in signal intensities and peak RTs in long analysis sequences and normalized. Long sequences can lead to changes in the LC-MS system, for example, build-up of contamination in the column and further column stationary phase degradation leading to poor chromatographic separation, or the contamination of ion source cone or needle, resulting in worse ionization efficiency [33]. Sample normalization is performed to account of bias in pre-instrumental analysis steps, which can lead to different amount of injected sample [30]. The methods used typically assume that most features do not change between similar samples [34]. The final step, illustrated in Figure 1.3, centering and scaling, is not commonly used in environmental non-target investigations, but rather in metabolomics. It is used to account for different response factors for individual compounds. In mass spectrometry, the change in signal response is not always linear with the concentration of the analyte as the ionization efficiencies are varied and can be influenced by the sample matrix or mobile phase additives in LC-MS.

Figure 1.3. Reprinted from Analytica Chimica Acta, Volume 1105, Pezzatti, J., Boccard, J., Codesido, S., Gagnebin, Y., Joshi, A., Picard, D., ... & Rudaz, S., **Implementation of liquid chromatography–high resolution mass spectrometry methods for untargeted metabolomic analyses of biological samples: A tutorial**, 28-44, CC-BY-NC-ND (2020), with permission from Elsevier

Figure 1.4. Reprinted from Environmental Science & Technology, Schymanski, E. L., Jeon, J., Gulde, R., Fenner, K., Ruff, M., Singer, H. P., & Hollender, J., **Identifying small molecules via high resolution mass spectrometry: communicating confidence.** CC-BY-NC-ND (2014), with permission from American Chemical Society

1.2. Compound identification in non-target mass spectrometry

1.2.1. Confidence and bias in identification

Schymanski et al. has proposed a scheme for reporting the identification confidence in non-target studies [22] based on originally published classification system by Goodacre et al. [35] for metabolomics. Figure 1.4 illustrates the system. Highest possible confidence level in structure identification is level 1. Level 1 indicates that the proposed structure is confirmed with a reference standard and all other criteria of identification are fulfilled – the precursor ion (MS level 1), fragmentation spectra (MS/MS) and retention time match for both the standard and proposed structure / identified substance. Level 2 or "probable structure" is the second-best confidence level that can be assigned and the best that can be assigned in a typical non-target study, when the reference standards are typically scarce or not available. It is obtained by unequivocal match of MS1 and MS/MS spectra of spectral libraries (level 2a), generated from reference standards. Level 2b is obtained by diagnostic evidence and the match of *in-silico* generated fragmentation spectra with those measured in sample. For both levels additional bonus points of identification are granted if the modeled retention times match with those in samples. Level 3 or "tentative candidate" confidence is assigned to compounds where not enough evidence might be present for an unequivocal identification and assignment of level 2, e.g. the presence of positional isomers or the confidence is depreciated due to the fact that the predicted compounds are an outlier of a retention time model (as was done in my work on non-target screening of food contact material substances). Level 4 and 5 identifications cannot be considered ambiguous and are assigned to compounds with no spectral or *in-silico* library matches to the fragmentation spectra present. For level 4 of identification the molecular formula is resolved based on the isotope pattern, but in no way that is considered an identification based on the molecular formula match in a database. Level 5 of confidence is typically assigned to compounds with observed exact mass at MS1 level.

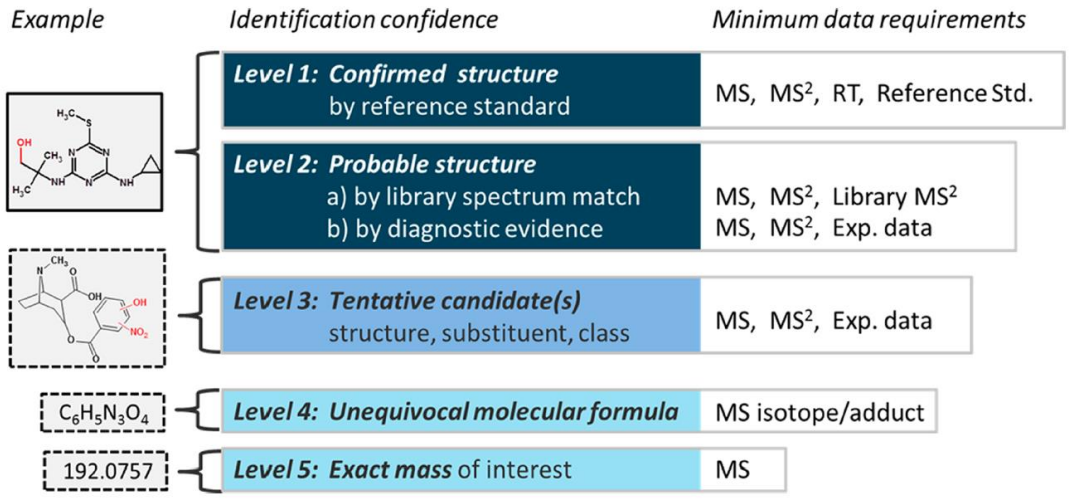

Figure 1.4. **The identification confidence levels as proposed by Schymanski et al.** [22]

Quality control in non-target screening

Quality assurance (QA) and quality control (QC) are an essential part of analytical chemistry. While both aim at controlling and minimizing all the variance and biases affecting the whole workflow, QC comprises the activities undertaken prior to data acquisition, while QC refers to the techniques implemented during or after data acquisition step [30,36]. In targeted analysis, it is a well-established process as there are whole protocols that describe the process of QC and QC. Targeted methods need to be validated, in order to prove the orderliness of the results by ensuring sufficient method accuracy and precision, and avoid false positive or negative results. On the contrary, there are no established regulations or protocols which underline any QC principles in non-target analysis [37]. Recently, efforts by the metabolomics community have led to guideline QA and QC processes published as tutorial type reviews, in which the authors describe the necessary measures [30,36].

In environmental and contaminant non-target analysis, the QA and QC processes are like those already applied in metabolomics workflows. Just as in targeted method development and application, system suitability samples and blank samples must be used to qualify the analytical process before and during the analysis of the samples of interest. Blank samples (also process blank samples) allow to detect any signals that could be interfering background, related to impurities in solvents, the contamination during sample preparation or of the analysis system, whether it is the LC or GC, the separation column, or the mass spectrometer. During the analysis, blank samples also allow to evaluate the presence of carry over contaminants. Invaluable is the fact that, in non-target approach, the blank samples are used for background subtraction and baseline correction in data processing workflows.

There are different types of system suitability samples (SST), which can include several reference standard substances or a reference matrix (environmental, food or biological fluid). SSTs can be used for system suitability testing. Standard substance SSTs act as a clean sample free of biological matrix effects [30] and are used to evaluate the system suitability for the scope of the analytes. Typically, these reference standard mixes should contain analytes across the whole method *m/z* range and chromatographic gradient. The standard mix should allow to evaluate the precision of MS method (i.e. *m/z* error less than 5 ppm, compared to theoretical mass) and the goodness of fit for the chromatographic method, by examining the deviation in retention times, the variability of peak areas and the shapes of peaks (incl. broadening, tailing, peak shoulders). Reference sample matrix is applied for the same purpose, and typically is used across the real sample analysis sequence. Inclusion of commercial reference materials is useful as a reference sample matrix and for comparison between various analysis sequences or long-term inter-laboratory studies [30,36].

A common type of SSTs are pooled QC samples, which are used on an intra-study basis. The pooled QC sample should reflect both the sample matrix and chemical composition. Data from pooled QC samples is used in a similar way to other SSTs – to evaluate the variance in data and monitor the

method quality control by specific intra-method scope markers (analytes) or using a non-selective approach, for example, using non-supervised statistical methods such as principal component analysis (PCA, Figure 1.5). If the variance is too high (i.e., RSD > 30%) for features detected in QC samples, then the corresponding features can be removed. In non-targeted workflows this is one of the first steps in the data analysis process. If pooled QC samples drawn from a single homogeneous source are used across multiple analytical batches, it is also possible to correct for between-batch systematic error. Often, changes in sensitivity can be observed between multiple analytical sequences. Once within-sequence systematic error has been corrected then multiple sequences can simply be aligned by mean response. This is done by a grand mean calculation across all sequences, and then error between each sequence mean and the grand mean is subtracted from all the samples in that analytical sequence [30,38]. However, this type of QC measure (pooled samples) is not widely used in non-target studies with the purpose to detect contaminants in the analyzed samples.

Furthermore, pooled QC samples can be used for other things than the measurement of precision. Pooled QC samples can be used to equilibrate, or stabilize the analysis system, prior to running the analysis sequence. This allows for higher reproducibility by removing the variance in retention times or the response measured by the detector.

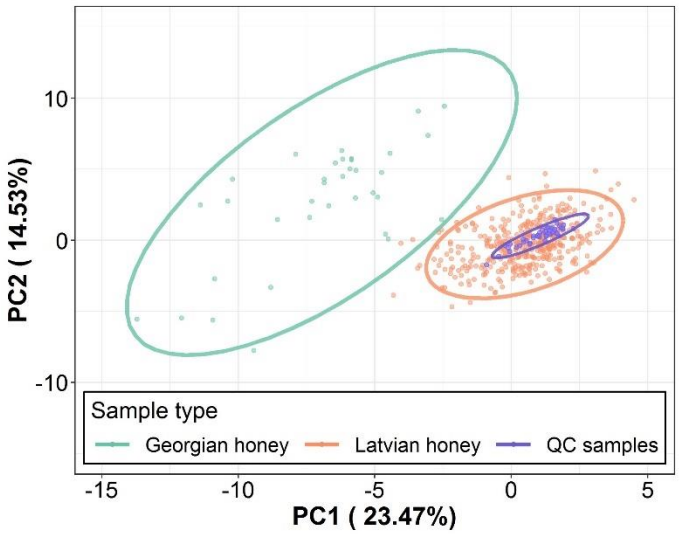

Figure 1.5. **An example of pooled QC samples used in a non-target study – PC scores plot of Latvian, Georgian and pooled QC samples; the QC data points cluster tightly in comparison to the total variance in projection**

During the work of my PhD I have focused on a couple of QC aspects which were essential for the investigated studies. In the anticoccidial veterinary drug suspect study, method development stage was all about the QA of analysis by throughout optimization of various sample preparation and instrumental aspects. SSTs consisting both of analytical standards and matrix components were used.

A stepwise process was implemented in the optimization. The instrumental stability was improved using the SSTs by optimizing the ion source and Orbitrap detector conditions. Later the method was validated and in routine application QC is performed as per targeted method basis (e.g. Levey-Jenning quality control plots, standard addition to samples). In the food contact materials application QA was assured by using control and process blank samples, and by randomizing the sample analysis order. QC was performed mainly in the post-analysis stage by treatment of data by intra-workflow peak area normalization.

1.2.2. Identification via mass spectra

Fragmentation spectra is a great tool to identify chemical structures, but it is not possible to identify all of compounds based on a single MS/MS spectrum. Firstly, to obtain full fragmentation spectra coverage, the compounds must be fragmented over a range of collision energies (i.e. 10, 20, 40, 60 NCE), and, if possible, MS^3 or MS^n experiments must be performed for unequivocal identification. However, this kind of experiments requires costly equipment (ion trap and quadrupole equipped Orbitrap tribrid models) and is rarely available. Furthermore, the mass spectra are not always unique or sufficiently informative [39], which can lead to equivocal identification of compounds. Also, the ability to identify compounds based on database fragmentation spectra match is based on the availability of reference spectra, which often is not available for the suspect of interest. Lastly, the knowledge and skillset of the operator is a crucial factor to avoid misidentification.

Comprehensive databases are an essential part of any suspect or unknown analysis workflow as the databases largely set the scope of analysis and the number of compounds compiled in the database lists is proportional to the features detected.

Most notable spectral libraries in environmental (e.g. non-biological) analysis are MassBank of North America (MoNA), MassBank, Global Natural Product Social Molecular Networking library (GNPS), NORMAN Suspect Exchange and many chemical lists available in the US EPA CompTox Chemistry Dashboard, among others. Notable is the fact that, Massbank allows for users to contribute to the growing amount of spectra records, by allowing to upload spectra of properly identified substances, preferably from reference standards.

In-silico tools for the generation of fragment spectra such as SIRIUS combined with CSI:FingerID [40], CFM-ID [41] and MetFrag [42] are most notable. Each tool serves a similar purpose, but additional features extend the usability. For all the tools not only graphical user interface versions is available, but also console versions, which allow to streamline large batches of analysis faster and, in a way, enable better reproducibility.

One of the first steps in structure elucidation is the correct assignment of molecular formula. It is a very well-integrated technique in most computational workflows, but quite often in non-target

analysis, the settings of formula assignment can be overlooked. High mass accuracy is required for proper identification of isotope pattern per compound basis, due to often overlapping mass signals. The most common set of elements abundant are carbon (C), hydrogen (H), oxygen (O), nitrogen (N), phosphorus (P) and sulphur (S). For each candidate molecular formula, an isotopic pattern is simulated and matched with the observed pattern and the distribution of intensities. Suspect databases help with the assignment of elements by limiting the maximum element types and count.

In the study of food contact materials, I applied molecular formula assignment using Compound Discoverer 2.1 software. Prior the assignment, we used the elements and element molecular ranges from the database, to simplify the molecular formula search by limiting the amount of candidate formulas generated.

Retention time prediction

Accurate prediction of retention time for the proposed suspects adds another level of confidence on top of identification via mass spectra. It has been widely adapted in proteomics for accurate peptide identification [43], but has been less pronounced in environmental and food non-target analysis. Researchers have shown that simple models of retention time plotted vs log K_{OW} can reduce the number of false positives by an average of 49% [37].

For more advanced chromatography methods employing hydrophilic interaction chromatography (HILIC), more advanced retention time prediction algorithms are needed. For example, Quantitative Structure-Retention Relationship (QSRR) models can search chemical space to define the correct polarity value for a compound in order to comprehensively understand the elution mechanisms in HILIC conditions [44]. The developed models in the mentioned study helped to accurately identify 10 new pharmaceutical transformation products and 28 biocides in influent and effluent of a wastewater treatment plant [44].

In our study of food contact materials, we also applied a linear regression model of retention time vs log K_{OW}, which helped to identify 6 outlier compounds for which the confidence was depreciated.

1.3. Biosensors

1.3.1. Biochemical strategies for the chemical detection

The search for a quick and easy detection of the neurotoxin levels in the environment has fostered the search for systems alternative to currently employed analytical methods. In particular, the development of sensors and biosensors for the precise detection and estimation of hazardous chemicals in a variety of sample matrices (i.e. water, human fluids, and tissue) has been gaining momentum.

The advantages of biosensors compared to the current technological approaches could be summarized in a few words: easy, cheap, and rapid.

Figure 1.6. illustrates the main building blocks of biosensors. Biosensors are characterized by a bio-recognition element, which is the biological part recognizing the substance, a transducer element, that transforms the biological interaction into a measurable signal, and a signal processor, that produces a readable output. Sometimes a signal amplifier can be used to amplify the signal improving the sensitivity of the biosensor [45,46].

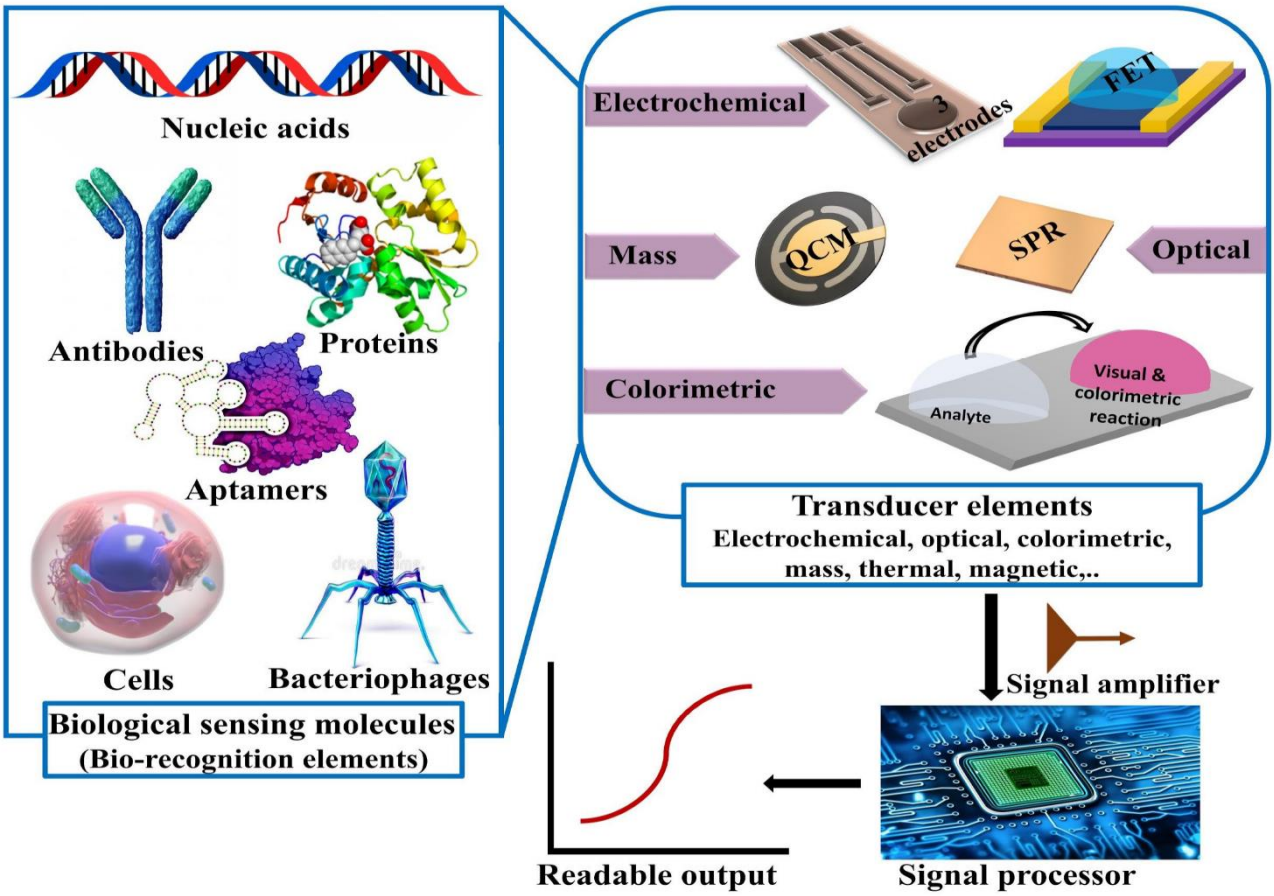

Figure 1.6. **Main components of biosensors**

Biosensors for chemical substances can be based on microorganisms, antibodies, enzymes, and nucleic acids [47–49]. The limit of detection for a number of these biosensors is comparable and sometimes better than common analytical techniques, such as mass spectrometry [50–53]. Further details on the characteristics of the most recent biosensors and on the advances in the development of these technologies can be found in several recent reviews and articles [45–47,49,54–56]. There are two distinguishable types of applications of biosensors – diagnostic use in clinical settings and the environmental monitoring of chemical substances. The recent development of diagnostic biosensors permits us to hypothesize about their possible use in routine clinical analysis [57–59].

New emerging biosensors for the analysis of environmental chemicals have been proposed in order to offer a simple alternative means of assessment approach, such as VHH antibodies (the antigen binding fragment of heavy chain antibodies) that combines the comparable performance of conventional antibodies with the affinity for small molecules [60], or genetically engineered microbial whole-cells, that respond to target chemicals and produce detectable output signals [61]. However, these advances in the field of environmental chemical monitoring are still far from producing a continuous real-time and on-line system for their detection.

Even though biosensors provide a valid alternative to the classical analysis techniques, compared to the possibilities of non-target analysis using mass spectrometry, the scope of analysis is often limited to target or suspect analysis. Based on the type of the bio-recognition element, biosensors are excellent for the analysis of similar chemical compound classes, for example, sulfonamides [62] or organophosphates [63,64], the development of which are within the scope of this thesis.

1.3.2. Principle of enzymatic biosensors

In Figure 1.7, a schematic illustration of an enzymatic biosensor is presented, the enzyme bonded to the surface of a generic support (membrane, gold, etc.) reacts with different analytes.

The resulting interaction, as the formation of specific products, mediated or not by other molecules and enzyme, is transformed by a transducer (optical, electrochemical, etc.) in an appropriate output signal to be used for the analyte detection.

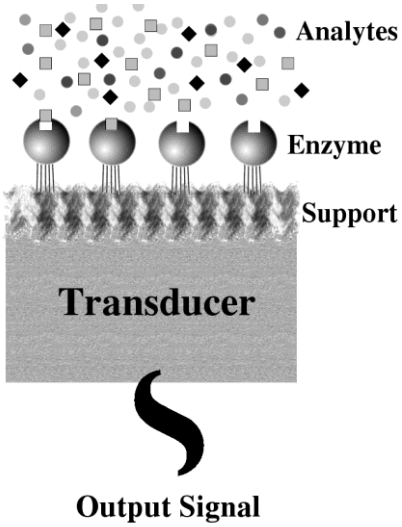

Figure 1.7. **Schematic illustration of an enzymatic biosensor**

Detection of analytes by enzymatic activity could be carried out by two different approaches: one is the measurement of the residual enzymatic activity after inhibition, and the other is the determination of the products after the hydrolysis of analytes. The first approach is most often based on the enzyme inhibition [65]. The inhibition mechanism takes place in the formation of an irreversible enzyme-inhibitor covalent complex.

A general protocol to measure the inhibitory activity of analytes provides a measurement of enzyme activity before the inhibition (A_{native}), the incubation of the enzyme in the presence of inhibitor, and the measurement of activity after inhibition ($A_{inhibited}$). The inhibition percentage is determined as $I\% = (A_{native} - A_{inhibited}) \times 100 / A_{native}$ or as $I\% = 100 - (A_{inhibited} / A_{native} \times 100)$.

Strictly depending on the detection system (transducer), different substrates could be used [66,67], as well as mediator compounds that enhance the detection sensitivity and minimize the contribution of other compounds to the total signal [67].

Direct detection by analytes hydrolysis is realized by detection of the product from the enzymatic hydrolysis at once or by other molecule/enzyme mediator using several transducers [67].

1.3.3. Detection of neurotoxic chemicals

Excluding neurotoxic poisons produced by certain fish, insects and reptiles (such as Bungarotoxin, Chlorotoxin, Conotoxin, and Tetrodotoxin), or by certain plants, algae and bacteria (such as Anatoxin-a, Tetanus and the Botulinum toxins), as well as some metals, such as lead and mercury, that can affect the activities of the nervous system, the most diffuse synthetic chemicals that impair the central nervous system are nerve agents, certain pesticides (for example, the organophosphates) and some organic solvents, such as hexane. These neurotoxins affect the transmission of chemical signals between neurons, causing several disorders and even fatality. In particular, the majority (the nerve agents and organophosphate pesticides) act as inhibitors of acetylcholinesterase activity [68]. Acetylcholinesterases are enzymes belonging to the carboxylesterase family, involved in the regulation of nerve signal transmission at the chemical synapses, by hydrolyzing acetylcholine and other choline ester neurotransmitters. The inactivation of this enzyme causes paralysis and even death. As this result, indeed, is the specific target of the above-mentioned toxic chemicals, this family of enzymes remains the one most extensively studied for use as bioreceptors in the development of biosensors for neurotoxic chemicals [69–71]. The principles of acetylcholinesterase biosensors are based on the measurement of the residual activity of the enzyme using different substrates, such as acetylcholine and thiocholine, that can be monitored using potentiometric, amperometric and optical devices [69–71]. The LODs that can be obtained using acetylcholinesterase activities, from insects, for the detection of these neurotoxic compounds, remain among the highest obtainable [72].

Recently, new alternative bioreceptors have been proposed, including new enzymes, microorganisms, antibodies, and aptamers [73–76], which represent a possible alternative to overcome the limitations involved in the use of acetylcholinesterases.

2. EXPERIMENTAL PART

2.1. Targeted suspect methodology – determination of anticoccidials

2.1.1. Chemicals and materials

Amprolium (APL), clopidol (CLOP), decoquinate (DEC), monensin (MON), nequinate (NEQ), toltrazuril (TOL), toltrazuril sulfone (TOLS), and toltrazuril sulfoxide (TOLX) were obtained from Sigma-Aldrich, Germany. Diclazuril (DCZ), lasalocid (LAS), and salinomycin (SAL) were purchased from Dr. Ehrenstorfer, Germany. Halofuginone (HAL) was obtained from WITEGA Laboratorien Berlin-Adlershof, Germany. The standards of maduramicin (MAD), narasin (NAR), nicarbazin (as marker compound DNC), robenidine (ROB), and semduramicin (SEM) were provided by the European Union Reference Laboratory for Residues of Veterinary Drugs (EURL). Internal standards of nigericin (NIG) (SigmaAldrich), robenidine-d_8 (ROB-d_8) (EURL), decoquinate-d_5 (DEC-d_5), halofuginone-$^{13}C_6$ (HAL-$^{13}C_6$), toltrazuril-d_3 (TOL-d_3), DNC-d_8 (WITEGA) were used in our study. All the compounds used in this study were of purity of 95% or higher, except for MON, NAR (86%) and SAL (80%). All compounds were dissolved in acetonitrile or DMSO and three diluted working mix solutions (two native compound solutions for each matrix and one internal standard solution) were prepared in acetonitrile at the concentrations given in Annex 1. Six intermediate native compound calibration solutions for standard addition samples for each matrix were prepared by diluting 50, 100, 200, 300, 400, and 600 µL of each working standard up to 1000 µL volume in acetonitrile.

Acetonitrile, methanol, formic acid (all MS grade), and DMSO (anhydrous, 99.5% purity) were purchased from Merck, Germany. Aqueous solutions were prepared in deionized water (resistivity >18 MΩ cm) obtained by using a Milli-Q purification system (Millipore, Billerica, MA, USA).

2.1.2. Samples and sample preparation

Two types of poultry – chickens raised for laying eggs and broilers, as well as two types of eggs – quail and chicken eggs were used for method validation. The samples were collected at a local poultry farm near Riga, Latvia. No information was available regarding possible previous treatment of these animals with veterinary drugs. The method specificity and the occurrence of anticoccidials were studied using another set of a variety of egg and poultry samples collected within the State monitoring program performed by the Institute of Food Safety, Animal Health and Environment – "BIOR" (Riga, Latvia).

The samples were homogenized using an Ultra-Turrax® T25 homogenizer system (IKA, USA) and frozen (−21 °C) immediately after collection, and thawed in small batches.

Homogeneous samples (5.00 ± 0.02 g) were weighed in 50 mL polypropylene (PP) tubes. Internal standard mixture (100 µL, 5 µg mL^{-1} of all compounds, 12.5 µg mL^{-1} of DNC-d_8) was added to all samples. Matrix-fortified calibration samples were prepared by adding 100 µL of the intermediate calibration solutions to blank control samples resulting in a total of six calibration levels for each matrix. The calibration concentrations were prepared at 0.25, 0.5, 1, 1.5, 2.0, and 3.0 times the ML or MRL values. The samples were vortexed and equilibrated for 20 – 30 min, then diluted with acetonitrile (20 mL) and vortexed again for 10 s. The samples were agitated in a rotary shaker at high speed for 20 min and then centrifuged for 15 min at 4750 rpm while cooling at 0 °C, followed by rapid (up to 5 min) transfer of 10 mL aliquots to 15 mL polypropylene vials. The sample extracts were found to be the most stable at this point and could be kept in a freezer (-20 °C) for at least one week. The extracts were then evaporated to dryness under nitrogen stream at 60 °C using a Turbovap LV system and then reconstituted in 500 µL solution of acetonitrile-aqueous sodium acetate (5 mM) (30:70, v/v). The samples were vortexed (1 min) and sonicated (5 min) prior to the LC-HRMS analysis. The final extracts were found to be stable for two days at -21 °C.

2.1.3. Parameters of UHPLC-HRMS method

Chromatographic analyses were conducted on an UltiMate 3000 (Dionex, Olten/Switzerland) HPLC system using a Kinetex C18 (100 mm × 2.1 mm i.d., 1.7 µm) analytical column (Phenomenex, Torrance, CA, USA). The column and autosampler temperatures were held at 35 °C and 10 °C, respectively. The mobile phase for baseline separation consisted of A – water, B – acetonitrile, and C – methanol, with all components containing 0.1% of formic acid. The following gradient elution program was used: the initial pre-run composition with equilibration for 6.0 min prior to injection – 7% B; 0–4.0 min – 7–80% B; 4.0–4.1 min – 80–95% B; 4.1–6 min – 95–100% B; 2 min hold at 100% B; 8.0–8.5 min – 100% B to 100% C; 2 min column washing at 100% C; 11.5–12.0 min – return to the initial conditions. The flow rate was 0.300 mL min^{-1}. The total run time was 18 min. The injection volume was 4 µL. Acetonitrile-water (30:70, v/v) mixture was employed as the solvent system for filling the sample loop and washing the needle.

The chromatographic system was coupled to a Q Exactive mass spectrometer (Thermo Scientific,Bremen, Germany) equipped with a Heated Electrospray Ionization Source II (HESI II). The qualification and quantification analyses were performed under heated electrospray ionization conditions in full scan/data-dependent MS^2 (FS-ddMS^2) mode in two separate runs for negative and positive ionization. Full mass range scans were used for quantification and ddMS^2 – for confirmatory analysis. The optimized HESI II conditions were: sheath gas, 20 arbitrary units (a.u.); auxiliary gas, 6 a.u. (positive ionization, +) or 10 a.u. (negative ionization, -); spray voltage, 4.5 kV (+) or -3.5 kV (-); capillary temperature, 265 °C (+) or 293 °C (-); heater temperature, 400 °C. In the FS-ddMS^2 mode the

Q Exactive HRMS instrument performed a full scan followed by a $ddMS^2$ scan. The full scan mass range was set to 100-1000 m/z with a resolution of 35 000 (FWHM at 200 m/z). The optimized automatic gain control (AGC) target was assigned a value of $5.0 \cdot 10^6$ (the maximum number of ions filling C-Trap) with the maximum ion injection time (IT) of 80 ms. For $ddMS^2$ scans, the precursor quadrupole isolation window was set to 0.6 m/z. The data-dependent settings (underfill ratio, apex trigger, charge exclusion, dynamic exclusion, excluded isotopes, and peptide match) were disabled. Selected precursor ions (Table 2.1.) were admitted for the activation of MS^2 fragmentation with collision energies specified in the inclusion list of the software. The default charge state was set to 1. The multiplex and loop count were set to 1 and 2, respectively, as appropriate for a Top 2 $ddMS^2$ method. Orbitrap resolution was set to 17 500 FWHM, the AGC target at $1.0 \cdot 10^5$, and IT was set at 20 ms for the $ddMS^2$ scan period. The instrument was calibrated using Pierce LTQ Velos ESI positive and negative ion calibration solutions.

Thermo Scientific Xcalibur™ and TraceFinder™ software suites were used for both qualitative and quantitative assessment of the obtained data. The native compounds and isotopically labeled internal standards were quantified by measuring a ratio of peak areas in FS EICs. The $ddMS^2$ transitions (qualifiers) were used to confirm the identity of the native analytes, but did not contribute to the quantification results.

2.1.4. Method optimization workflow

In order to obtain the optimal performance of mass spectrometer, such as signal stability and sensitivity, a chemometric approach was applied by using the MiniTab 17 software (Minitab, State College, PA, USA). The optimization strategy consisted of several steps, during which particular experiments were performed. A stepwise plan of all procedures performed in this work is shown in Figure 2.1.

The compound-specific collision energies were optimized by adding the individual standards at 1 μg mL^{-1} concentration in reconstitution solvent with a syringe at a flow rate of 5 μL min^{-1}. Using the Q Exactive tune program, the precursor ions of the corresponding anticoccidial drug residues were selected by setting the quadrupole in the t-MS/MS mode and the intensities of product ion signals were assessed by increasing the Normalized Collision Energy (NCE). The value of NCE was optimal when complete fragmentation of precursor ions occurred. The monoisotopic masses of the monitored ions and the optimal NCE values are shown in Table 2.1. The LC conditions were defined at this point by selecting the appropriate mobile and stationary phases to achieve the necessary resolution and reasonable chromatographic peak shape.

Table 2.1

Mass spectral properties of the investigated analytes

			Precursor ions (quantifiers)				Product ions (confirmatory)				
	ISTD	Charge	[M ± Adduct]	Monoisotopic exact mass (m/z)	Absolute mass error[b] (ppm)		NCE [a]	[M]	Ion 1 exact mass (m/z)	[M]	Ion 2 exact mass (m/z)
					Egg matrix	Poultry matrix					
APL	HAL-$^{13}C_6$	+	$[C_{14}H_{18}N_4+H]$	243.1604	3.6	4.6	10	$[C_8H_{12}N_3]$	150.1026	$[C_6H_8N]$	94.0651
CLOP	HAL-$^{13}C_6$	+	$[C_7H_7Cl_2NO+H]$	191.9977	4.4	3.9	90	$[C_5H_6Cl]$	101.0153	$[C_4H_4Cl]$	86.9996
DEC	DEC-d_5	+	$[C_{24}H_{35}NO_5+H]$	418.2588	4.7	4.1	35	$[C_{22}H_{32}NO_5]$	390.2275	$[C_{22}H_{30}NO_4]$	372.2169
DCZ	TOL-d_3	-	$[C_{17}H_9Cl_3N_4O_2-H]$	404.9718	0.2	0.2	25	$[C_{15}H_7Cl_3N_3]$	333.9711	$[C_{15}H_7Cl_2N_3]$	299.0023
HAL	HAL-$^{13}C_6$	+	$[C_{16}H_{17}{}^{80}BrClN_3O_3+H]$	416.0193	4.8	5.4	30	$[C_5H_{10}NO]$	100.0757	$[C_8H_{10}N]$	120.0808
LAS	HAL-$^{13}C_6$	+	$[C_{34}H_{54}O_8+Na]$	613.3711	5.3	3.6	35	$[C_{21}H_{38}NaO_4]$	377.2662	$[C_{34}H_{50}NaO_6]$	577.3470
MAD	HAL-$^{13}C_6$	+	$[C_{47}H_{80}O_{17}+Na]$	939.5288	4.6	5.8	20	$[C_{46}H_{78}NaO_{14}]$	877.5284	$[C_{46}H_{80}NaO_{15}]$	895.5389
MON	HAL-$^{13}C_6$	+	$[C_{36}H_{62}O_{11}+Na]$	693.4184	4.8	4.0	50	$[C_{25}H_{42}NaO_6]$	461.2874	$[C_{25}H_{44}NaO_7]$	479.2979
NAR	NIG	+	$[C_{43}H_{72}O_{11}+Na]$	787.4967	4.5	3.9	40	$[C_{23}H_{36}NaO_6]$	431.2404	$[C_{29}H_{48}NaO_7]$	531.3292
NEQ	HAL-$^{13}C_6$	+	$[C_{22}H_{23}NO_4+H]$	366.1700	6.5	4.8	30	$[C_{21}H_{22}NO_4]$	352.1543	$[C_{21}H_{20}NO_3]$	334.1438
DNC	DNC-d_8	-	$[C_{13}H_{10}N_4O_5-H]$	301.0578	0.1	0.6	10	$[C_6H_5N_2O_2]$	137.0346	$[C_3H_7O_4]$	107.0350
ROB	ROB-d_8	+	$[C_{15}H_{13}Cl_2N_5+H]$	334.0621	5.3	5.6	40	$[C_7H_5ClN]$	138.0105	$[C_7H_8ClN_2]$	155.0371
SAL	HAL-$^{13}C_6$	+	$[C_{42}H_{70}O_{11}+Na]$	773.4810	5.4	4.3	40	$[C_{23}H_{36}NaO_6]$	431.2404	$[C_{29}H_{48}NaO_7]$	531.3292
SEM	HAL-$^{13}C_6$	+	$[C_{45}H_{76}O_{16}+Na]$	895.5026	5.3	3.7	20	$[C_{44}H_{74}NaO_{13}]$	833.5022	$[C_{44}H_{76}NaO_{14}]$	851.5049
TOL	TOL-d_3	-	$[C_{18}H_{14}F_3N_3O_4S-H]$	424.0584	0.9	0.5	-	$[C_{18}H_{14}F_3N_3O_4S-H]$	425.0608	$[C_{18}H_{14}F_3N_3O_4S-H]$	426.0576
TOLS	TOL-d_3	-	$[C_{18}H_{14}F_3N_3O_5S-H]$	440.0533	0.8	0.4	-	$[C_{18}H_{14}F_3N_3O_5S-H]$	441.0557	$[C_{18}H_{14}F_3N_3O_5S-H]$	442.0526
TOLX	TOL-d_3	-	$[C_{18}H_{14}F_3N_3O_6S-H]$	456.0483	0.1	0	-	$[C_{18}H_{14}F_3N_3O_6S-H]$	457.0506	$[C_{18}H_{14}F_3N_3O_6S-H]$	458.0477
DEC-d_5		+	$[C_{24}D_5H_{30}NO_5+H]$	423.2902	4.5	4.4					
DNC-d_8		+	$[^{13}C_6C_{10}H_{17}{}^{80}BrClN_3O_3+H]$	422.0393	5.9	5.3					
HAL-$^{13}C_6$	-	-	$[C_{13}D_8H_2N_4O_5-H]$	309.1081	0	0.1			-		
NIG		+	$[C_{40}H_{68}O_{11}+Na]$	747.4654	6.1	4.8					
ROB-d_8		+	$[C_{15}H_5D_8Cl_2N_5+H]$	342.1123	6.8	5.9					
TOL-d_3		-	$[C_{18}D_3H_{11}F_3N_3O_4S-H]$	427.0773	0.9	0.8					

[a] The actual HCD energy is calculated on a basis of mass and charge of the selected precursor ion.

[b] Average mass error obtained at validation level for each matrix during 4 day validation period. (n=8)

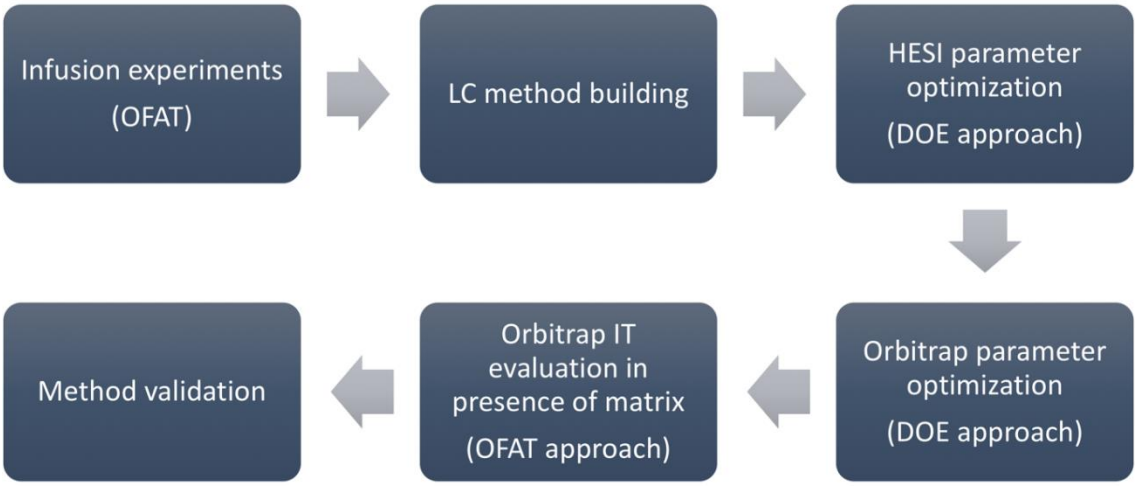

Figure 2.1. **Step-by-step plan of general work strategy**

The HESI II ionization source parameters and Orbitrap MS detector conditions were optimized using Box-Behnken response surface designs (BBD). The campaign of experiments for optimization of ion source parameters involved 5 different factors at 3 levels, for a total of 46 runs. The Orbitrap parameters (AGC, IT, and resolution) were optimized at three levels for a total of 15 runs. A total of 5 replicate runs were planned for the ion source and 3 replicate runs for the optimization of Orbitrap parameters. The experiments were conducted in both positive and negative ionization modes and in randomized order.

The ion source and Orbitrap analyzer conditions were optimized using analytical standards at 20 μg kg^{-1} concentration. The injection time was studied by one factor at a time (OFAT) optimization using matrix-matched standards at 20 μg kg^{-1} concentration for both matrices. The experimental factors were tested by both BBD and OFAT approaches. The optimization experiments are compiled in Table 2.2.

Table 2.2

The optimization steps performed and statistical methods used in the study

	Parameter	Abbrevation	-1	0	1
1. Optimization of HESI conditions (BBD)	Sheath gas flow[a]	A	20	40	60
	Auxiliary gas flow[a]	B	6	12	18
	Spray voltage, positive (kV)	C_1	+2.5	+3.5	+4.5
	Spray voltage, negative (kV)	C_2	-1.5	-2.5	-3.5
	Capillary temperature (°C)	D	250	300	350
	Auxiliary gas temperature (°C)	E	300	350	400
2. Optimization of mass spectroscopic parameters (BBD)	Resolution	F	35 000	70 000	140 000
	AGC	G	$5.0 \cdot 10^4$	$5.0 \cdot 10^5$	$5.0 \cdot 10^6$
	Injection time (ms)	H	20	100	180
			Variables		
3. The effect of injection time in the presence of matrix (OFAT)	Injection time (ms)	20	40	60	80
		100	120	140	180

[a] Arbitrary units

2.1.5. Method validation

To evaluate the performance and suitability of the developed LC-HRMS method for the determination of anticoccidial veterinary drugs, it was validated according to the predefined criteria summarized in Table 2.3. A matrix-comprehensive in-house validation concept was applied using the InterVAL software according to 2002/657/EC [77] for a quantitative confirmatory method.

Table 2.3

Validation criteria used in the study

Validation parameter	Requirement/Criteria		
Selectivity	No interfering peaks at the defined analyte RT and a confirmatory fragmentation scan.		
Decision limit (CCα) and detection capability (CCβ)		Set validation levels from lowest ML/MRL (μg kg^{-1})	
		Egg matrix	Poultry meat matrix
	APL	10	50
	CLOP	10	50
	DEC	20	500
	DCZ	2	500
	HAL	6	10
	LAS	150	60
	MAD	2	2
	MON	2	8
	NAR	2	50
	NEQ	10	10
	DNC	300	50
	ROB	25	200
	SAL	3	5
	SEM	2	10
	TOL	10	100
	TOLS	10	100
	TOLX	10	100
	$CC_\alpha = ML/MRL + 1.64 \cdot (RSD_{wR})$ (1) $CC_\beta = CC_\alpha + 1.64 \cdot (RSD_{wR})$ (2) , where ML/MRL- maximum limit/maximum residue limit (μg kg-1); RSD_{wR} - standard deviation of the within-laboratory reproducibility at validation level.		
Recovery	-30 to +10% at concentration range 1 - 10 (μg kg^{-1}); -20 to +20% at concentrations higher than 10 (μg kg^{-1}).		
Linearity	$R^2 > 0.90$, where R^2 - coeficcient of determination of calibration graph.		
Reproducibility / repeatability	< 45% at concentration range 1 - 10 (μg kg-1); < 32% at concentration range 10 - 100 (μg kg-1); < 23% at concentration range 100 - 1000 (μg kg-1); < 16% at concentrations higher than 1000 (μg kg-1).		
Uncertainty	Freely chosen criteria: 100% at 95% confidence interval (k = 2). $U = k \cdot RSD_{wR} = 2 \cdot RSD_{wR}$ (3) , where U - uncertainty at 95% confidence interval (%); k - overlapping coefficient; RSD_{wR} - standard deviation of the within-laboratory reproducibility at validation level.		

The validation levels for poultry and eggs were chosen according to the ML and MRL values of the target anticoccidial drugs in the relevant European Commission regulations and were set at 0.5, 1, 1.5, and 2 times the ML and MRL values. Substances without defined MRL were validated at 5, 10, 15, and 20 μg kg^{-1} concentrations. The whole validation study for each matrix type consisted of 8 replicate standard addition experiments, which were performed by two operators over two days. Fresh matrix calibration series and three matrix blank samples fortified with the internal standard were additionally prepared on both days in order to prove the specificity and the lack of susceptibility to matrix interference during the validation. Four validation levels per experiment, two calibration and blank series resulted in a total of 50 samples per each type of eggs (chicken and quail eggs) and 50 samples per each poultry (chickens raised for laying eggs and broilers) matrix. Additional selectivity evaluation experiments were performed post-validation using different samples of eggs (n = 20) and meat (n = 5) to further ensure the robustness of the method.

The stability of anticoccidials in spiked (20 μg kg^{-1}) sample extracts was evaluated by using reconstituted extracts. The extracts were stored at -20 °C and monitored for a week, with aliquots analyzed after 1, 2, 4, and 7 days. A fresh reference sample was prepared on each day of analysis to evaluate and compare the recoveries. Five sample injections were performed and a narrow recovery threshold of -20 to +10% was applied, taking into account a previous study involving such evaluation [78].

2.2. Non-target methodology - food contact materials

2.2.1. Sampling and sample preparation

In total, 17 commercially available straw samples were purchased at local catering outlets in Riga, Latvia. One sample was made from recycled biodegradable, transparent plastic, the rest were from paper or multilayer composite paper. The samples were separated into two groups – large diameter (8 mm, n = 5) and small diameter straws (6 mm, n = 12). No information was available regarding the detailed material composition and the technology used in the manufacture of these FCMs. Most of the paper and plastic straws were labelled as “biodegradable” and “biologically friendly”. A detailed list of samples and their characteristics, as well as dates and outlets of purchase, origin or products is available in Annex 5. No information was available regarding the detailed material composition and the technology used in the manufacture of these FCMs.

To account for any background contamination, before the extraction, all non-disposable glassware, e.g., Erlenmeyer flasks, glass vials and measuring cylinders were soaked in 95% ethanol for at least 8 hours and heated at 200 °C for a minimum of 12 h. All plastic equipment was also soaked in 95% ethanol for at least 8 hours and dried overnight in room temperature. Crimp top chromatography

vials with inlets (BGB Analytic AG) and Vivaspin® 500 Centrifugal filter vials (0.2 µm) were used as received.

Two straws were used per leeching experiment. The straws were flattened out with some reminder of open volume in the middle and cut in 6-8 mm long pieces with cleaned scissors. Samples were then transferred to clean Erlenmeyer flasks, with 25 and 40 mL of warm (35 – 40 °C) extraction solution added to smaller and larger diameter straws, respectively. The solvents were chosen based on simulants described for plastics testing in Commission Regulation 10/2011 and were 3% acetic acid in deionized water (w/v) as simulant B and 50% ethanol in deionized water (v/v) as simulant D1. Two negative control samples were prepared solely with 40 mL of extraction solvents. The flasks were capped and sealed with a plastic clamp, transferred into airtight bags, and submerged in a water bath for 24 hours at 40 °C. After 24 hours, the extracts were transferred to clean 50 mL glass vials, cooled down to room temperature and stored in 4 °C in the dark. Additional leaching trend experiments were undertaken, to determine the rate of compound migration in simulants. For the leaching trend experiments, aliquots of 0.2 mL were taken and analyzed immediately.

The extracts were filtered with centrifugal filter vials and transferred to chromatography vials prior to LC-MS analysis.

2.2.2. Databases used as basis for suspect screening

Databases

The choice and volume of "suspect" compound lists largely influences the result of investigation. Databases for chemicals of concern (COC) as well as regulatory and non-regulatory FCM substance lists were obtained based on the previously published and reviewed inventories by Geueke et al. [9]. The COC databases retrieved were: Substitute It Now! (SIN); Substances of Very High Concern (SVHC); The Endocrine Disruption Exchange (TEDX). The databases of FCM substances were: USFDA indirect food additive list; USFDA SCOGS (Generally Recognized As Safe or GRAS substances); EFSA Scientific cooperation (ESCO) coatings, colorants, cork and wood, paper and board, printing inks, rubber and silicones; EU Plastics regulation (Union list). Additionally, native Thermo extractables and leachables list was included as provided by the software manufacturer. The non-specific public online databases (PubChem, ChemSpider) were avoided, as fitting the experimental data would allow for a high risk of false positive results. The entries from databases were acquired in December 2018.

Processing of databases

The extracted CASRNs were processed using a modified version of the MS-Ready workflow [79] (Figure 2.2) based on the opensource environment KNIME Analytics platform 3.7.0. Chemical Identifier Resolver (CIR) extension was used to process the CASRN and to obtain SDF identifiers prior to the MS-Ready workflow.

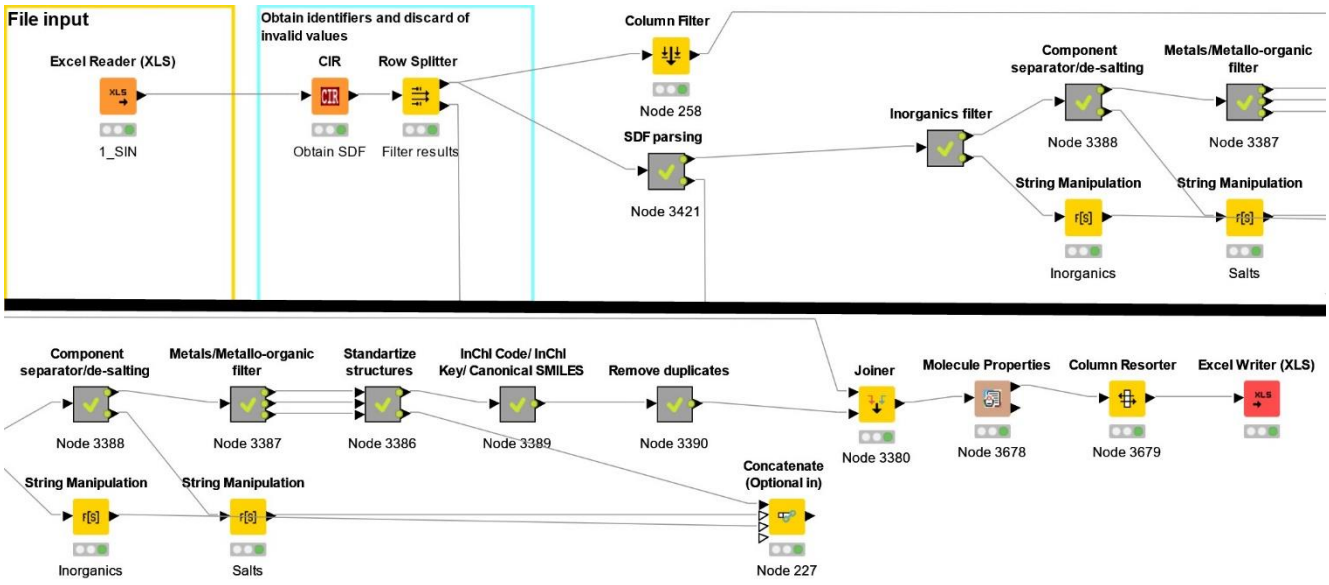

Figure 2.2. **A modified version of MS-ready workflow by the addition of chemical identifier parsing nodes**

The CIR extension node used the network service by the CADD Group at the NCI/NIH as a resolver for different chemical structure identifiers and allowed to convert a given structure identifier into another representation or structure identifier. Cheminformatic steps were performed using an updated version of Indigo 2 nodes. In addition to the MS-Ready workflow nodes, we also added nodes to obtain the molecular formulas and monoisotopic masses for the import into Compound Discoverer 2.1. The processed databases are available as a .csv file in the Harvard Dataverse repository [80].

The obtained molecular formulas were used to obtain the atomic ranges for the prediction of molecular formula node in Compound Discoverer. For the purpose of determining the maximum element counts, a ChemRegex Visual Basic (VBA) macro was used. The formulas were predicted using the 99.8th percentile values of the calculated maximum element count from all the compounds in extracted databases. The VBA macro is available in Annex 6. The resulting maximum ranges are available together with Compound Discoverer 2.1 parameters in Annex 7.

2.2.3. Parameters of UHPLC-HRMS method

The conditions for the instrumental LC-HRMS analysis based on modified previously published methods [81]. The order of experiments was as follows: two different MS experiments were carried out in positive ion mode. First, all samples, control samples and blank solvents were run in full scan (100 - 1200 Da) – data-dependent mode (FS-ddMS^2) with no inclusion list provided, referred to as the **screening experiment**. After preliminary data processing, an inclusion list was created based on the most prominent chromatographic and mass features in the sample pool (see Data Processing section). A second batch of experiments were then performed using the same samples, but with the inclusion list attached to the FS-ddMS^2 method (the **identification experiment**), providing the most prevalent precursor masses. The resolution of 70,000 full width at half maximum (FWHM) at 200 m/z was used in the FS mode and the ddMS2 resolution was set to 17500 at 200 m/z. Normalized collision energy (NCE) of 40% was applied in the screening experiment and three levels of 20%, 40% and 60% of NCE were applied in the identification experiments. The top three most intense precursor MS/MS spectra were collected per each scan cycle.

Chromatographic analyses were conducted on an UltiMate 3000 (Dionex, Olten/Switzerland) HPLC system using a Kinetex C18 (100 mm × 2.1 mm i.d., 1.7 μm) analytical column (Phenomenex, Torrance, CA, USA). The column and autosampler temperatures were held at 40°C and 4°C, respectively. The mobile phase for baseline separation consisted of A – water, B – acetonitrile, and C – methanol, with all components containing 0.1% of formic acid. The following gradient elution program was used: the initial pre-run composition with equilibration for 6.0 min prior to injection – 7% B; 0–4.0 min – 7–80% B; 4.0–4.1 min – 80–95% B; 4.1–6 min – 95–100% B; 2 min hold at 100% B; 8.0–8.5 min – 100% B to 100% C; 2 min column washing at 100% C; 11.5–12.0 min – return to the initial conditions. The flow rate was 0.300 mL min^{-1}. The total run time was 18 min. The injection volume was 4 μL. Additionally a Kinetex C18 (50 mm × 2.1 mm i.d., 1.7 μm) analytical column (Phenomenex, Torrance, CA, USA) was placed between the HPLC pump and the injection valve for the retardation of substances originating from the mobile phase and the analytical instrument.

The chromatographic system was coupled to a Q Exactive mass spectrometer (Thermo Fisher Scientific, Bremen, Germany) equipped with a Heated Electrospray Ionization Source II (HESI II) set at C position. The screening and identification analyses were performed under heated electrospray ionization conditions in full scan/data-dependent MS^2 (FS-ddMS^2) mode in separate runs for negative and positive ionization. The HESI II probe was set to C position depth. The conditions for HESI II were: sheath gas, 40 arbitrary units (a.u.); auxiliary gas, 10 a.u.; spray voltage, 4.5 kV (positive ionization, +) or -3.5 kV (negative ionization, -); capillary temperature, 280 °C; heater temperature, 400 °C. The S-lens RF level was set to 50. In the FS-ddMS^2 mode the Q Exactive HRMS instrument performed a full scan followed by multiple ddMS^2 scans. The full scan mass range was set to 100–

1200 m/z with a resolution of 70’000 full width at half maximum (FWHM) at 200 m/z. The automatic gain control (AGC) target was assigned a value of $5.0 \cdot 10^6$ (the maximum number of ions filling C-Trap) with the maximum ion injection time (IT) of 100 ms.

For $ddMS^2$ scans, the precursor quadrupole isolation window was set to 0.6 m/z. The data-dependent settings (underfill ratio, apex trigger, charge exclusion, dynamic exclusion, excluded isotopes, and peptide match) were disabled. Selected precursor ions after the screening experiment were admitted for the activation of MS^2 fragmentation. The default charge state was set to 1. The multiplex and loop count were set to 1 and 3. Orbitrap resolution was set to 17 500 FWHM at 200 m/z, the AGC target at $1.0 \cdot 10^5$, and IT was set at 20 ms for the $ddMS^2$ scan period. The instrument was calibrated using Pierce LTQ Velos ESI positive and negative ion calibration solutions.

Thermo Scientific Xcalibur™ software suite was used for sequence setup and acquisition.

2.2.4. Data processing and compound identification

The acquired data for both experiment types were processed using Compound Discoverer 2.1 (Thermo Scientific) analysis workflow nodes including peak alignment, unknown compound detection, grouping, gap filling, composition prediction, mass lists, mzCloud, mzVault, ChemSpider search and compound annotation.

A background subtraction was performed by Mark Background Compounds node. Detailed parameters for each node are available in Annex 7. The conceptual workflow for the analysis and identification of potentially hazardous chemicals is presented in Figure 2.3 and was as follows:

- Peak lists were generated by Compound Discoverer from the exact mass chromatograms of the samples, extraction solvent blanks and control samples;
- Retention time alignment was performed and the peaks detected in negative control samples were subtracted from the real samples;
- All peaks with the maximum area of less than 500000 across all the sample pool were filtered out;
- Compounds with retention time less than 1 min were filtered out;
- Exact masses of the remaining peaks were searched against suspect databases and filtered;
- Molecular formulas were generated based on the isotope pattern fit;
- Candidates with a spectrum fit score (SFit) greater than 80% were filtered;
- The remaining candidates were included in an Xcalibur inclusion list for $ddMS^2$ analysis and the samples were re-run;
- Fragmentation spectra of candidates were searched against MassBank, MassBank of North America (MoNA), mzCloud and mzVault;

● Fragmentation spectra of candidates were averaged between 20%, 40% and 60% NCE, then matched and ranked against MetFrag [42] search. Individual spectra were also submitted to SIRIUS 4 [40]. Both tools were populated with SMILES and InChlKeys from the suspect database.

In-house R script that was used to implement the spectra averaging and search against MetFrag is available upon request. The levels of confidence for the identification of the detected compounds matched those used by [22], where level 2 was assigned to the probable structure, subdivided into two levels – 2a (spectral library match) and 2b (diagnostic evidence and in silico prediction match). Level 2ab was assigned to candidates for which both spectral library and diagnostic evidence provided unanimous agreement.

Level 3 was assigned to tentative candidates, when there was not enough evidence for level 2 confirmation and level 4 to candidates with unequivocal molecular formulas. The original spectra and average spectra of final candidates, exported in .csv format, are available at Harvard Dataverse repository [80]. For the candidates with multiple isobaric compounds, spectra were collected from the highest intensity peaks.

Multivariate model regression analysis of retention time and the logarithm of the octanol-water partitioning coefficient ($\log K_{OW}$) for the annotated structures were used to check retention time plausibility and to evaluate the outliers by applying Cook's distance.

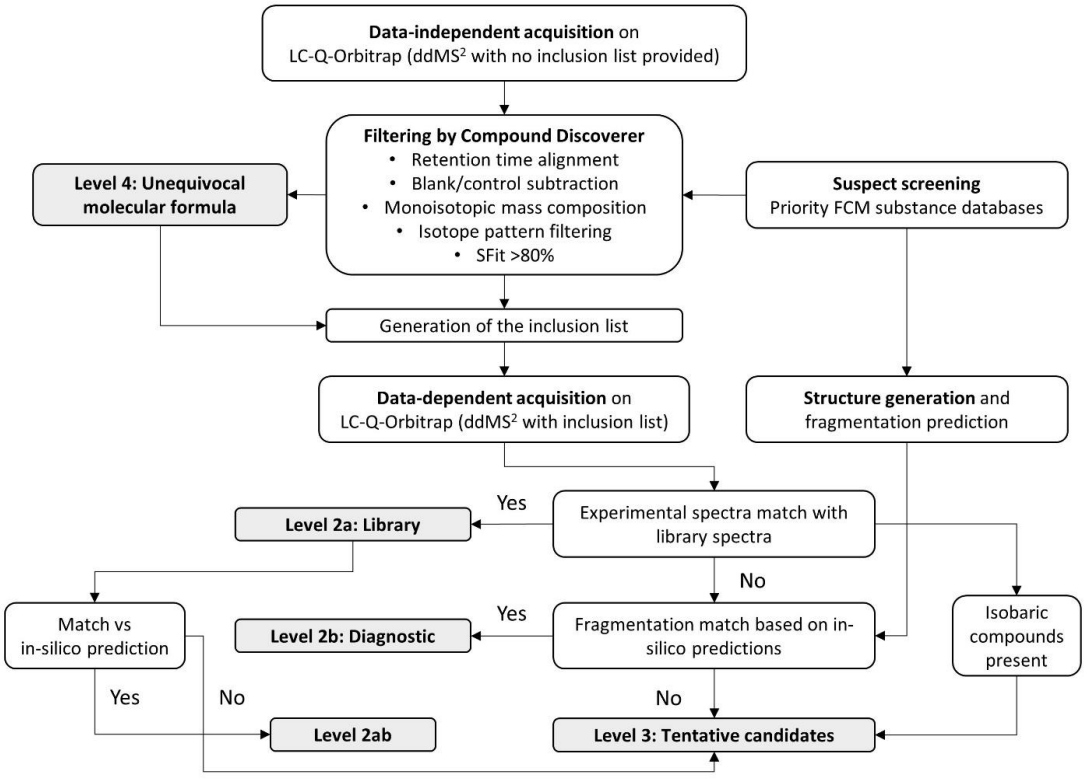

Figure 2.3. **Conceptual workflow for the analysis, identification and ranking of the suspects**

2.2.5. Toxicological endpoint screening

To assess whether any experimental data concerning mutagenicity or carcinogenicity may be already available for any of the compounds tentatively identified in this study, the free software application OECD QSAR Toolbox v4.3 [82] was used for in-silico analysis of the toxicity of individual compounds, serving as a reference database comprising experimental toxicity data for different endpoints. Information retrieval from the OECD QSAR Toolbox v4.3 was performed as described in [83]. In short, with a focus on the endpoints of mutagenicity and carcinogenicity, all databases provided under the headline "Human Health Hazards" within the "Endpoint" tool were used to (i) extract the number of experimental studies being available within these databases, and to (ii) extract the number of experimental studies indicating that the respective substance was mutagenic or carcinogenic.

In addition, the compounds tentatively identified in this study also were subjected to (Q)SAR analyses for in silico toxicity predictions. Five (Q)SAR tools were used for the prediction of mutagenicity and three tools were used for carcinogenicity predictions following an approach adapted from [83]. In short, TEST (https://www.epa.gov/chemical-research/toxicity-estimation-software-tool-test) was used for mutagenicity predictions; VEGA (https://www.vegahub.eu/) and LAZAR (http://lazar.in-silico.de/predict) were used to predict mutagenic and carcinogenic endpoints.

The Toxicity Estimation Software Tool (TEST; v4.2.1) provided by the USEPA predicts mutagenicity using three different QSAR methodologies based on either hierarchical clustering, the so-called FDA approach as applied by the USFDA, a nearest neighbor approach, and a consensus model. The output given by TEST models was a numeric value within the limits of 0 and 1; when no output results were produced the mutagenic score was set to the value of 0.5. For the cumulative analysis using all the models, the consensus score was used following normalization as suggested in [83].

The VEGA platform v1.1.4 [84] comprises an array of toxicity estimation models including four models (CAESAR, SarPy/IRFMN, ISS and KNN/Read-Across) for mutagenicity predictions later combined in a consensus model and four carcinogenicity models (CAESAR, ISS, IRFMN/Antares and IRFMN/ISSCAN-CGX). In accordance with [83], the VEGA results obtained were translated into numeric values. The models provided two different types of information for every individual compound. The first layer of information was a simple yes/no prediction for mutagenicity (carcinogenicity); in addition, compounds could be marked as suspected mutagens. The second layer of information was related to the reliability of the prediction made by the respective model. The possible outputs were "experimental activity", "good reliability", "moderate reliability", or "low reliability". Following the approach described in [83], these two types of information were combined and translated into a numeric value in the range between 0 and 1, which then served as mutagenic

(carcinogenic) scores for the respective model of the VEGA platform. For the cumulative analysis using all the models for mutagenicity, the consensus model score was used.

LAZAR (lazy, structure–activity relationship) [85] comprises one model for mutagenicity and three models for carcinogenicity. The mutagenicity model yields binary yes/no answers, which are presented alongside probability scores (0 to 1) that indicate to which class the prediction belongs to. Binary and probability outputs were combined, translated into numeric values, and normalized to obtain a single LAZAR mutagenicity score in the range of 0 to 1. Accordingly, the results of the LAZAR carcinogenicity models were translated into normalized carcinogenic scores for LAZAR.

Following the individual (Q)SAR analysis, the three normalized mutagenic scores and the carcinogenic scores (all of the VEGA model scores and the LAZAR scores) were combined by calculating the mean values for each predicted endpoint and the tentatively identified compounds were sorted and ranked according to their final cumulative mutagenic and carcinogenic scores.

The R script implemented in this case study including the output data are available at Harvard Dataverse repository [80] as a .rmd file and in Annex 8.

2.3. Biosensors

2.3.1. Reagents

All reagents were of analytical grade and obtained from commercial sources. 2-[4-(2 Hydroxyethyl)-1-piperazino]ethansulfonic acid (HEPES), 4-methylumbelliferyl butyrate (4-MUBu), 4-methylumbelliferone (4-MU), N-bromosuccinimide (NBS), diethyl (4-nitrophenyl)phosphate (paraoxon), diethoxy-(4-nitrophenoxy)sulfanylidenephosphorane (parathion), 3-chloro-7-diethoxy-phosphinothioyloxy-4-methyl-chromen-2-one (coumaphos), dimethoxy-(4 nitrophenoxy)-sulfanylidenephosphorane (methyl parathion), diethoxy-(4- methylsulfinylphenoxy)-sulfanylidene-phosphorane (fensulfothion), O-4-cyanophenyl O,O-dimethyl phosphorothioate (cyanophos), diethoxysulfanylidene- (3,5,6-trichloropyridin-2-yl)oxyphosphorane (chlorpyrifos), diethoxy-(6-methyl- 2-propan-2-ylpyrimidin-4-yl)oxy-sulfanylidene-phosphorane (diazinon), N-(mercapto-methyl)phthalimide S-(O,O-dimethyl) phosphorothionate (phosmet), O-(2-(diethylamino)- 6-methyl-4-pyrimidinyl) O,O-dimethylphosphorothioate (pirimiphos), O,Odimethyl O-(2,6-dichloro-4-methylphenyl) phosphorothioate (tolclofos), were from Sigma-Aldrich (St. Louis, MO, USA).

2.3.2. MU standard calibration curve in HEPES

Stock solution of 1 mM methylumbelliferone (MU) in 100 % DMSO was prepared as a standard reference for the calculation of the reaction product concentrations in our experimental conditions. Fluorescence emission was measured at 445 nm after excitation at 365 nm for MU solution aliquots at

different concentration levels in the range from 0.01 to 0.66 mM. The slopes obtained from the plotted fluorescence intensities versus the MU concentrations were used for the determination of fluorescence intensity coefficients, further used to quantify the amount of MU released during the hydrolysis of MU by EST2. All measurements were carried out at least three times, and the acquired data was analyzed using the software QtiPlot 0.9.7.10 (Copyright 2004–2009 Ion Vasilief, IONDEV SRL - Bucuresti, Romania).

2.3.3. Enzyme purification

EST2 was over-expressed in the mesophilic host *E. coli* strain BL21 (DE3) and purified as previously described in Manco et al. [86]. Purity was tested by SDS-PAGE. The protein concentration was estimated by the optical absorbance at 280 nm, using a molar extinction coefficient of $1.34 \times 10^5\ M^{-1}\ cm^{-1}$ in 40 mM sodium phosphate buffer, pH 7.1 (slightly alkali), at 25 °C, as described in Manco et al. [86].

2.3.4. Fluorescence standard enzymatic assay

The standard assay was prepared in a 0.5 mL final volume reaction mixture containing 25 mM HEPES buffer, pH 7.0 (neutral), 1% $C_{14}H_{22}O(C_2H_4O)_n$ (TRITON X-100) and 1 mM 4-MUBu (from a stock solution of 40 mM 4-MUBu in 100% DMSO). After 2 min incubation at 30 °C, aliquots of EST2 (1.46 pmol) in 25 mM HEPES at pH 7.0 were added to the assay solution. Fluorescence measurements were carried out in a JASCO FP-777 spectrofluorometer (Jasco Analytical Instruments, Tokyo Japan), equipped with an external thermostatic bath Julabo F25 (Julabo GmbH, Seelbach, Germany) at the temperature of 30 °C, using a quartz cuvette of 1 cm optical path. The rate of 4-MUBu hydrolysis by the EST2 enzymatic activity was determined by monitoring the increase of the fluorescence emission at 445 nm (Ex = 365 nm) due to the release of 4-MU as a reaction product. The coefficient of 4-MU fluorescence intensity, determined as previously described, was used for the calculation of the concentration of reaction products. One unit of enzymatic activity was defined as the amount of enzyme required to release 1 μmol min^{-1} of 4-MU under the indicated experimental conditions.

2.3.5. Kinetic constants

Enzyme kinetic constants on 4-MUBu were determined under standard assay conditions at substrate concentrations in the range from 0.1 to 4 mM. The kinetic constant values (K_M and k_{cat}) were calculated by plotting the reciprocals of EST2 hydrolysis rates versus the substrate concentrations (Lineweaver-Burk transformation plot). All measures were carried out at least three times, and the data

were analyzed by the software QtiPlot 0.9.8.9 (Copyright 2004–2011 Ion Vasilief, IONDEV SRL - Bucuresti, Romania).

2.3.6. Inhibition Assay of EST2 in Presence of Pesticides

Ten mM stocks of paraoxon, coumaphos, fensulfothion, methyl-parathion, parathion, cyanophos, pirimiphos and diazinon in 100% DMSO, and 20 mM stocks of phosmet, chlorpyrifos and tolclofos in 100% DMSO, were prepared in order to use as EST2 activity inhibitors. The inhibition assays were carried out under the standard assay conditions by incubating aliquots of 1.46 pmol of EST2 in presence of increasing concentrations of each inhibitor in the range from 0 to 2.1 pmol in a final volume of 10 μL. After 1 min incubation, aliquots of inhibited enzyme were removed from the mixture and the residual activity was measured in the standard assay conditions. The inhibition percentage was calculated based on the following as previously described [72] equation:

$$\frac{(I_0 - I)}{I_0} \times 100$$

in which I_0 represents the inhibition percentage in absence of inhibitor and I the percentage of inhibition at the indicated inhibitor concentration. All measurements were carried out at least three times and the data analyzed by the software QtiPlot 0.9.8.9 (Copyright 2004–2011 Ion Vasilief).

2.3.7. Docking analysis

Computer simulations were carried out as described in Carullo et al. [75] using the 3D crystallographic structure of EST2 resolved at 2.6 Å (ID number 1EQV from the Protein Data Bank (http://www.rcsb.org/pdb/)). In particular, the EST2 pdb file was opportunely edited by removing the 4-(2-hydroxyethyl)-1-piperazine ethanesulfonic acid bound to the serine 155 residue in the catalytic site, and the 2-amino-2-hydroxymethyl-propane-1,3-diol molecule bound to the protein during the crystallization process. Using Avogadro software (https://avogadro.cc/), the resulting structure was optimized through a brief energy minimization, by using the Assisted Model Building with Energy Refinement (AMBER) force field with the steepest descent algorithm, in order to remove potential problems, such as bad contacts, clashes and nonphysical contacts/interactions. The 4-MUBu and p-nitrophenyl butyrate 3D structures were generated using Avogadro software (https://avogadro.cc/) and the structures optimized through the MMFF94 force field with the steepest descent algorithm. The docking analysis was carried out using Autodock Vina, that employed the Broyden-Fletcher-Goldfarb-Shanno algorithm, significantly improving the average accuracy of the binding mode predictions with

respect to AutoDock 4 [87]. A box of about 89 $Å^3$ was used to include both catalytic protein pockets, with an exhaustiveness of 8. During the docking procedure, both the protein and ligands are considered as rigid, because the rigidity of the double ring of 4-MUBu and of the thermophilic proteins at room temperature. The structures were analyzed and the images produced by using the PyMOL (Schrödinger - New York, NY, USA) molecular graphic software [88].

2.3.8. Phosphorothionate pesticide oxidation by NBS

The chemical oxidation of phosphorothionate compounds was carried out by incubating these compounds in the presence of NBS. Aliquots of NBS (90 mM in water) were added at the final concentration of 300 μM to aliquots of OPs which possess the sulphur atom in binding with phosphate, at room temperature, in a ratio 1:90, and immediately mixed. After 5 min of incubation, the mixture was used in the inhibition assays of EST2. Incubation time and concentration ratio were determined by measuring the inhibition efficiency of oxidized-parathion on EST2 activity and the lack of NBS effects in the enzymatic activity.

2.3.9. MS analysis of NBS-oxidized pesticides

The chemical oxidation of phosphorothionate compounds by NBS was tested by using LC-MS. LC steps were performed with a Nexera X2 series UHPLC system (Shimadzu, Kyoto, Japan). The chromatographic separation was achieved on a Symmetry C18 column (5 μm, 4.6 × 150 mm, Waters, Dublin, Ireland). The column oven temperature was kept at 40 °C and the temperature of autosampler was set at 10 °C. Flow rate was set at 0.400 mL min^{-1}. Compounds were separated with a gradient of water (A) and ACN (B), both with added 4 mM ammonium acetate and 0.1% acetic acid. Gradient conditions were as follows: 5 min equilibration at initial 5% B, then increased to 60% B at 2 min with a further increase to 90% B at 5 min, followed by final increase to 95% B at 12 min. Gradient was returned to initial conditions of 5% B during 0.5 min and allowed for 2.5 min re-equilibration. Total analysis time was 20 min. Injection volume was set to 10 μL. MS analysis was performed with a 4500 QTrap mass spectrometer (AB Sciex, Courtaboeuf, France), equipped with turbo ion spray interface (ESI), operated in positive ionization mode. The source conditions were as follows: ion spray voltage, 5.5 KV; curtain gas pressure, 25 psi; nebulizer and heating gas pressure, 50 psi. The source temperature was set at 500 ◦C. Data acquisition was performed with the MRM mode. The declustering potential, the collision energy and the cell exit potential were found from literature data. Detailed MRM transitions, voltage settings and literature references are shown in Annex 9. Data were plotted by using the software QtiPlot 0.9.8.9.

2.3.10. Determination of EST2 activity in presence of NBS

The effect of NBS on the activity of EST2 was measured by pre-incubating 1.46 pmol of EST2 in the presence of several concentrations of NBS in the range from 0 to 50 mM in a final volume of 10 µL. After 1 min of incubation, aliquots of EST2 were taken from the mixture and the residual activity was measured in the standard assay conditions. All measurements were carried out at least in triplicate and the data analyzed by the software QtiPlot 0.9.8.9.

2.3.11. EST2 assay on robotic workstation and OP screening

Enzyme activity assay in the presence of irreversible inhibitors for pesticide screening and fingerprint purpose was carried out in 96 well micro-plates V-bottom, black, from Greiner Bio-one (Kremsmünster, Austria), using a Microlab® STAR Liquid Handling Workstation (Hamilton Europe, Bonaduz, Switzerland), equipped with an eight-channel liquid handler arm and a Hamilton Microlab® iSwap robotic arm, a gripper tool that can access plates on or off the deck, and Hamilton Heater Shaker. The STAR line workstation is equipped with a sensor for the control of temperature set in our experiments at 20 °C and controlled from a Microlab® Star Vector software 4.0. The workstation was also connected to a VICTOR™ X3 Multi-label Plate Reader (PerkinElmer, Waltham, MA, USA) a luminescence, fluorescence, and UV-Absorbance reader, equipped with a dispenser module and a shaker with adjustable speed. In Figure 2.4a, the layout of the robotic workstations worktable is described. In the worktable column 1 the first solvent reservoir carrier (total volume of about 250 mL) was filled with 50 mL of 0.025 M HEPES buffer pH 7.0, and 96-well micro-plates were placed in the worktable columns 3, 4 and 5. As described in Figure 2.4b, the mother plate in the temperature controller (set at 20 °C) of column 3 in Figure 2.4a, was prepared manually by the operator to contain 150 µL of EST2 enzyme at the final concentration of 0.7 µM in 0.025 M buffer HEPES pH 7.0 in the well 4A, and 11 different NBS treated OP inhibitors (10 µL each) at a final concentration of 3.3 µM in 3.3% DMSO, pre-incubated in presence of 300 µM NBS, in the wells from 1B to 2D, and a blank reference sample containing 3.3% DMSO and 300 µM NBS in water in the well 1A.

Incubation mixtures were prepared by the robotic liquid handler in the plate of worktable column 4, using the solutions from the solvent reservoir in column 1 and the plate in column 3, and dispensing in the wells from 1A to 2D the following solutions: 187 µL of 0.025 M HEPES buffer pH 7.0, 10 µL of EST2 (7 pmol). Then 3 µL of reference sample in the well 1A and 3 µL of each inhibitor (9.9 pmol) in the wells from 1B to 2D (Figure 2.4c). The plate was agitated in the shaker for 5 s and 10 µL aliquots, containing 0.35 pmol of fully inhibited enzyme with 0.495 pmol of the inhibitors, were withdrawn and dispensed in the plates in the worktable column 5 (each mixture had four replicates) for the assay of enzymatic residual activity (Figure 2.4d). The Microlab® iSwap robotic arm was used to

transfer the plate to the Victor X3 plate reader, where the internal temperature was set at 30 °C, and the dispenser added to a single well 250 µL of a reaction mixture containing 25 µM MUBu in 0.025 M HEPES pH 7.0, 1% Triton X-100. Then the plate was shaken for 5 s and the increase in fluorescence at 445 nm, after excitation at 350 nm, was measured for 30 s. The instrument automatically was set to repeat the entire process of dispensation/agitation/reading for each well, until all the inhibitors were tested. All measurements were carried out four times and the data analyzed by the software QtiPlot 0.9.8.9.

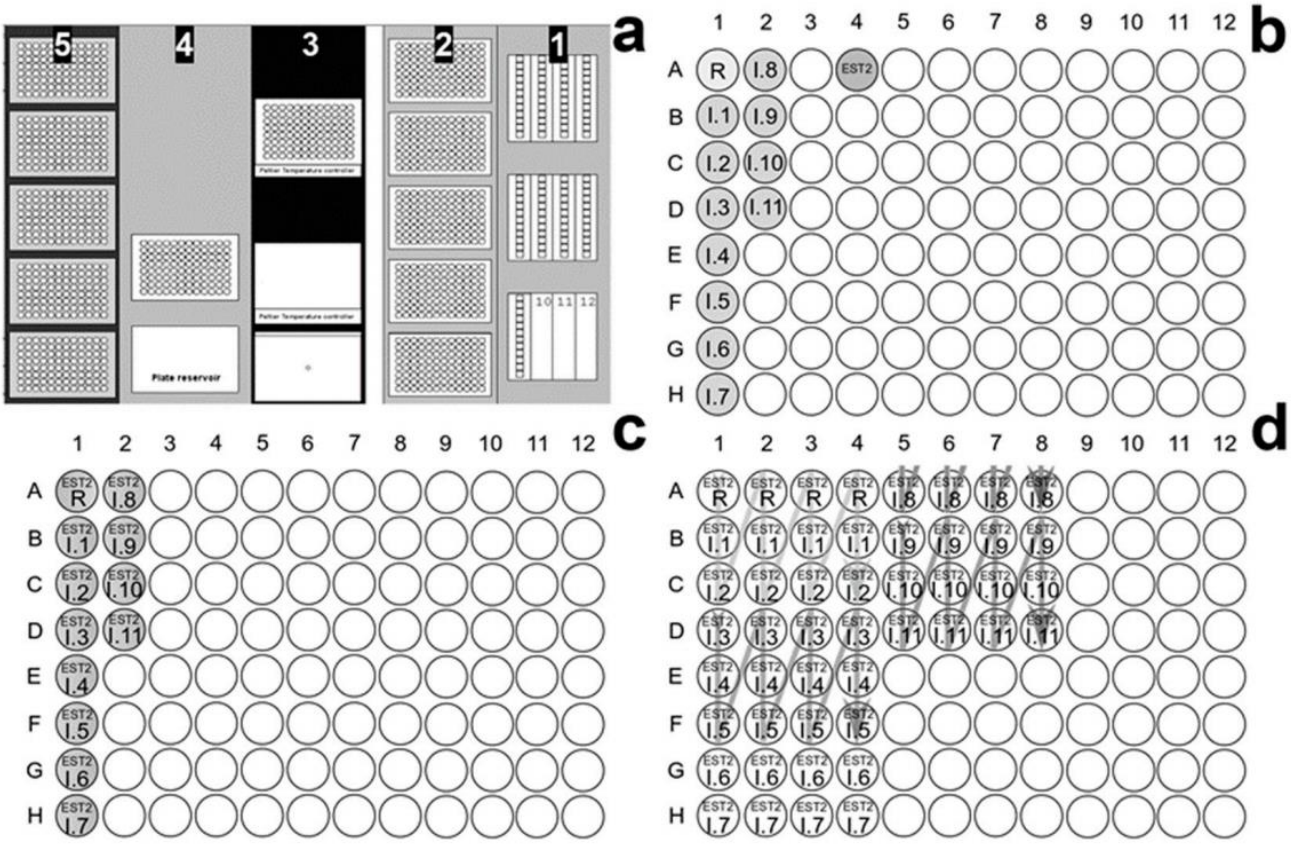

Figure 2.4. **Representation of the robotic workstation worktable and plates layout for the measurement of EST2 residual activity. (a) In the worktable column 1 the solvent reservoir carriers, in column 2 disposable tip carriers (10, 200, 1000 µL), in column 3 the stock solution and reagent plate in the temperature controller, in column 4 the incubation plate on the heated shaker, and in column 5 the plates for the enzymatic residual activity assays, were placed. (b) Plate placed in column 3 of (a), prepared by the operator manually, containing the enzyme (EST2) and the NBS treated OP inhibitors (I.1, I.2, … I.n) and a blank reference (R). (c) Plate in column 4 of (a), containing the incubation mixtures (enzyme-inhibitors) prepared by the robotic liquid handler. (d) Plate layout in column 5 for the assays of enzymatic residual activity, samples are divided in three groups for the assay of each mixture. The arrows indicated the direction of measurements for each group**

2.3.12. Collection of human urine and blood samples

All samples were collected in accordance with European ethical guidelines, and those who agreed to participate in this study provided written consent. Human urine samples were collected from two healthy adult volunteers in 50 mL sterile falcons. After centrifugation at 14,000 rpm for 10 min to remove particulate matter, all urine samples were used immediately after collection in the fluorescence experiments.

Human blood samples of 10 mL were collected from two healthy adult volunteers in a sterile tube. After 30 min to allow the blood to clot, serum was separated by centrifugation at 2000 rpm for 10 min and stored at 4 °C to be used in the fluorescence experiments.

2.3.13. EST2 residual activity in human urine

Aliquots of a urine sample in the concentration from 0 to 10 % were added to a solution (50 µL final volume) containing 1.46 pmol of EST2 in buffer 25 mM HEPES, pH 7.0, and incubated for 5 min at 25 °C. Aliquots of 45 µL were withdrawn from the mixture, and the activity of EST2 was then measured in the standard assay conditions in the presence of 1 mM 4-MUBu. All measurements were carried out at least three times, and the data were analyzed by the software QtiPlot 0.9.8.9 (Copyright 2004–2011 Ion Vasilief, IONDEV SRL - Bucuresti, Romania).

2.3.14. Paraoxon inhibition assay of EST2 in human urine

Aliquots of 1.46 pmol of EST2 were incubated in a solution (50 µL final volume) containing 4% urine in buffer 25 mM HEPES, pH 7.0, and increasing concentrations of paraoxon in the range from 0 to 2.1 pmol. After 1 min incubation, aliquots of 45 µL were removed from the mixture and the EST2 residual activity was measured in the standard assay conditions. All measurements were carried out at least three times, and the data were analyzed by the software QtiPlot 0.9.8.9 (Copyright 2004–2011 Ion Vasilief, IONDEV SRL - Bucuresti, Romania).

3. RESULTS AND DISCUSSION

3.1. Targeted suspect methodology – determination of anticoccidials

3.1.1. Sample extraction

During the initial stage of method development, a convenient sample preparation procedure for routine samples was optimized. Since poultry and eggs contain large amounts of problematic matrix components such as fats and proteins, some basic clean-up is mandatory. Considering the previous studies [89–95], acetonitrile was chosen as the extraction solvent and partitioning clean-up at moderately low temperature (0 °C) was applied.

3.1.2. Liquid chromatography

The selection of UHPLC method and the choice of specific conditions were influenced by previous studies [95–97]. First, we tested a gradient system of 0.5% formic acid in water and methanol systems [96], which led to a good overall performance, except for polyether ionophore anticoccidials that showed poor results, including notable tailing. A modified method developed by Pereira et al. [97] was found to be applicable in our case. Excellent peak shapes for all compounds were observed using a Hypersil Gold (50 mm × 2.1 mm, 1.9 μm particle size) column, but co-elution of some peaks occurred. A longer Kinetex C18 column (100 mm × 2.1 mm, 1.7 μm particle size) was chosen as a compromise. The selected gradient program produced excellent peak shapes and chromatographic separation, while also effectively removing the matrix components and thus reducing the noise level, decreasing the risks of carry-over effect, and minimizing column deterioration. During the method development, validation and sample analysis, the retention time of analytes did not deviate by more than ± 0.1 min.

A solution of acetonitrile-aqueous sodium acetate (5 mM) (30:70, v/v) was used as the injection solvent. Polyether ionophore anticoccidials are known to favor sodium adducts [95,98] and a significant increase in signal was observed. Another reason in favor of using this solution was the increased stability of analytes under mildly basic (pH = 7–8) conditions [95]. The injection volume of 4 μL was found to be satisfactory for balancing the sensitivity and selectivity of the method.

3.1.3. MS conditions

TOL, TOLS, and TOLX did not produce suitable fragment ions while using the electrospray ionization interface. Previous studies have shown that the confirmatory fragmentation criteria for these three compounds can be met by MS systems operating in atmospheric pressure chemical ionization mode [99]. In our work, however, the confirmation of species derived from TOL was possible by using

full scan spectra and confirming the presence of monoisotopic target ions with the expected isotope pattern and applying a narrow (10 ppm) window of mass tolerance to all the aforementioned species.

3.1.4. Optimization of MS parameters

The responses were assessed as absolute peak areas in arbitrary units. A series of diagnostic tests (e.g., residual normal probability test, residuals vs. run order, histograms) did not indicate the presence of any significant outliers which would indicate experimental errors for any of the statistical DoE. BBD and OFAT optimization parameters are shown in Table 2.2. The analysis of variance (ANOVA) results for all the factor interactions along with the final coefficients for BBD equations in terms of actual and coded response factors regarding all the analytes both for the ion generation region and the optimization of analyzer are available upon request.

Source conditions

The HESI source factors exerting significant effects on the MS response were identified through simultaneous batch screening and optimization experiments using a BBD model. Five main source parameters – the sheath (A) and auxiliary (B) gas flow rates, spray voltage (C1 for positive and C2 for negative ionization), capillary (D) and auxiliary gas heater temperatures (E) were considered as independent variables. A wide range of values were chosen and the original Orbitrap software auto-tune settings were selected as the center point of BBD. The BBD models showed a good fit for most of the compounds analyzed, with $R^2 > 0.9$ in most of the cases. Significant lack-of-fit was observed for MAD ($p < 0.001$), MON ($p < 0.001$), and NAR ($p < 0.05$), indicating that the model did not fit the data within the observed variations among replicate samples. The fit values were insignificant for other compounds, showing a good fit with the experimental model. The terms were found to be significant at 95% confidence interval with the p values of the F-test being lower than 0.05 (statistically significant) or 0.001 (statistically highly significant).

The experimental study showed differences in the most significant parameters depending on the ionization modes used. For all the compounds analyzed in positive ionization mode, ANOVA allowed to identify three parameters (A, B, and C1) and the corresponding linear terms that most affected the response with a high statistical significance ($p < 0.001$). Four out of 11 compounds were also significantly affected by parameters D and E. As for the squared interactions, 9 compounds out of 11 showed significant ($p < 0.05$) interaction for A^2, 5 compounds out of 11 for B^2, 4 compounds out of 11 for $C1^2$ and D^2, and E^2 was found to be significant for HAL. Response surface curvature was found for some 2-way interactions and ANOVA confirmed the significance of BC (auxiliary gas flow × spray

voltage) interactions for 7 compounds, as well as AB, AD, AE, and BD interactions for 2 compounds. The AC, BE, and DE interactions were significant for only one compound in each case.

The significance of the linear term A in the case of negative ionization was observed with 5 compounds out of 6, and 4 compounds out of 6 for the term C. The linear terms of B, D and E had a significant impact on individual compounds. The squared interaction of C2 2 was evident for 3 compounds out of 6, while A2 and D2 affected 2 compounds. Statistically significant ($p < 0.05$) and visible (surface curvature) 2-way interactions were AB and AE for 3 compounds out of 6; BC for 2 compounds out of 6; AC and DE for 1 compound each.

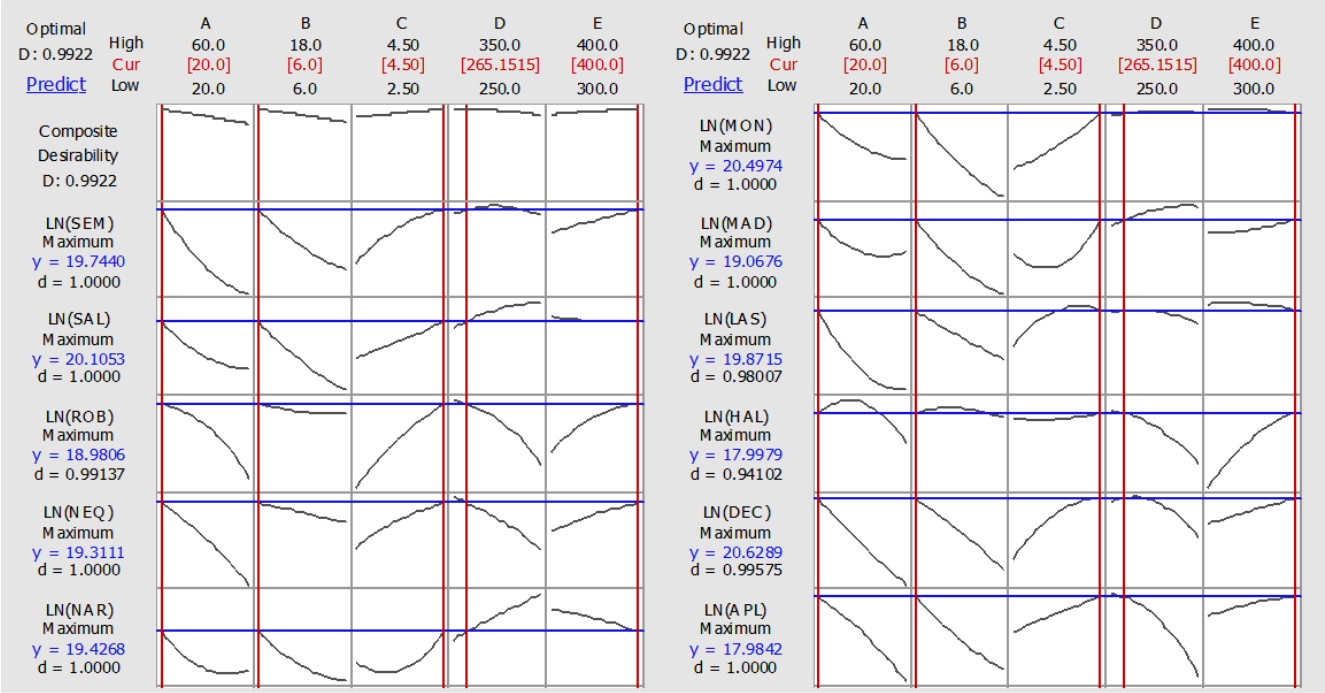

Figure 3.1. **Desirability plots for optimization of HESI source conditions in positive ionization**

The optimal source parameter values were established separately for positive and negative ionization by using the integrated response optimizer function (Figures 3.1 and 3.2). The target compound responses were optimized simultaneously with the goal to maximize the intensities and to achieve the highest composite desirability. The overall value of composite desirability combines the individual desirability of compounds and reflects the relative importance of the responses. The higher the desirability, the closer it is to 1 (measured on a scale from 0 to 1). Composite desirability of 0.9922 was achieved in positive ionization mode and 0.9135 in negative ionization mode for 11 and 6 target compounds, respectively. The maximum simultaneous responses for all compounds in positive ionization mode were obtained with the following parameters: sheath gas flow rate 20 a.u., auxiliary gas flow rate 6 a.u., capillary voltage + 4.5 kV, capillary temperature 265 °C, auxiliary gas heater temperature 400 °C.

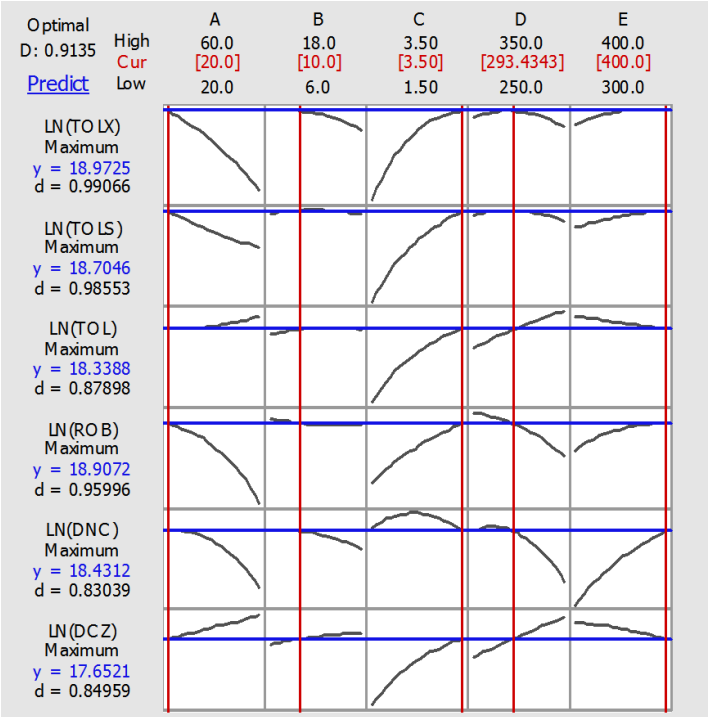

Figure 3.2. **Desirability plots for optimization of HESI source conditions in negative ionization**

The finalized parameter values in negative ionization mode were: sheath gas flow rate 20 a.u., auxiliary gas flow rate 10 a.u., capillary voltage −3.5 kV, capillary temperature 293 °C, auxiliary gas heater temperature 400 °C. The desirability contour plots for anticoccidials and their residues analyzed in positive and negative ionization modes are shown in Figures 3.1 and 3.2, respectively. Another way to interpret the data is shown in tables provided in Annexes 2 and 3, which contain center point levels of source variables for methods used in the optimization and the resulting relative responses and RSD values for HESI ionization source conditions according to the BBD design.

Orbitrap detector conditions

The AGC values were expressed as decimal logarithms as they differed from each other by a factor of 10 (Log(G), further G) and the resolution values were normalized using natural logarithm so the difference between the levels was constant (Ln(F), further F). Center-reducing the data yielded [−1; 0; +1] values that were expected to fit in the BBD levels. The rest of the variables for the MS system, which were found in the previous steps, were set at the values optimized for these experiments.

The BBD models did not fit as well for the factors associated with the mass analyzer as for those of the ionization source, with generally lower R^2 values observed. Significant ($p < 0.05$) lack-of-fit was observed for APL, CLOP, MON, while the lack-of-fit was very significant ($p < 0.001$) for DEC and NEQ. Otherwise, the statistical model performed quite well. The terms were found to be significant at

95% confidence interval, with the p values of the F-test being lower than 0.05 (statistically significant) or 0.001 (statistically highly significant).

Yet again, various parameters affected the response, depending on the ionization modes used. The BBD models revealed that the most significant linear term affecting the response in positive ionization mode was resolution ($p < 0.001$ for 7 compounds out of 11; $p < 0.05$ for 3 compounds; no significance of resolution setting for 1 compound). Among the squared terms, F^2 was found to be significant ($p < 0.001$ for 7 compounds; $p < 0.01$ for 1 compound; $p < 0.05$ for 3 compounds) and the 2-way term of FG showed the p-values of < 0.01 for APL and DEC and < 0.05 for SEM.

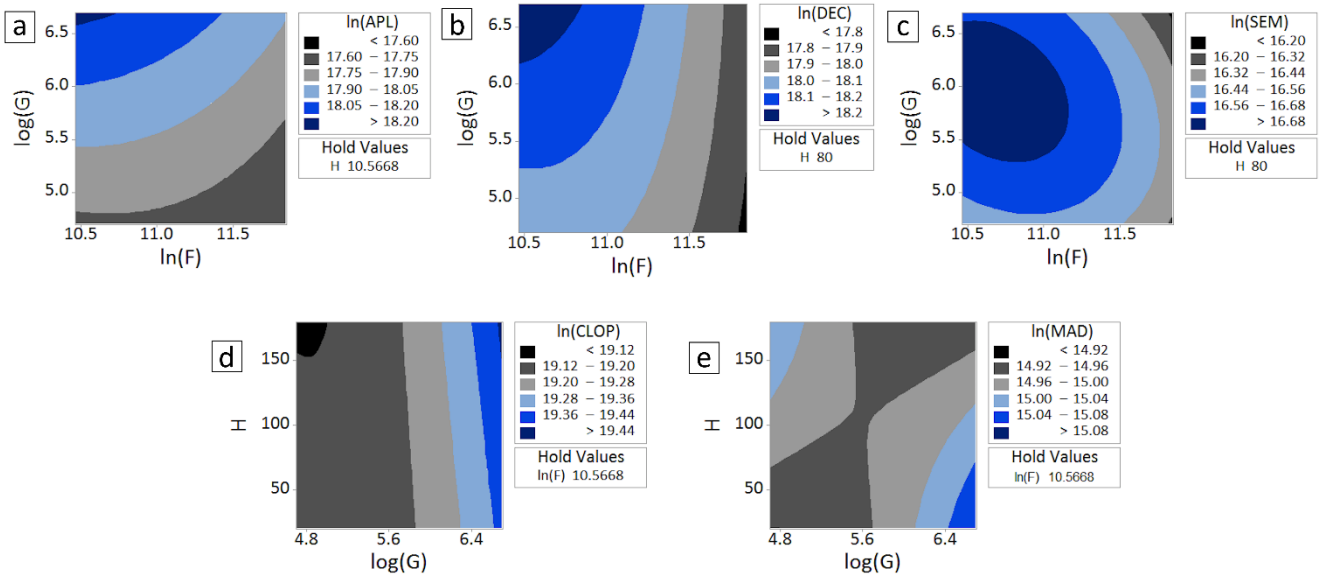

Figure 3.3. **Contour plots illustrating the most significant interactions of parameters and their effects on the Orbitrap detector response, where dark blue area represents the highest response. Plots: (A) – APL signal response plotted versus resolution (ln(F)) and AGC (log(G)) value, (B) – DEC vs ln(F), log(G), (C) – SEM vs ln(F), log(G), (D) – CLOP vs log(G), injection time (H), (E) – MAD vs log(G), H**

The terms G and G^2 were found significant for 4 compounds with *p*-values <0.01. The 2-way interaction of GH was significant for CLOP and MAD, with the *p*-values of <0.05 and <0.01, as shown by the contour plots of interactions in Figure 3.3 D and E, accordingly. Longer injection times were favored in the case of CLOP, but not in the case of MAD, as it can be seen both in the Figure 3.3 contour plot E and Figure 3.4 desirability plot.

For compounds analyzed in the negative ionization mode, the change of terms had barely any effect on the total response according to ANOVA. ROB was the only compound affected by the linear terms of F and G, the squared terms of F^2 and G^2, and the 2-way term FG ($p < 0.001$). As a matter of fact, the collection time of ions or the injection time (H) in both the positive and negative ion modes

had no significant influence on the signal intensity. C-trap typically reached the AGC target value in fewer milliseconds than set, before the time interval allotted for ion gathering. This observation conforms with the findings by Lemonakis et al. [100] who showed that suppression effects can occur in an Orbitrap MS analyzer in the presence of a difficult matrix with barely any clean-up.

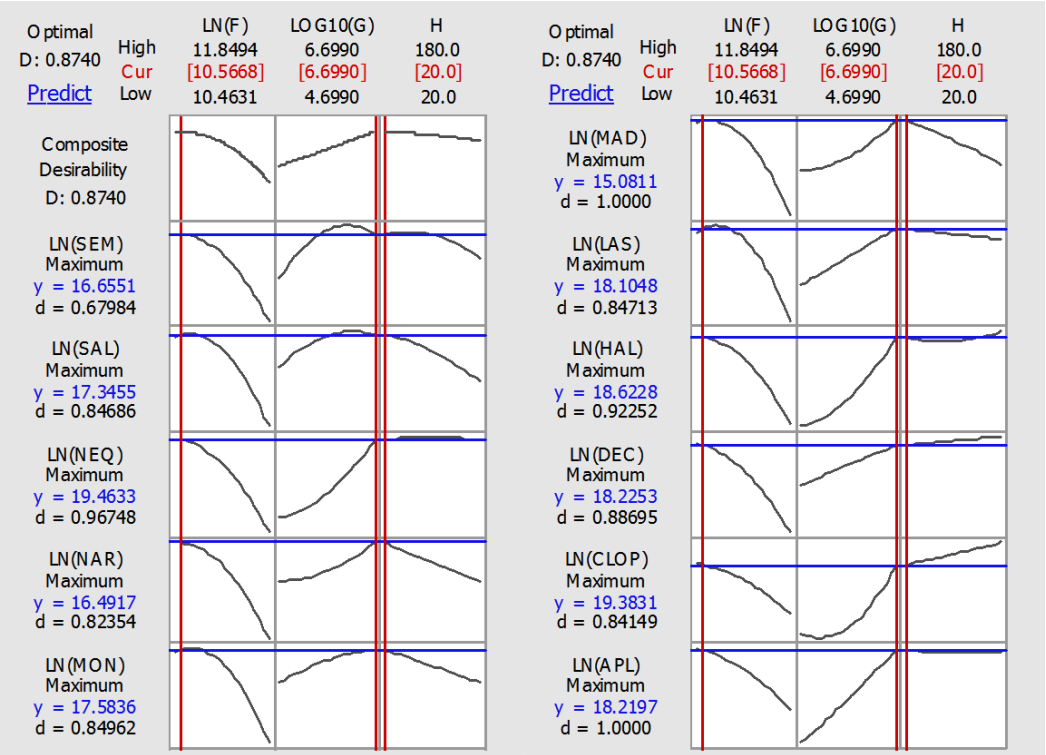

Figure 3.4. **Desirability plots for optimization of Orbitrap detector conditions for compounds analyzed in positive ionization**

The optimal values were established separately for the positive and negative ionization modes, as two separate runs were required for the analysis. The target compound responses were optimized simultaneously with the goal to maximize the signal intensities and to achieve the highest composite desirability. The composite desirability was achieved with a desirability coefficient of 0.8740 in the positive ionization mode and 0.8386 in the negative ionization mode for 11 and 6 target compounds, respectively. The optimization results were quite similar for both ionization modes – the response was the highest when the resolution was kept low (35 000 FWHM), the AGC was set to represent the maximum loading capacity of the C-trap (target of $5 \cdot 10^6$ ions), and IT was kept low (20 ms for positive and 26 ms for negative ionization). The effect of resolution on the Orbitrap sensitivity was an interesting finding that was backed up by statistically significant experiments. A plausible explanation could be the loss of ion energy during the travel time and distance, which is more pronounced at high resolution. This observation could be particularly relevant when trying to achieve the required MRLs for specific compounds at low concentrations. We did not find a correlation between the mass to

charge ratios of particular compounds and the observed effect and additional studies may be needed to further explore this phenomenon. If the aim is to look for a specific analyte in a pool of isobaric compounds, the selectivity still can be improved by using fragmentation mode transitions to compensate for the relatively low resolution.

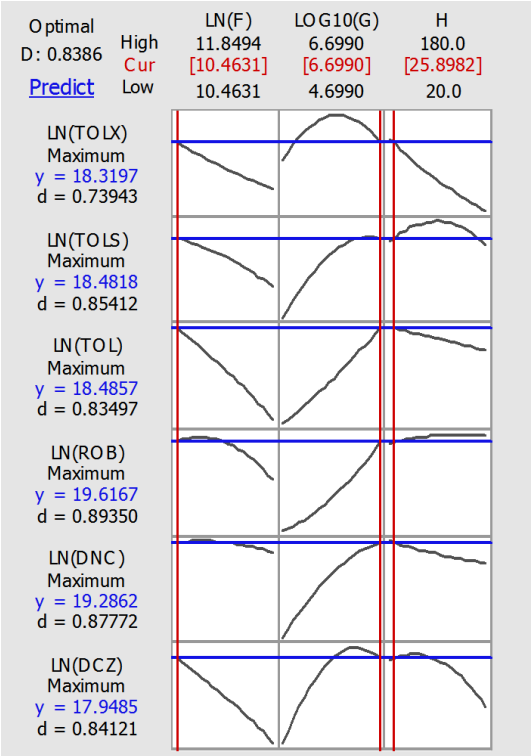

Figure 3.5. **Desirability plots for optimization of Orbitrap detector conditions for compounds analyzed in negative ionization**

The desirability contour plots for Orbitrap detector optimization are shown as Figures 3.4 and 3.5 for anticoccidials and their residues analyzed in the positive and negative ionization modes, respectively. Annex 4 contains a table with methods and levels with the corresponding relative responses and RSD values used for the optimization of Orbitrap detector conditions using the BBD design.

Optimization of the ion injection time in the presence of matrix

The injection time was further optimized by the means of OFAT experiments through a stepped increase of injection time over the range from 20 ms to 180 ms, same as previously done in BBD experiments, but this time including the food matrix. Poultry and egg samples spiked at 20 µg kg^{-1} level were analyzed in five replicates for each injection time. The values were normalized against the responses obtained for injection time of 20 ms (Figures 3.6 and 3.7).

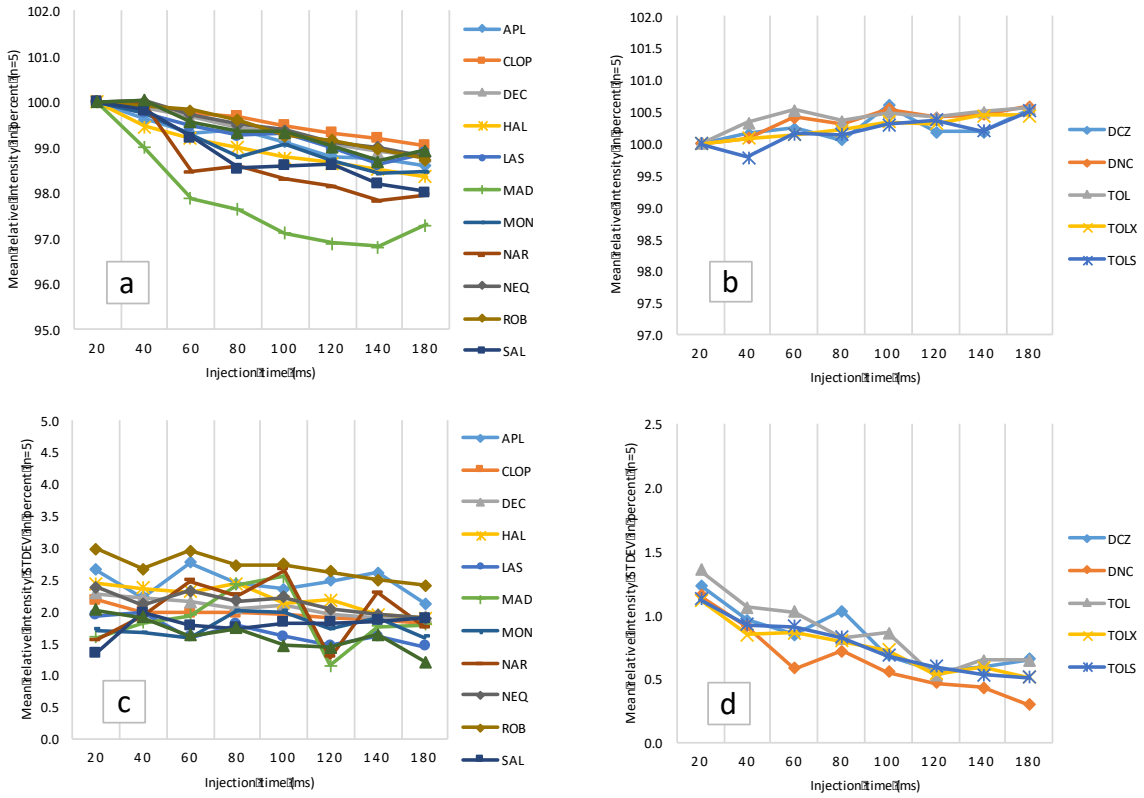

Figure 3.6. **Influence of injection time in presence of egg matrix; a, b – relative intensities, c, d – corresponding RSD values**

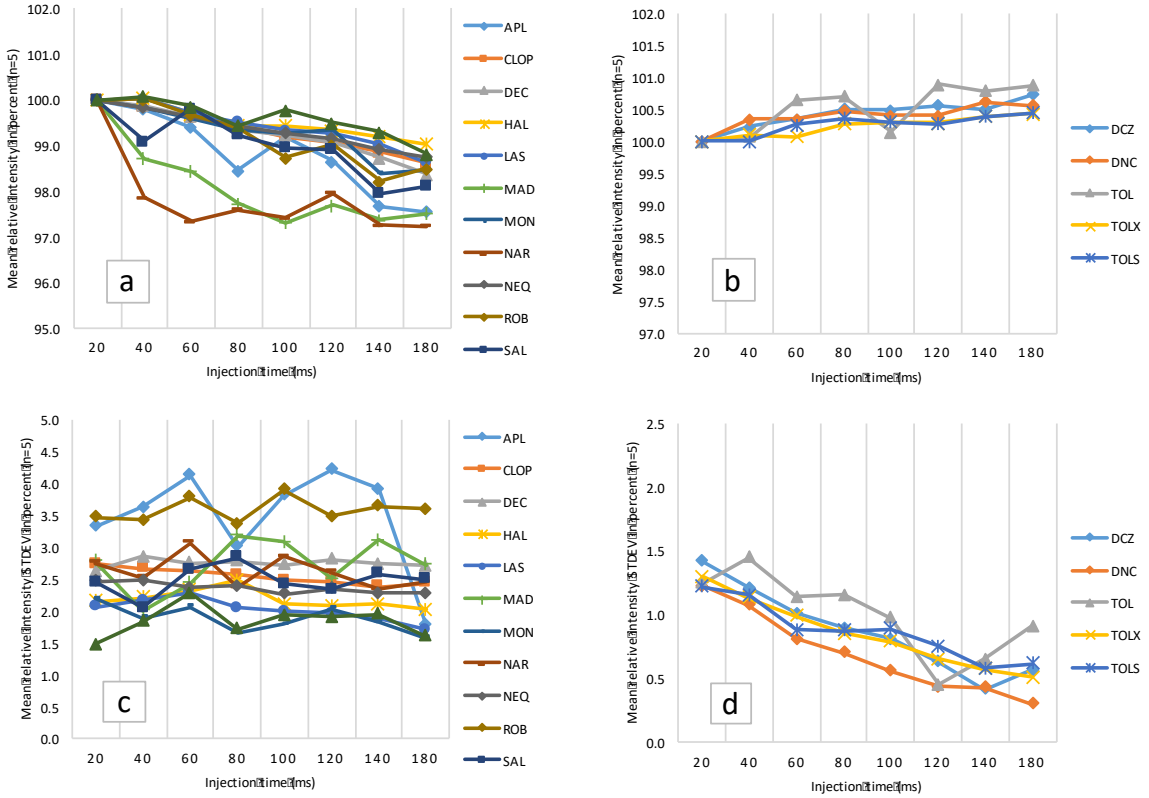

Figure 3.7. **Influence of injection time in presence of meat matrix; a, b – relative intensities, c, d – corresponding RSD values**

The observations for egg and poultry matrices were the same. In positive ion mode, a small suppression of signal was observed ranging from 0.5 to 3%, with the RSD values not significantly influenced by the change of injection time. On the other hand, a small but notable increase of signal by 0.5% occurred in negative ion mode for all the analyzed compounds, while the RSD also tended to vary less. In the presence of egg matrix, the compound most affected by the injection time was MAD, due to the particularly strong signal of co-eluted unidentified matrix components observed in TIC. Short injection times (20–40 ms) produced jagged peaks and occasionally even loss of signal, so we preferred 80 ms injection time both for the positive and negative ionization modes.

Optimization of data-dependent acquisition

Data-dependent scans were introduced as a source of fragmentation criteria and used to further reduce the chance of false positive results. The ddMS^2 events occur when there is a precursor ion detected in the full scan measurement. The following scan cycles include the fragmentation scan events of the detected precursors. A single data-dependent scan provides full scan spectra of an isolated and fragmented precursor ion, which contains confirmatory fragment ions. Rajski et al. described the overall FS-ddMS^2 workflow superiority over other confirmation modes, with greater repeatability at low concentration levels and equal selectivity than that of targeted single reaction monitoring (SRM). It was also superior to other non-targeted Orbitrap methods (all ion fragmentation (AIF) and variable data-independent analysis (vDIA)) [2]. Similar work has been done by Kumar et al. [101].

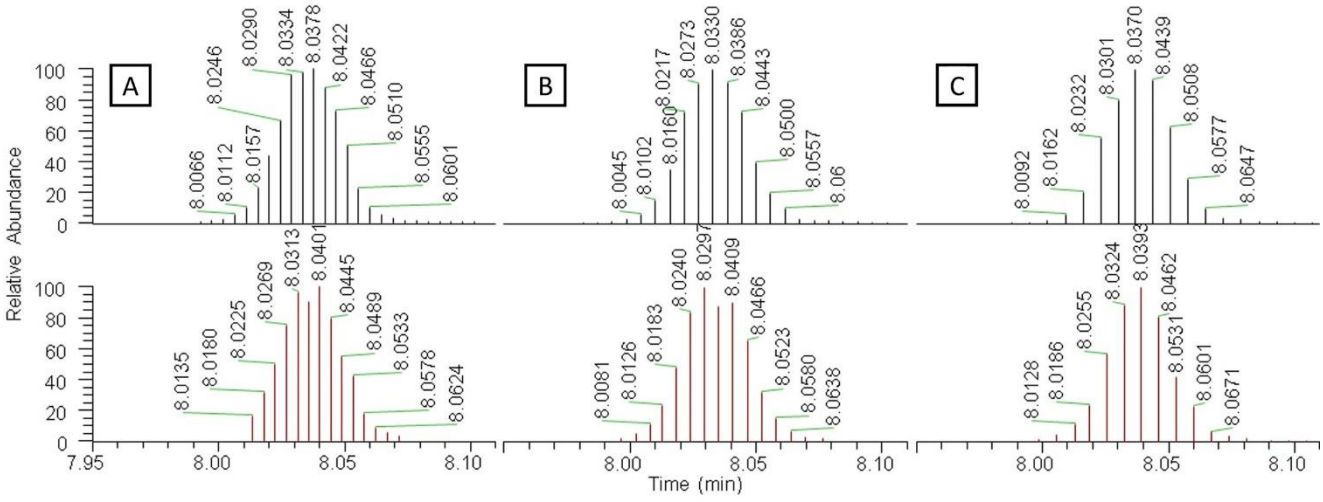

Figure 3.8. **The effect of ddMS^2 method loop count (N) on the number of scans per peak in full scan (first row) and data-dependent MS^2 (second row). Loop count: (A) – 1, (B) – 2, (C) – 3**

The ddMS^2 procedure was optimized by taking account the number of co-eluting analytes, which correspond to the parameter *N* in Top *N* approach. Since the maximum number of co-eluting analytes was 2 and the other analytes were baseline separated, the loop count was set to 2, thus making the method a Top 2 approach. The number of scans acquired per very narrow 3.2 s peak of SAL using a Top 2 approach is illustrated in Figure 3.8B. The total scan cycle time was 340 ms, allowing for one full scan and two fragmentation scans per cycle. The peak was covered by 9 full scans for quantitative purposes and 9 fragmentation scans for qualitative purposes. When the loop count was set to 1, the Q Exactive instrument prioritized the ddMS^2 scan for the precursor ion of the highest intensity (Figure 3.9).

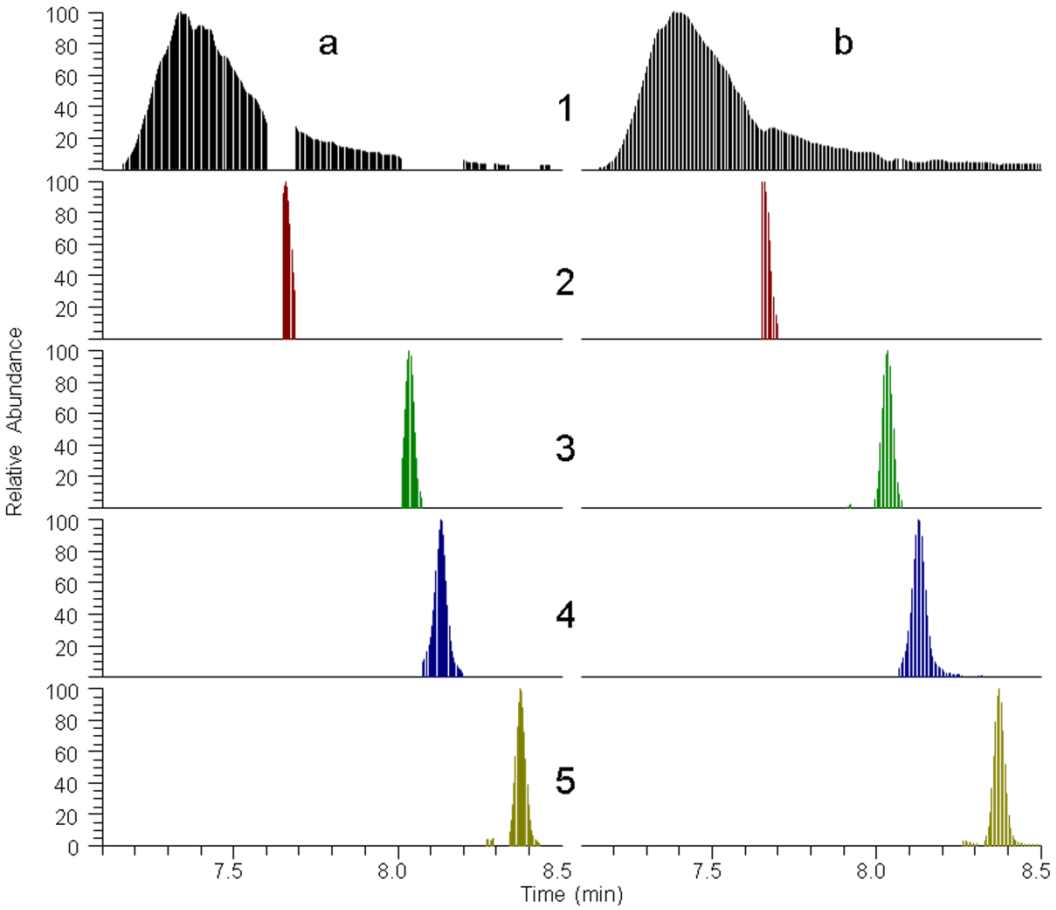

Figure 3.9. **Co-elution of peaks vs. Selected loop count. Columns: A – 1 loop, B – 2 loops. Rows: 1 – DEC, 2 – MAD, 3 – SAL, 4 – MON, 5 – NAR**

In the case of signal overlap between different compounds, this feature increased the chance of missed confirmatory scans. Thus, even though more scans were acquired, there was a slight chance of a false negative result. It should be noted that the ddMS^2 data can also be used for quantitation purposes in the case when full-scan interference is present. Figure 3.10 illustrates the scheme of FS-

ddMS^2 data acquisition and gives an example for the achieved selectivity of DNC and SAL, in positive and negative ionization modes, accordingly.

The ddMS^2 workflow also enabled the specificity needed for confirmation using the ion ratios. The non-targeted fragment acquisition modes such as AIF and vDIA were susceptible to altered ion ratios in the presence of isobaric fragmentation ions, while the selectivity of ddMS^2 was improved tremendously due to the narrow (0.6 *m/z*) isolation window of quadrupole. The known fragmentation patterns of precursor ions enabled the use of intensity ratios of two fragment ions determined in preliminary experiments as confirmation criteria.

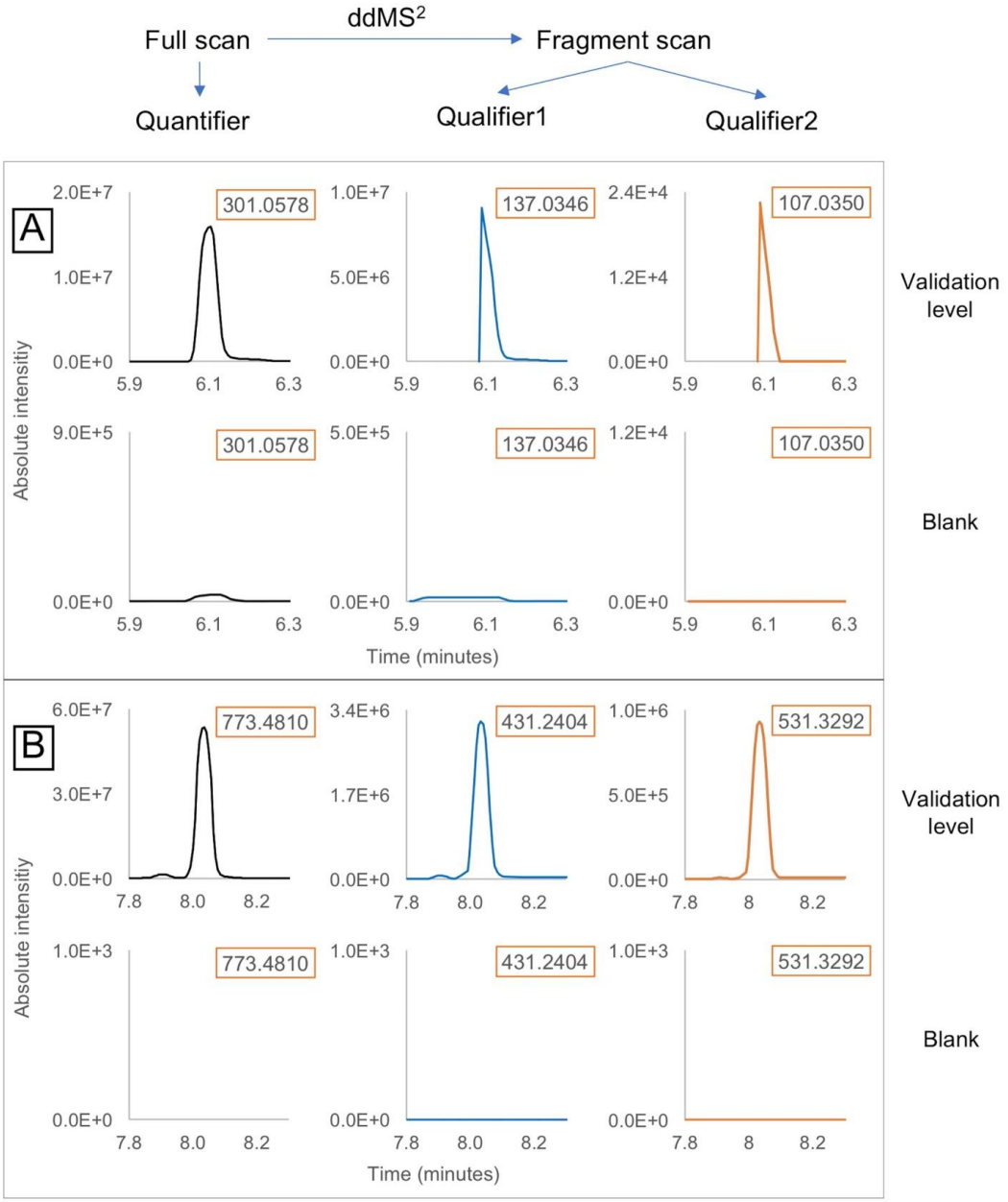

Figure 3.10. **Scheme of FS-ddMS^2 data acquisition. Extracted ion chromatograms for quantifier and qualifier ions for DNC (A) and SAL (B) at the validation and blank concentration levels in egg matrix are displayed**

The isolation of fragment ions was performed by the means of inclusion list of specified target compound masses, retention times, and compound-specific collision energies. The data-dependent scan was set to trigger when the accurate mass of precursor ion was detected within the bounds of 10 ppm. The fragment ion ratio measurements during the method development, validation and sample analysis were within ± 20% from the original ratios observed in the standard solutions, thus the HCD-induced ddMS^2 fragmentation was deemed to be a suitable confirmatory tool. Table 3.1 contains the calculated ion ratios within the ddMS^2 scanning mode, observed in the standard sample analysis.

Table 3.1

Ion ratios of the investigated compounds within the ddMS^2 scans

	Relative abundance (%)			Ion ratio	
	Quan	Ion 1	Ion 2	(Ion 1 / Precursor)	(Ion 2 / Precursor)
APL	2	100	35	50	18
CLOP	47	100	91	2	2
DEC	4	100	21	25	5
DCZ	8	100	10	13	1
HAL	4	100	53	25	13
LAS	6	100	41	17	7
MAD	1	100	6	100	6
MON	10	100	95	10	10
NAR	7	100	42	14	6
NEQ	9	100	7	11	1
DNC	1	100	8	100	8
ROB	4	100	85	25	21
SAL	7	100	42	14	6
SEM	4	100	14	25	4
TOL					
TOLS				-	
TOLX					

Results of the optimization

Numerical optimization steps led to an impressive overall signal improvement for most of the compounds, even in the presence of either poultry meat or egg matrices. Repeated analysis of spiked (20 µg kg^{-1}) sample extracts showed 10–99% increase of signal intensity for 16 out of the 17 anticoccidials, as illustrated in Figure 3.11 a minor (10%) decrease of signal intensity was observed for HAL, but it was more than compensated by the significant gains of sensitivity obtained for other analytes.

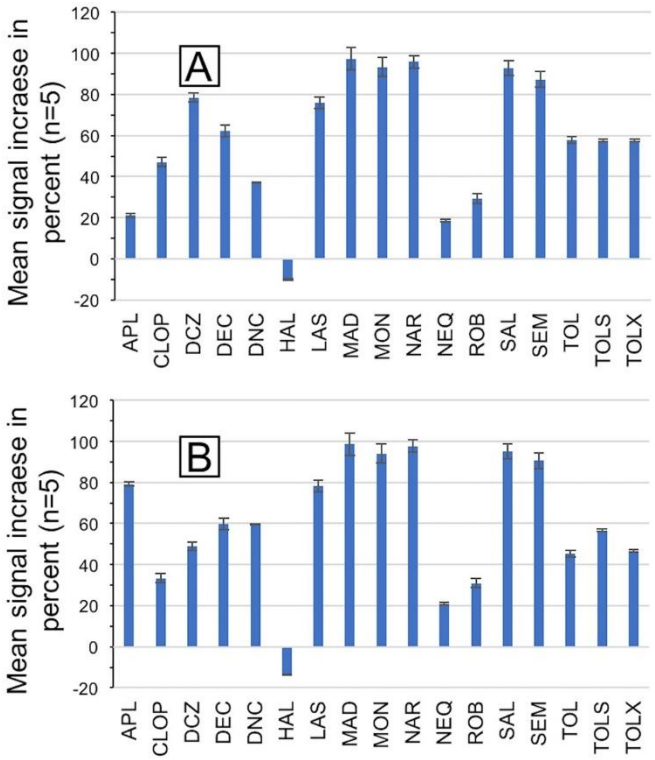

Figure 3.11. **Mean signal increase after the performed optimization procedures; (A) – spiked (20 µg kg^{-1}) egg sample, (B) – spiked (20 µg kg^{-1}) poultry meat sample**

3.1.5. Analytical method validation

The optimized methodology was validated to confirm its applicability for routine analysis of samples and to assess the reliability of results. The parameters evaluated were repeatability, within-laboratory reproducibility, recovery, selectivity, CCα, and CCβ. The results of this validation fulfilled the defined validation criteria and are summarized in Table 3.2. The recovery was corrected using isotopically labeled internal standard addition and matrix calibration to account for possible matrix effects. After the additional selectivity evaluation experiments, no significant interference was observed at the expected retention time of analytes after the analysis of negative samples (n=20 for eggs, n=5 for poultry meat). The final sample extracts were found to be stable for 2 days, after which the recoveries for some of the analytes dropped below 80% when compared to freshly prepared sample extracts. The results are in agreement with those of Spisso et al. [95].

Overall, the method covered a wide and unique range of analytes, with only a couple of previously published methods providing such scope for the analysis of multiclass anticoccidials in poultry and eggs.

Table 3.2

The validation results for fortified egg and poultry meat samples

	Egg matrix							Poultry matrix						
	MRL/ML level (µg kg^{-1})	[a] RSD S_r (%)	[b] RSD S_{wR} (%)	Corrected recovery (%)	Total uncertainty [c] at VL (%)	CCα (µg kg^{-1})	CCβ (µg kg^{-1})	MRL/ML level (µg kg^{-1})	[a] RSD S_r (%)	[b] RSD S_{wR} (%)	Corrected recovery (%)	Total uncertainty [c] at VL (%)	CCα (µg kg^{-1})	CCβ (µg kg^{-1})
APL	10	8.4	10.3	96.8	10.5	12	15.8	50	6.9	8.6	101.9	8.7	58.5	73.6
CLOP	10	20.3	20.9	97.7	21.3	13.8	> 20.0	50	5.4	10.8	99.2	11.3	62.8	90.2
DEC	20	14.5	15.3	96.3	15.6	26.2	37.6	500	5.5	7.7	105.2	7.8	577	721
DCZ	2	11.8	12.8	105.8	13	2.54	3.54	500	8	9.4	100.8	9.5	589	749
HAL	6	5.5	7.5	97.2	7.5	6.79	8.21	10	5.5	7.5	99.2	7.5	11.4	13.9
LAS	150	10.4	11.6	97.8	11.8	183	255	60	11.8	13.4	102	13.6	77.9	109
MAD	2	15.6	16.4	99.2	16.8	2.64	3.78	2	19.4	20.1	91.6	20.4	2.64	3.74
MON	2	2	5.4	100.5	5.4	2.2	2.58	8	12.6	13.6	97.3	13.8	9.95	14.2
NAR	2	13.5	15	99.9	15.3	2.55	3.52	50	6	8.4	102.6	8.5	58.4	75.1
NEQ	10	6.8	8.6	99.5	8.7	11.6	14.4	10	6	7.8	105.7	7.9	11.5	14.1
DNC	300	3.6	6.1	101.2	6.2	336	401	50	3.6	6.2	104.4	6.3	56	67.2
ROB	25	8.9	10.2	102.9	10.4	30.1	39.3	200	7.3	9.7	99.9	9.9	238	310
SAL	3	12.7	13.6	101.2	13.9	3.77	5.13	5	9.4	11	99.1	11.2	5.97	7.79
SEM	2	19.7	20.7	94.1	21.1	2.71	3.96	10	14.3	15.1	97.2	15.4	12.9	17.9
TOL	10	1.4	5.2	101	5.2	12.5	12.9	100	1.2	5.1	100.2	5.2	110	129
TOLS	10	11.7	12.8	102.9	13	12.5	16.9	100	7.9	9.4	101.5	9.5	118	150
TOLX	10	10	11.2	99.6	11.4	12.2	16	100	7.4	8.9	102.5	9	117	147

[a] RSD S_r - repeatability

[b] RSD S_{wR} - within-laboratory reproducibility

[c] Total uncertainty takes into account the within-laboratory reproducibility standard deviation and additionally the uncertainty of recovery correction

3.1.6. Method applicability

The present method has been applied to eighty-one egg samples and three poultry muscle samples over a 5-month time, as a part of the 2017 Latvian national monitoring program. The results are displayed with uncertainty. One egg sample was found to be non-compliant, with 102 ± 7 μg kg^{-1} concentration of TOLS, along with TOL and TOLX at the levels of 10.2 ± 0.5 and 4.0 ± 1.1 μg kg^{-1}, respectively. The same sample contained DNC at the level of 10.1 ± 4.1 μg kg^{-1}. Among the rest of the samples, five contained the target compounds at levels lower than the MRL. DNC was found in 3 samples at the levels of 1.4 ± 0.6, 49 ± 6, and 133 ± 11.9 μg kg^{-1}. Another two samples contained TOL and its metabolites. The first sample contained 7.0 ± 1.2 μg kg^{-1} of TOLS, 1.9 ± 0.4 μg kg^{-1} of TOL, with trace levels of TOLX detected. The second sample contained 2.9 ± 1.4 μg kg^{-1} of TOLS and trace levels of TOL and TOLX. One sample contained 2.4 ± 0.4 μg kg^{-1} of SAL and 1.8 ± 0.3 μg kg^{-1} of NAR.

3.2. Non-target methodology application for a case study of food contact materials

3.2.1. Data acquisition and processing

A total of 17 samples in each extraction solvent, two negative control samples and two extraction solvent samples were analyzed in the initial screening experiment, resulting in 38 data files. After the identification experiments, the LC-HRMS analysis resulted in 114 data files to be deconvoluted by the "Detect Unknown compounds" node of Compound Discoverer.

A total of 21'380 unique chromatographic peaks were extracted from the data files. After the subtraction of negative control samples, the number of candidates was reduced to 18'432. To exclude the candidates that could later present difficulties in structure elucidation, the candidates were filtered based on the peak area. The candidates with peak areas of less than 500'000 were excluded, as isobaric compounds in full scan spectrum can mislead the accuracy of formula prediction based on isotope pattern. Also, area (max.) > 500'000 was necessary to acquire MS/MS spectra as low intensity of precursor ion signals results in low quality of fragmentation spectra. The area cutoff gave the largest reduction of suspects to 2817 (84.7% reduction). Additionally, masses with retention times less than 1 minute were excluded to avoid the compounds that elute with the void volume and form unresolvable peaks.

The remaining peaks were searched against the databases and yielded 279 assigned peaks across all samples. Hits against any of the compounds on the mass list were registered in the inclusion list for the identification experiment. The most useful reference was the Thermo native EFS database (Figure 3.12), with 114 unique mass hits that also matched the molecular formula composition. Other

notable hits were 49 hits from the SIN database, 51 hits from the endocrine disruptor database, and ESCO printing inks database with 52 mass hits.

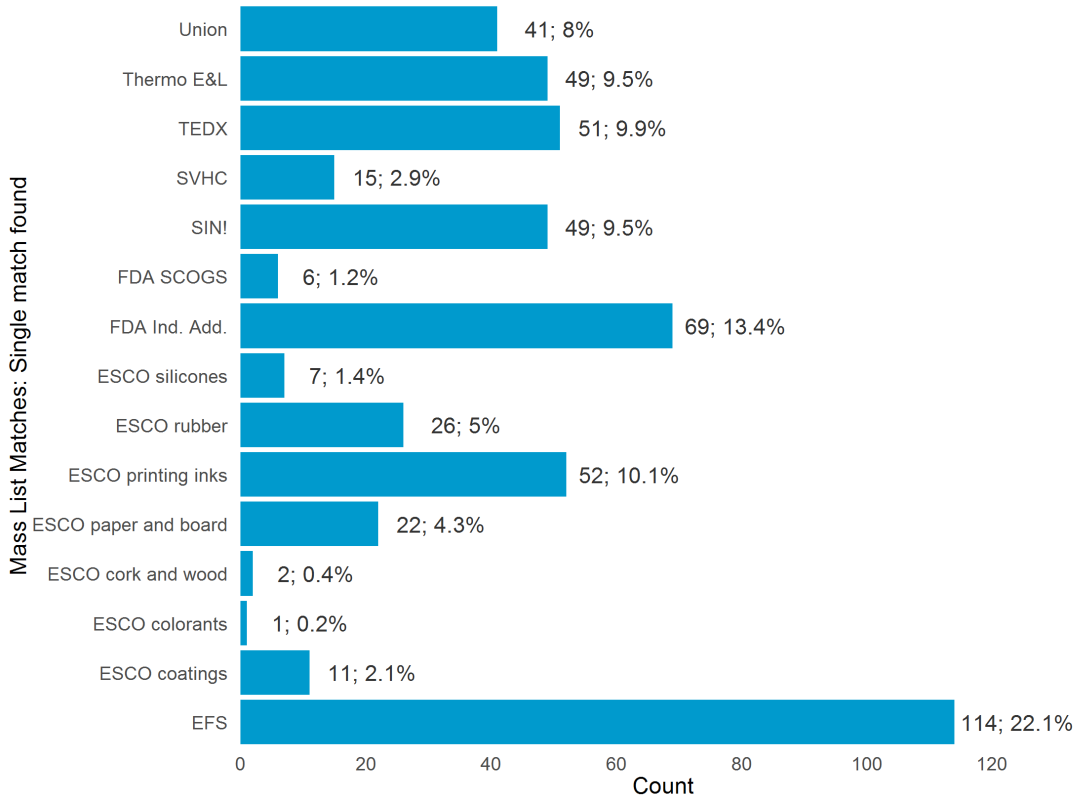

Figure 3.12. **Hits of the monoisotopic mass search *vs.* mass lists**

The assigned peak isotope patterns and peak intensities were inspected against the predicted molecular composition. The predicted compositions node in Compound Discoverer lists the possible chemical formulas based on the accurate monoisotopic mass values. Full match was achieved for 209 compounds. Goodness of fit was evaluated for the predicted compositions by enabling strict criteria of SFit > 80%. SFit is a value which resembles the spectrum fit to the proposed molecular formula. This function compares the mass shifts and intensities of the centroids in the isotope pattern for the detected compound to a set of defined mass shifts and relative intensities. The fit range is from 0 to 100%, with a higher value given for a better fit. Altogether, 31.6% of the 209 remaining peaks were excluded, with 143 compounds left to be identified. Systematic filtering or data reduction strategies are critical for prioritizing the most relevant masses or compounds in the samples on which the effort should focus for subsequent identity assignment. In our study we have efficiently used the filtering strategy to refine the valid chromatographic peaks resulting in a total of 0.67 % of the initial features. The filtration steps taken for candidate list pruning are briefly covered in Table 3.3.

Table 3.3

Reducing the number of candidates by various filtering steps

No	Filtering step	Number of candidates	% filtered out
	Total Peaks	21380	-
1	Background, negative control subtraction	18432	13.8
2	Area (max.) > 500’000	2817	84.7
3	Retention time > 1 min	2500	11.3
4	Mass list match	279	88.8
5	Predicted compositions – Full match	209	25.1
6	Predicted compositions – SFit > 80%	143	31.6
7	Reference spectra available	37	-
8	*In silico* match successful	74	-

3.2.2. Identification of migrating compounds - method performance

Of the 143 remaining candidates, 74 candidates were assigned with a unique molecular formula composition. Of these, 23 candidates were with more than one isobar and 51 with a single detected isobar. For the molecular formulas with more than one isobar, only level 3 and 4 identification was possible. However, for most of the compounds with only one isobar present, level 2 or 3 confidence was assigned.

In total, the methodology yielded a list of 40 compounds annotated at the highest level of confidence possible without reference standards and for all of them a plausible structure was assigned. The suspects identified at the level 2 are summarized in Table 3.4. For a full table containing all the tentatively identified compounds, as well as a table listing the corresponding linked spectra matches to the libraries and the search results from batch MetFrag query, the readers are welcome to refer to the Supplementary workbook of published online version of the FCM article [102].

The levels of confidence for the suspects were based on multiple criteria:

- presence of reference MS/MS spectra;
- agreement of *in silico* predictions between MetFrag and SIRIUS;
- high structural similarity in SIRIUS;
- not being an outlier according to the retention time model;
- no interference from isobaric compounds (instant downgrade of confidence to level 3);
- the substance is known to be used in the manufacture of paper FCMs.

Table 3.4

List of candidates of the highest confidence levels, confirmed by library spectra and/or *in silico* fragmentation prediction match

ID	Compound	CASRN	Unequivocal molecular formula	Presence across suspect lists*	Confidence level	Substance classification	Use in FCM manufacture***	Occurrence in paper FCMs, bibliographical reference
#1	1,4-Dihydroxybenzene	123-31-9	$C_6H_6O_2$	8/15	2ab	IAS**	Coloring Additive, Photosensitive Chemical	[103]
#2	2-Methyl-4-isothiazolin-3-one	2682-20-4	C_4H_5NOS	6/15	2ab	IAS**/NIAS	Antimicrobial	[103,104]
#7	Acetamidocyclohexane	1124-53-4	$C_8H_{15}NO$	1/15	2b	NIAS	Byproduct/Intermediate/Reactant	
#9	Phthalic anhydride	85-44-9	$C_8H_4O_3$	5/15	2ab	IAS**	Byproduct/Intermediate/Reactant, Plasticizer	[103]
#10	Phenol, Isobutylenated	68610-06-0	$C_{10}H_{12}O$	3/15	2b	NIAS	Antimicrobial, Antioxidant	
#11	5-Chloro-2-methyl-4-isothiazolin-3-one	26172-55-4	C_4H_4ClNOS	3/15	2ab	IAS/NIAS	Antimicrobial	[104]
#13	1,2-Benzisothiazolin-3-one	2634-33-5	C_7H_5NOS	6/15	2ab	IAS/NIAS	Antimicrobial	[104]
#20	1,4-Cyclohexanedicarboxylic acid	1076-97-7	$C_8H_{12}O_4$	4/15	2ab	IAS**	Byproduct/Intermediate/Reactant, Coloring additive	
#21	4-Styrenesulfonic acid	98-70-4	$C_8H_8O_3S$	2/15	2b	IAS**	Byproduct/Intermediate/Reactant, Coloring additive	
#22	6-Hydroxy-2-naphthalenecarboxylic acid	16712-64-4	$C_{11}H_8O_3$	1/15	2b	IAS**	Byproduct/Intermediate/Reactant	
#24	4,4'-Oxydianiline	101-80-4	$C_{12}H_{12}N_2O$	4/15	2ab	NIAS	Byproduct/Intermediate/Reactant	[105]
#25	Diphenyl phosphine oxide	4559-70-0	$C_{12}H_{11}OP$	1/15	2ab	NIAS	Byproduct/Intermediate/Reactant	
#27	Diphenylphosphinic acid	1707-03-5	$C_{12}H_{11}O_2P$	2/15	2ab	NIAS	Byproduct/Intermediate/Reactant	
#29	2,4,6-Trimethylbenzophenone	954-16-5	$C_{16}H_{16}O$	1/15	2b	NIAS	Byproduct/Intermediate/Reactant, Photosensitive Chemical	[106]
#35	Ethyl 2-cyano-3,3-diphenylacrylate	5232-99-5	$C_{18}H_{15}NO_2$	3/15	2ab	IAS**	Photosensitive Chemical	
#36	2-Ethylhexyl 4-(dimethylamino)benzoate	21245-02-3	$C_{17}H_{27}NO_2$	4/15	2b	NIAS	Coloring Additive, Photosensitive Chemical	[103,107,108]
#37	Linolenic acid and isomers	463-40-1	$C_{18}H_{30}O_2$	4/15	2ab	IAS**	Surfactant	
#40	Dimethoxy ethyl phthalate	117-82-8	$C_{14}H_{18}O_6$	4/15	2ab	NIAS	Byproduct/Intermediate/Reactant, Plasticizer	[109]
#41	Hexaethylene glycol	2615-15-8	$C_{12}H_{26}O_7$	2/15	2ab	NIAS	Adhesive additive	
#42	2,6-Di-*tert*-butyl-4-phenylphenol	2668-47-5	$C_{20}H_{26}O$	2/15	2b	NIAS	Byproduct/Intermediate/Reactant, Antioxidant	
#43	Octyl 4-methoxycinnamate	5466-77-3	$C_{18}H_{26}O_3$	3/15	2b	NIAS	Photosensitive Chemical	
#45	Tridemorph	24602-86-6	$C_{19}H_{39}NO$	2/15	2ab	IAS/NIAS	Fungicide	
#47	Dehydroabietic acid	1740-19-8	$C_{20}H_{28}O_2$	4/15	2ab	NIAS	Byproduct/Intermediate/Reactant, Degradation product	[10,103]
#48	Pigment Orange 64	72102-84-2	$C_{12}H_{10}N_6O_4$	1/15	2b	NIAS	Coloring Additive	
#49	Abietic acid	514-10-3	$C_{20}H_{30}O_2$	5/15	2ab	IAS**	Coloring Additive, Adhesive Additive, Surfactant	[12]
#55	Heptaethylene glycol	5617-32-3	$C_{14}H_{30}O_8$	1/15	2ab	NIAS	Adhesive additive	
#57	Dipropyleneglycol dibenzoate	20109-39-1	$C_{20}H_{22}O_5$	2/15	2ab	NIAS	Coloring Additive, Adhesive Additive	[10]
#58	2-Benzyl-2-(dimethylamino)-1-(4-morpholin-4-ylphenyl) butan-1-one	119313-12-1	$C_{23}H_{30}N_2O_2$	3/15	2b	NIAS	Coloring Additive, Photosensitive Chemical	[103]
#59	Tetraethylene glycol mono(*p*-nonylphenyl) ether	7311-27-5	$C_{23}H_{40}O_5$	2/15	2b	NIAS	Surfactant	
#60	Dibutoxyethoxyethyl adipate	141-17-3	$C_{22}H_{42}O_8$	3/15	2ab	NIAS	Byproduct/Intermediate/Reactant, Plasticizer	
#61	Dodecaethylene glycol	6790-09-6	$C_{24}H_{50}O_{13}$	1/15	2b	NIAS	Adhesive additive, Plasticizer	
#64	Behenamide	3061-75-4	$C_{22}H_{45}NO$	4/15	2ab	IAS**	Adhesive Additive	
#65	Methyl 9,10-dihydroxystearate	1115-01-1	$C_{19}H_{38}O_4$	1/15	2b	NIAS	Byproduct/Intermediate/Reactant, Photosensitive Chemical	
#66	Diethylene glycol dibenzoate	120-55-8	$C_{18}H_{18}O_5$	2/15	2ab	NIAS	Byproduct/Intermediate/Reactant, Plasticizer	[109]
#69	*N*-Butylbenzene sulfonamide	3622-84-2	$C_{10}H_{15}NO_2S$	1/15	2ab	NIAS	Byproduct/Intermediate/Reactant, Plasticizer	[12]
#70	Tributyl citrate	77-94-1	$C_{18}H_{32}O_7$	4/15	2ab	NIAS	Coloring Additive, Plasticizer	
#71	4,4'-Bis(diethylamino)benzophenone	90-93-7	$C_{21}H_{28}N_2O$	1/15	2ab	NIAS	Coloring Additive, Photosensitive Chemical	[106]
#72	Benzophenone	119-61-9	$C_{13}H_{10}O$	6/15	2ab	IAS**	Byproduct/Intermediate/Reactant, Photosensitive Chemical	[103,106–108,110]
#73	Dodine	2439-10-3	$C_{13}H_{29}N_3$	3/15	2ab	IAS/NIAS	Fungicide	
#74	Stearamide	124-26-5	$C_{18}H_{37}NO$	6/15	2ab	IAS**	Adhesive Additive	[10,103]

* Number of databases in which the unique candidate monoisotopic mass is listed

** Defined by Commission Regulation 10/2011 as amended

*** In case the compound is labeled as Byproduct/Intermediate/Reactant, the exact usage of compound might be uncertain

The fragmentation spectra of the candidates and some of the isobaric compounds were submitted to all spectral libraries mentioned in chapter regarding databases and mass lists, with annotations returned for 37 candidates. All the candidates were annotated by MetFrag and SIRIUS, however, the candidate ranking was occasionally different between the two tools. Based on the retention time regression analysis and outlier treatment by Cook's distance, 5 compounds were dismissed as less likely candidates and the confidence level was depreciated (data available at the Harvard Dataverse repository [80] and as Figure 3.13).

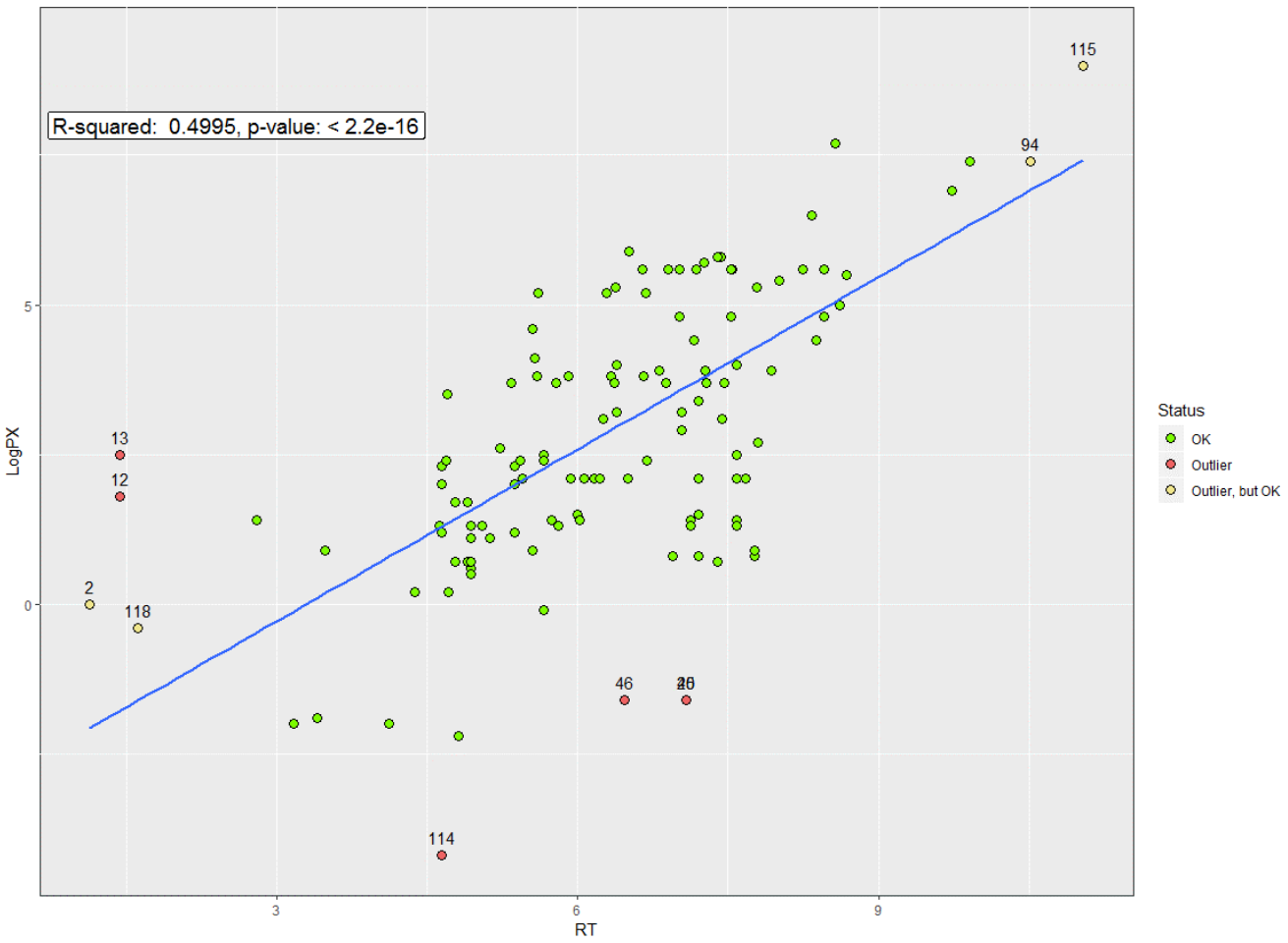

Figure 3.13. **Linear regression for the identification of outliers based on Cook's distance**

3.2.3. Leaching of the materials

The migration pattern was similar for both simulants, however, the ethanol-based simulant D1 showed higher leaching rate. In additional time trend leaching experiments, observations were made that more than half of the maximum relative peak area was already achieved for most compounds within 5 minutes of simulation (Figure 3.14). The mean relative peak area for the sum of the compounds increased in the time trend, however, the migration rate was sample and material dependent, with a slightly different trend observed for various samples (Figures 3.14-18). For some

compounds, the relative peak area at early migration stages corresponded to as much as 200% of the observed peak area in the 24-hour extracts, which can be explained by matrix-related signal suppression in electrospray ionization by the leached compounds in later migration stages.

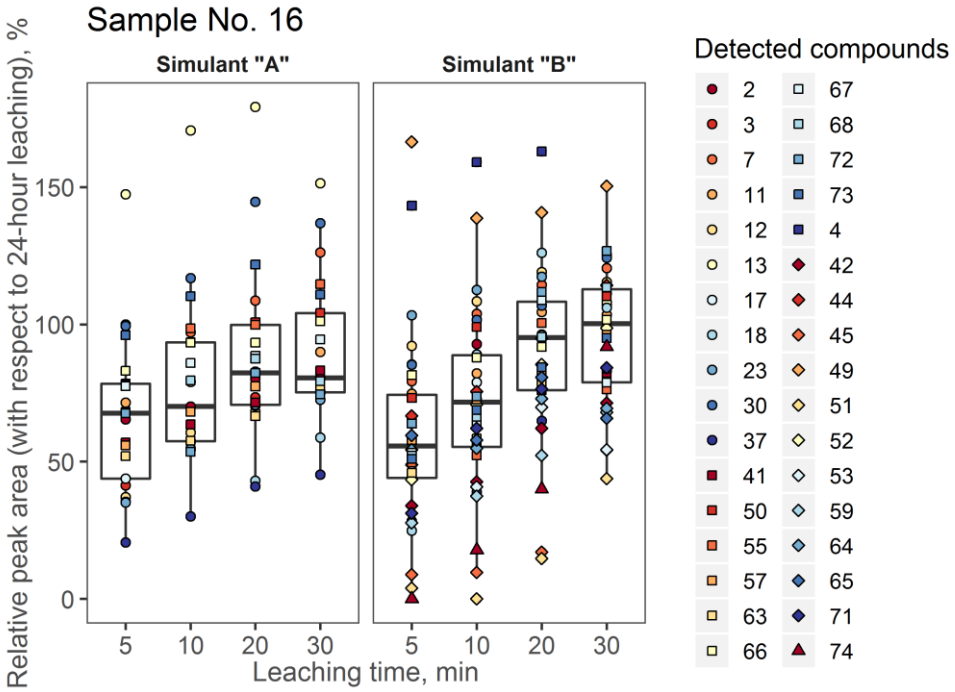

Figure 3.14. **Box plot representation of the leaching time trend for sample No. 16**

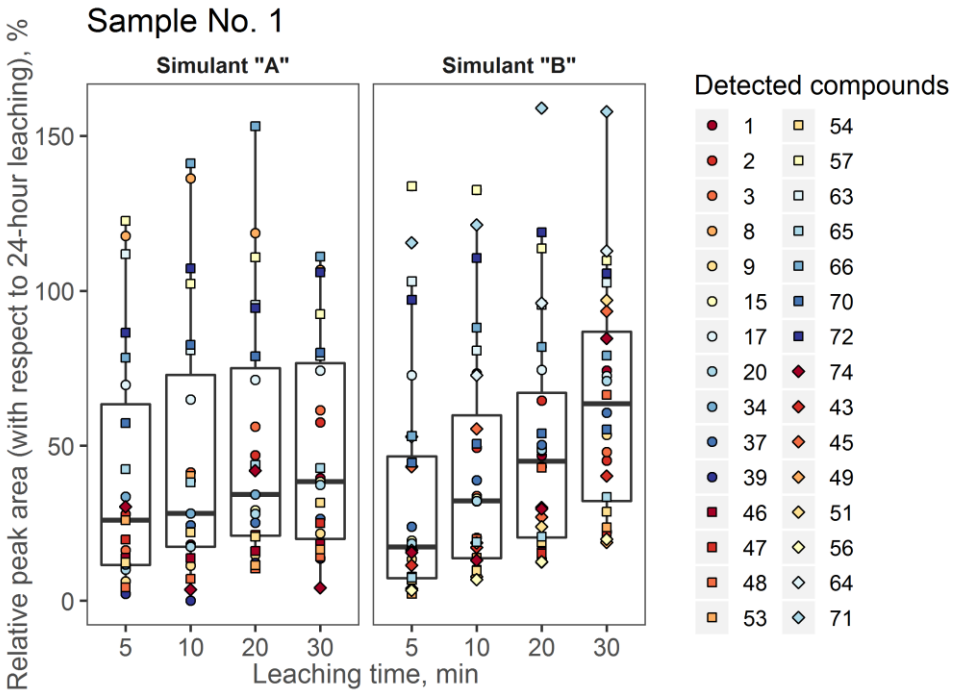

Figure 3.15. **Box plot representation of the leaching time trend for sample No. 1**

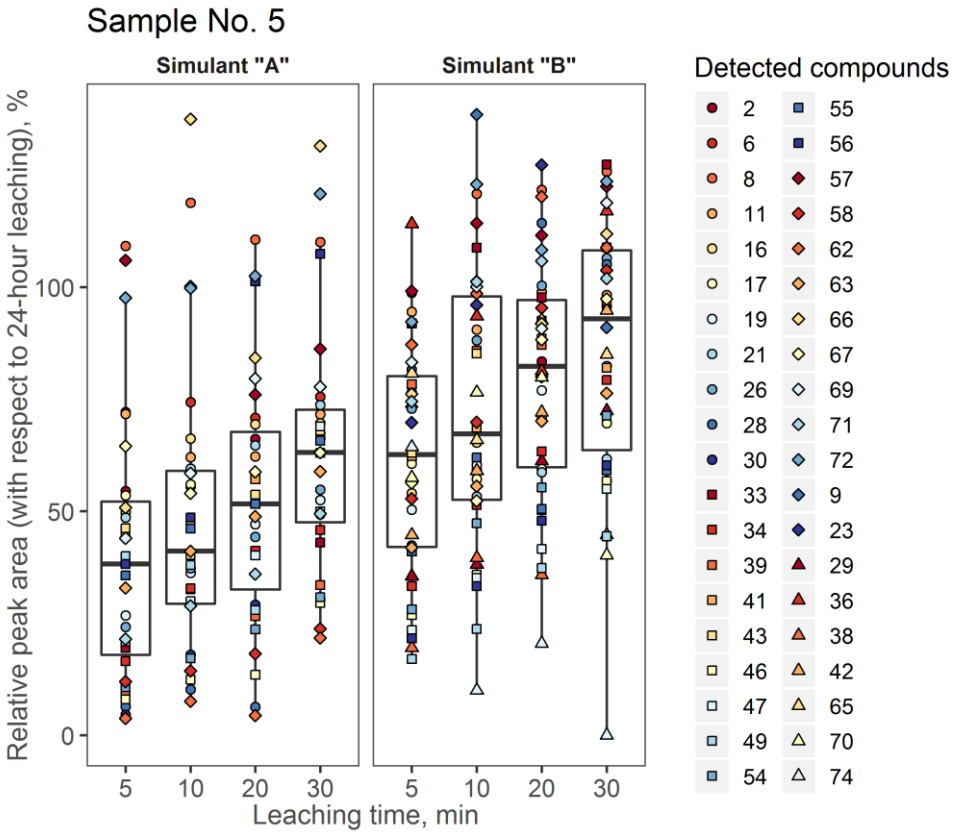

Figure 3.16. **Box plot representation of the leaching time trend for sample No. 5**

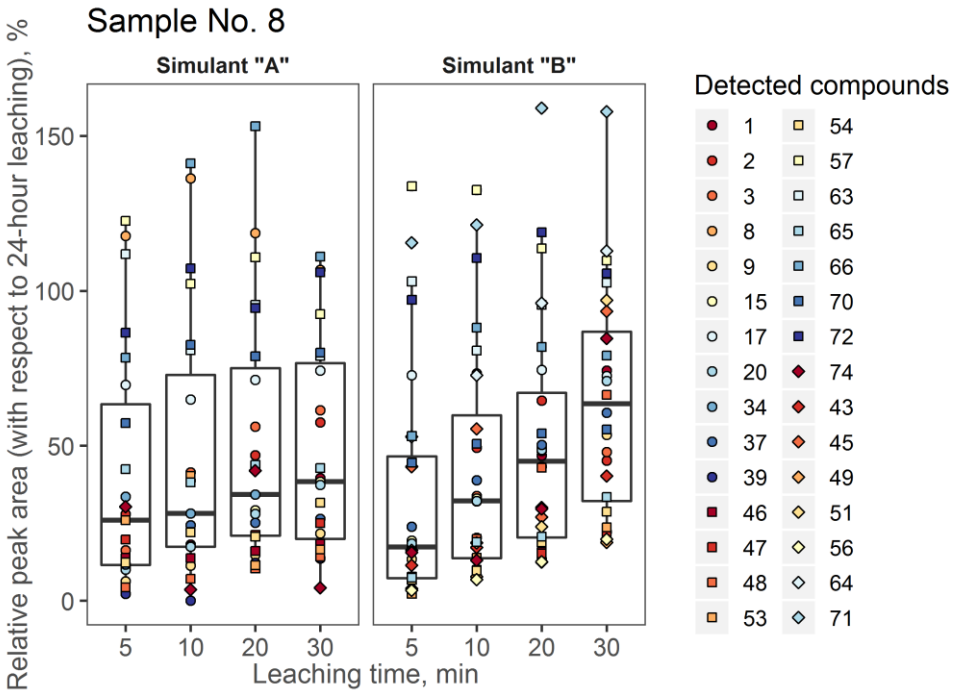

Figure 3.17. **Box plot representation of the leaching time trend for sample No. 8**

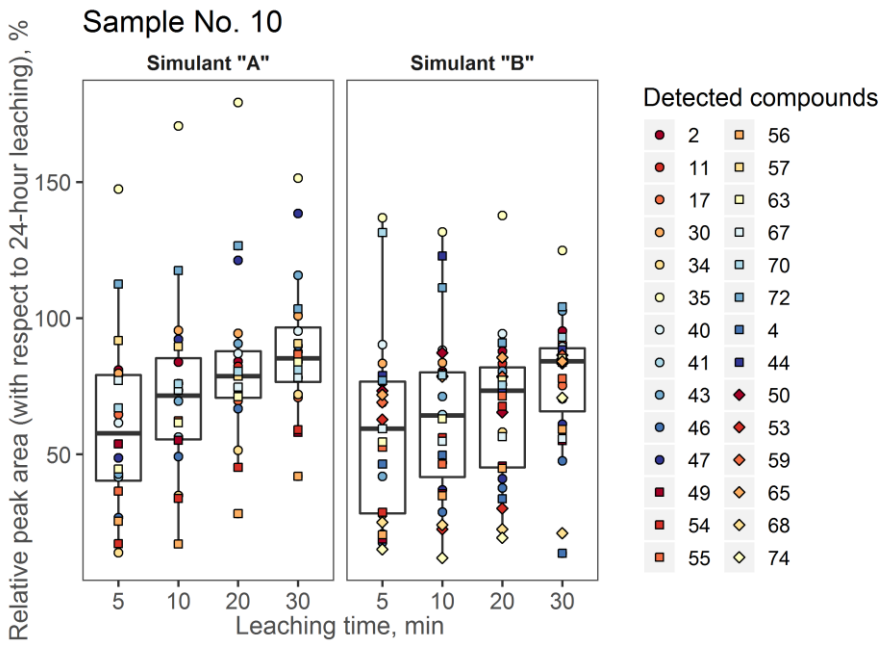

Figure 3.18. **Box plot representation of the leaching time trend for sample No. 10**

Since the main focus of the study was the investigation of paper materials, only one plastic straw sample (sample 6) was examined. It was observed from the base peak chromatogram (Figure 3.19) and the sample 6 row in Figure 3.20 that generally fewer compounds migrated and the peaks were of lower intensity. For a better understanding and elucidation of the migrants leaching from the plastic straws, concentration or cleanup procedures would be necessary.

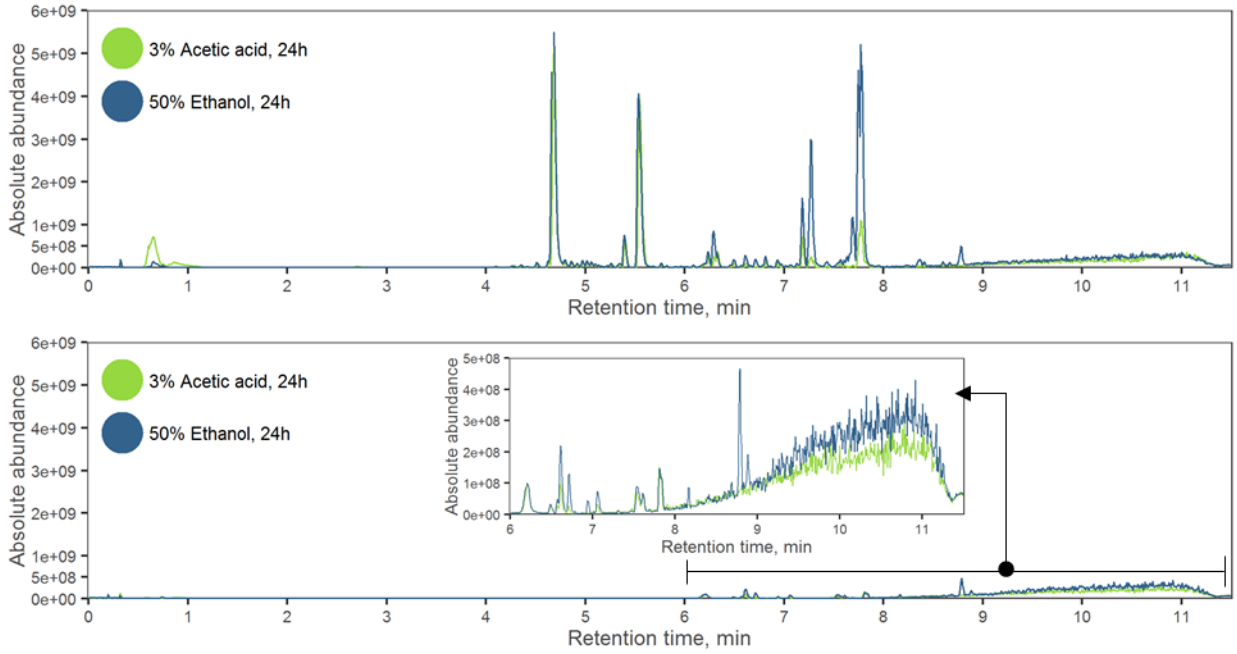

Figure 3.19. **Overlaid base peak chromatograms of 24-hour migration in two simulant types; (upper section) chromatogram of migration from paper straw sample 1; (lower section) chromatogram of migration from biodegradable plastic straws**

3.2.4. Characteristics of the identified substances

Considering the nature of samples used in this study, the tentative identification of compounds matching the profile of the FCMs was prioritized. We identified various additives that serve in the roles of adhesives, chemical intermediates, UV stabilizers and other photosensitive chemicals, plasticizers, ink and coating additives, and preservatives. A similar pattern of added chemicals was observed between the samples of the same countries of origin (also manufacturers, indicated in Figure 3.20), within the groups 1-5, 7-9, 10-13, and 14-17.

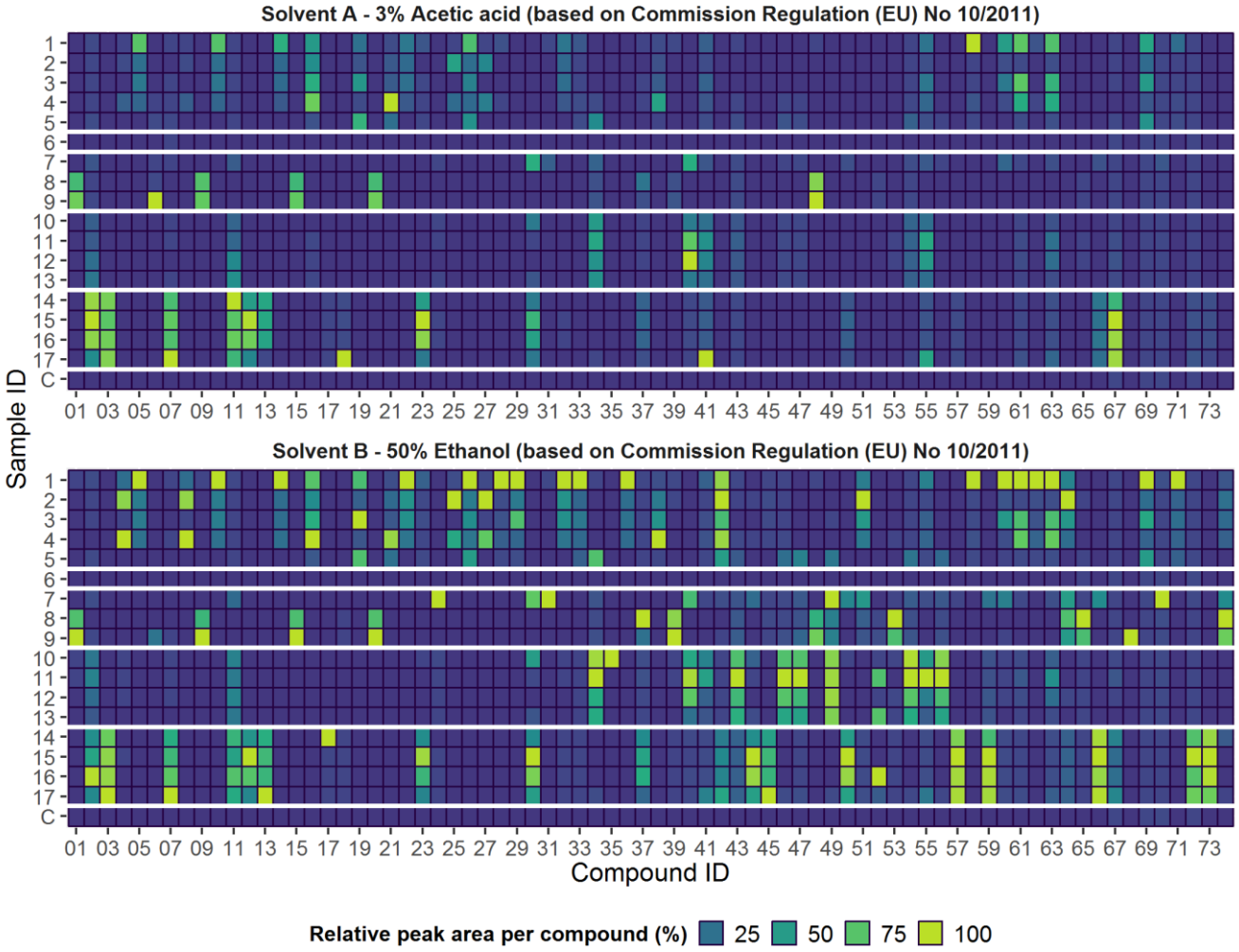

Figure 3.20. **Relative peak areas for compounds identified in the samples after 24-hour leaching; samples grouped within groups of the same manufacturer**

Primarily, the substances can be categorized into two major groups – intentionally added substances (IAS) and non-intentionally added substances (NIAS). The latter can be broadly defined as side products, breakdown products and contaminants of the added chemicals [111], however, the definition is open to interpretation as there are more elaborate definitions available. The former, IAS

can be defined as compounds added in the production process to the final articles, as starting materials, or to improve certain properties of the material. The interpretation and classification of substances belonging to these two groups depends on the form of the final article in which the substances occur.

In the present study, we attempted to classify the substances in either of the two categories and provided the application notes for each of the identified compounds. The information is presented in Table 3.4 for the substances of highest structural confidence and in the Supplementary workbook (available in the online version of [102]) for all the tentative candidates. Most of the substances were classified as NIAS, however, there is no general authorization or listing of NIAS, which means that the listing of a substance in suspect databases may or may not cover them. Exceptions were made and IAS classification was assigned for the substances that are listed in the Union list, according to Commission Regulation No 10/2011 [6]. The Union list encompasses substances that have been authorized for use in plastic FCMs and includes monomers, other starting materials, macromolecules obtained from microbial fermentation and additives.

In some cases, no unequivocal assignment could be made. For example, the identified microbial and fungicide substances could be considered both IAS and NIAS, depending on the material formulation. The largest groups of identified substances regarding their purpose in the FCMs consisted of coloring additives (n=17), adhesive additives (n=10), photosensitive chemicals (n=13), antimicrobials or fungicides (n=7), as well as byproducts/intermediates/reactants (n=34).

3.2.5. Hazard identification and risk prioritization

Tentatively identified compounds with the highest structural confidence levels of 2 and 3 (n = 72) were used for toxicological endpoint assessment. To screen and theoretically evaluate mutagenic and carcinogenic potential of the identified compounds, experimental toxicity data (when available) was collected using the OECD Toolbox v4.3a. The OECD Toolbox provided experimental mutagenicity data for 23 substances and carcinogenicity data for 9 out of the 72 substances detected in the present study (see Table 3.5). In addition, (Q)SAR based toxicity prediction and prioritization approach recently described in [83] was employed. In the present work, original model-specific classifications were recoded as described in [83] and the output of the five and three different predictions tools for mutagenicity and carcinogenetic, respectively are presented in form of numeric values ranging from “0” and “1”. The higher the value associated with a prediction the higher the probability that the substance detected is mutagenic or carcinogenic. The candidates with available experimental data and the corresponding (Q)SAR model score mean values are shown in Table 3.5; Figure 3.21 depicts a representation of the results of the *in-silico* analysis regarding both endpoints

investigated for all the candidates. Detailed lists of the model outputs, as well as the script implemented for model processing is available in Harvard Dataverse repository [80].

Table 3.5

Substance experimental data and the corresponding (Q)SAR model scores

ID	Compound	CASRN	Confidence level	Mean (Q)SAR mutagenicity [a]	Experimental mutagenicity data [b]		Mean (Q)SAR carcinogenicity [a]	Experimental carcinogenicity data [b]	
					In vitro	*In vivo*		*In vitro*	*In vivo*
#1	1,4-Dihydroxybenzene	123-31-9	2ab	0.21	5/19	2/2	0.93	1/1	9/10
#2	2-Methyl-4-isothiazolin-3-one	2682-20-4	2ab	0.4	0/12		0.5		
#3	Indole	120-72-9	3	0.14	0/11		0.44		0/1
#6	N-Isopropylaniline	768-52-5	3	0.05	0/21		0.67		
#9	Phthalic anhydride	85-44-9	2ab	0.14	2/24		0	0/5	0/6
#11	5-Chloro-2-methyl-4-isothiazolin-3-one	26172-55-4	2ab	0.67		0/1	0.5		
#12	Triethylene Glycol	112-27-6	3	0.57	1/11		0.32		0/2
#13	1,2-Benzisothiazolin-3-one	2634-33-5	2ab	0.54	0/8		0.5		
#14	Methyl paraben	99-76-3	3	0.11	0/11	1/1	0.21		
#24	4,4'-Oxydianiline	101-80-4	2ab	1	24/43	7/9	1	2/2	14/14
#26	Ethoxyquin	91-53-2	3	0.1	0/15	0/1	0.31		0/3
#31	1,3-Bis(2-isocyanato-2-propyl) benzene	2778-42-9	3	0.39	0/1		0.46		
#32	Diallyl phthalate	131-17-9	3	0.05	2/24	0/1	0.1		0/3
#33	4,4'-bis(dimethylamino)benzophenone (Michler's ketone)	90-94-8	3	0.78	11/22	2/2	1	1/1	13/13
#37	Linolenic acid and isomers	463-40-1	2ab	0.2	0/16		0.37		
#40	Dimethoxy ethyl phthalate	117-82-8	2ab	0.62	1/1		0.43		
#43	Octyl 4-methoxycinnamate	5466-77-3	2b	0.03	0/21		0.42		
#45	Tridemorph	24602-86-6	2ab	0.14	0/1		0.53		
#49	Abietic acid	514-10-3	2ab	0.08	0/11		0.46		
#56	Dicyclohexyl phthalate	84-61-7	3	0.01	0/21		0.5		
#67	Diglyme	111-96-6	3	0.15	0/21		0.73		
#72	Benzophenone	119-61-9	2ab	0.11	0/27	0/2	0.54		3/3
#74	Stearamide	124-26-5	2ab	0.14	0/9		0.45		

[a] Mean score as provided from normalized (Q)SAR model output

[b] Positive experimental tests; Data provided by QSAR Toolbox v4.3

Following the procedure described in [83], for further interpretation of the combined (Q)SAR output, mean model scores were classified into three areas: (i) compounds with a mutagenic (carcinogenic) score higher than 0.66 may be considered mutagenic (carcinogenic) with a high probability, (ii) scores between 0.33 and 0.66 indicate that reliable prediction of mutagenicity (carcinogenicity) cannot be made, and (iii) compounds with scores below 0.33 may be considered non-mutagenic (non-carcinogenic).

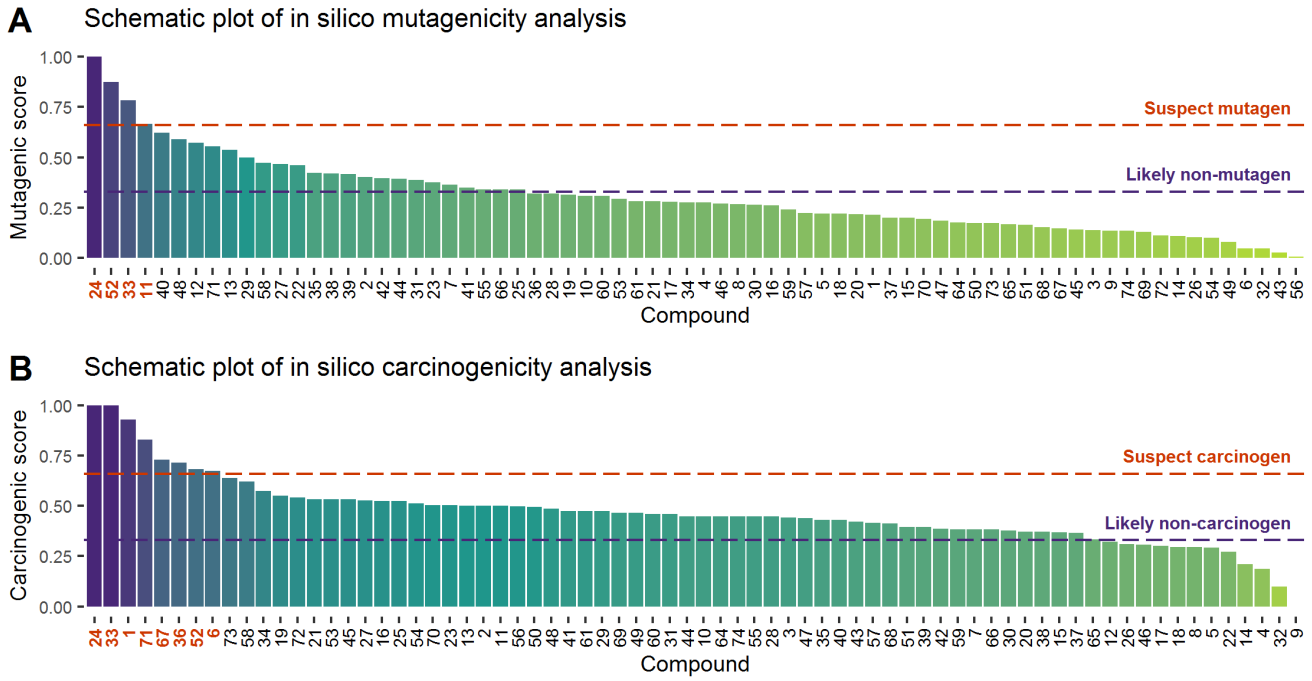

Figure 3.21. **Schematic representation of the results of the *in-silico* analysis in regard to the endpoints (A) mutagenicity and (B) carcinogenicity**

Regarding predicted mutagenicity, the mean model probability scores of four substances were higher than 0.66. For two out of four compounds – 4,4'-oxydianiline (compound ID #24) and Michler's ketone (#33) the experimental results were in consensus as these substances have been tested positive for mutagenicity. Third substance – 5-chloro-2-methyl-isothiazolin-3-one or CMI (#11) with a probability score of 0.67 had been tested negative in a single *in vivo* experiment. The Toolbox did not provide experimental data for the fourth compound predicted to be mutagenic - quinacridone (#52). A total of 22 compounds, were found to obtain equivocal (Q)SAR mean summary scores ranging from 0.33 to 0.66 and the bulk of the substances detected in the present work (n = 46) were considered non-mutagenic, with mean model scores of less than 0.33. Two substances of the latter two groups were identified as experimentally positive according to the OECD Toolbox data, namely 1,4-dihydroxybenzene (#1, score 0.21) and dimethoxy ethyl phthalate (#40, score 0.62), accordingly.

The investigation of the carcinogenicity endpoint by the (Q)SAR tools yielded the scores higher than 0.66 for eight compounds which could be considered carcinogenic. The provided experimental results were in agreement for #1, #24 and #33. For the remaining five – N-isopropyl aniline (#6), 2-ethylhexyl 4-(dimethyl amino) benzoate (#36), quinacridone (#52), diglyme (#67) and 4,4'-bis(diethylamino) benzophenone (#71) there were no available experimental data. Only 12 substances were considered non-carcinogenic with the model scores less than 0.33, however, the equivocal gray area provided by model results was rather large – 52 compounds. Single substance was found positive

in vivo for carcinogenicity experimentally – benzophenone (#72), however it was assigned an equivocal mean (Q)SAR model score of 0.54.

When applying a screening battery of complementary (Q)SAR systems using different mathematical algorithms and different training data sets conflicting predictions might occur. Mathematical predictions of toxicity are not yet predictable with sufficient reliability and will always be less favorable than any experimental data of a given substance provided for by *in vivo* or *in vitro* studies [83]. Therefore, future work, should focus on experimental (*in vitro* or *in vivo*) validation of the findings obtained in the present work. In addition, alternative combine and conquer strategies for (Q)SAR analyses should be investigated and their performance in priority ranking evaluated. Regardless, of the current limitations when applying (Q)SAR tools, the present study demonstrated the benefits of combining high throughput mass spectrometry-based detection and *in silico* hazard ranking of novel contaminants in FCMs.

3.2.6. General remarks regarding the analysis of paper food contact materials

Potential limitations of the study, similarly to other studies investigating FCMs, are associated with the recovery of analytes from FCMs. A multitude of factors such as the selectivity of extraction solvents, temperature, time, material thickness and density can influence the results of analysis. Multiple scenarios can be possible under non-simulated circumstances and a multitude of variables should be considered, as straws can be used in various types of beverages with different exposure time. When it comes to the assessment of risk to human health, for precautionary reasons usually the worst-case scenario is considered [83]. Since this study was performed with a qualitative approach, we have scrutinized the worst possible endpoints, as the real degree of risk is difficult to evaluate.

In order to obtain reliable occurrence and exposure data, suitable analytical methodologies need to be developed. In this study, novel HRMS instrumentation and data processing methodologies were used to identify the suspects. However, mass spectrometry is not intrinsically quantitative and differences in ionization efficiency can lead to relative intensities of compounds not accurately reflecting their concentrations [112], as it was observed in the time trend leaching investigation. The method applied for the identification of the substances was designed to be as comprehensive as technically achievable. However, without the use of reference substances, we might not have the best quality of evidence for the occurrence of various added chemicals, but untargeted methodology allowed to screen and tentatively identify hundreds and thousands of possible suspects. These methods are not intended to create a comprehensive inventory of the chemicals in the FCMs and are not intended to replace hazard assessment and migration testing.

For many of the identified compounds no toxicological data are available. To overcome this limitation, (Q)SAR modeling can be implemented, best used as a combination of multiple tools [11,83], as the models can have different simulation principles and produce different outcomes. While *in silico* modeling suffers from various limitations it provides helpful evidence for the investigation of the toxicological properties of compounds which can be obtained rapidly, at low cost and without excessive experimental testing [8,113]. What is more, applying *in silico* toxicity predictions for efficient priority ranking of substances of most concern can be performed and provide a basis for the selection of compounds for future exposure and subsequent risk assessments [83].

3.3. Determination of organophosphate suspects by biosensors

This chapter summarizes the outcome of the research performed during the EU-FORA fellowship, granted by European Food Safety Agency. During the fellowship, the work was carried out at the Institute of Protein Biochemistry, a part of National Research Council of Italy. Since then, the Institute has been merged and at the time of writing this thesis is now Institute of Biochemistry and Cell Biology.

The main results from the scientific work are shown in two parts. Firstly, an automated robotic workstation method was developed for organophosphate pesticide analysis using enzymatic biosensors. Secondly, the method was adapted for the determination of paraoxon in human urine.

The main results from the scientific work at the institute are published in two publications and one manuscript is in preparation for submission (non-disclosed research).

3.3.1. A robotic system for an automated biosensor analysis

In vitro pesticides activation by using NBS

Considering the massive presence on the market of phosphorothionate OPs, we investigated the ability of EST2 to detect these compounds. EST2 similarly to acetylcholinesterase activities showed less affinity toward thio-OP, although it can reversibly bind many of these compounds such as parathion and chlorpyriphos [75,114]. Starting from the evidence that thio-OPs are required to be in the active form of oxon-OP products, in order to irreversibly inhibit the acetylcholinesterase activities [115], the sample principle was applied in this research for the irreversible inhibition of EST2. Inhibition assay experiments were carried out in combination with an oxidant pre-treatment of the thio-OP compounds using a selective and rapid oxidant agent NBS (Figure 3.22b), obtaining a complete conversion to oxon form within 5 min as described by Bavcon et al. [116]. The MS measurements of NBS treated thio-OPs, such as parathion, in a ratio 90:1 for 5 min, indicated the complete transition from thio-OP compounds to the oxon-OP counterparts (Figure 3.22c). In Figure 3.22c, the MS signal

for parathion mass transition 292.0 -> 236 m/z (baseline 1) and for paraoxon mass transition 276.1 -> 220. m/z (baseline 2), were reported. Before the oxidation step, only parathion was present in the chromatogram and, as indicated by the baseline, it is all converted to paraoxon after the oxidation.

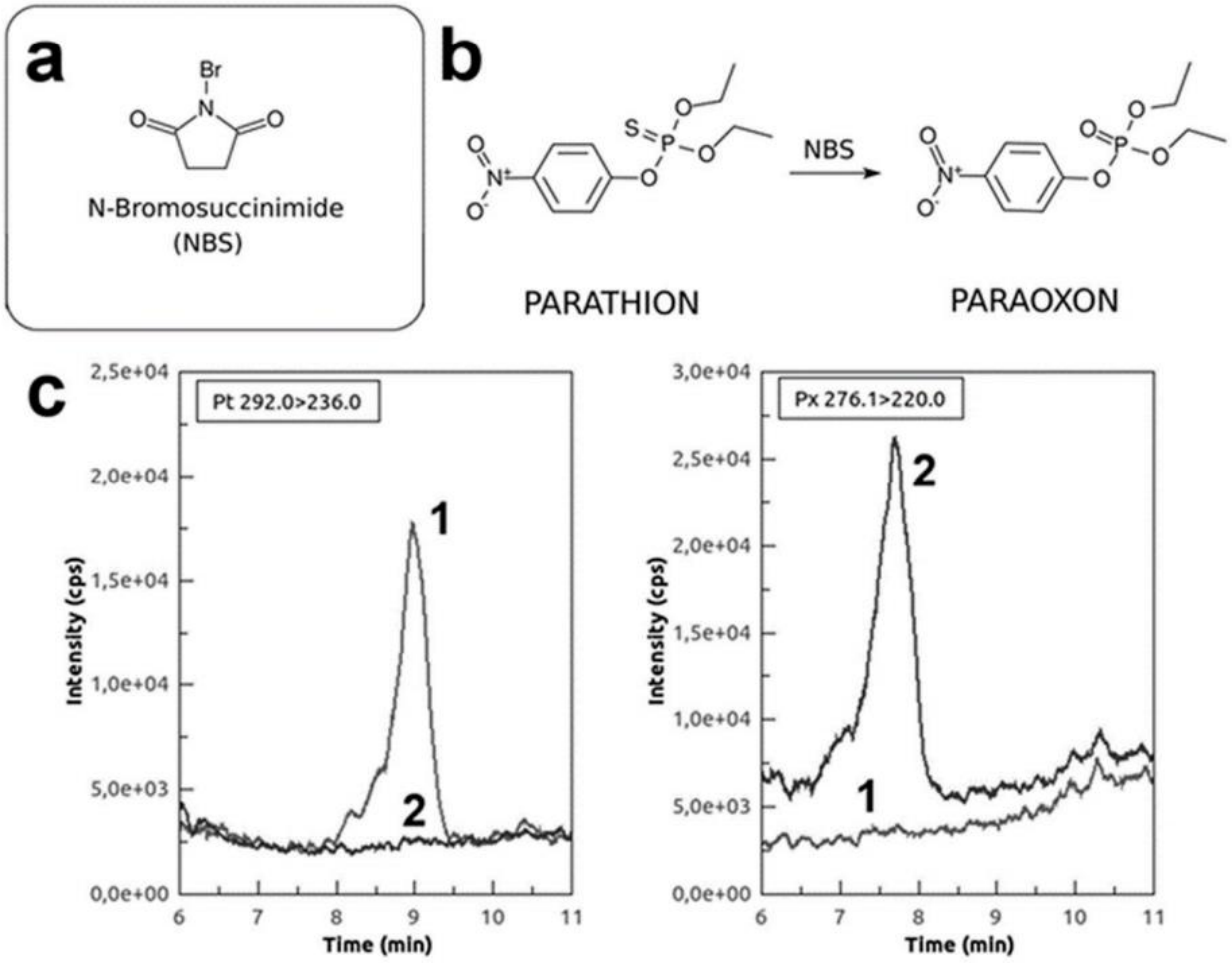

Figure 3.22. **NBS-oxidized pesticides detection in water. (a) Chemical structures of N-bromosuccinimide and general formula of thio- and oxo-organophosphates. (b) NBS-mediated parathion/paraoxon transition. (c) LC-MS plot of transformation from parathion (baseline 1) to paraoxon (baseline 2), before (on the left) and after (on the right) the NBS oxidation step**

Effects of NBS on EST2 activity

Measurement of the EST2 residual activity in the presence of NBS indicated that the chemical modification reagent slightly influenced the enzyme activity. Only 9.3 ± 1.9% of the EST2 activity was inhibited by 30 μM NBS (Figure 3.23), corresponding to the final amount of oxidant in the inhibition assay of NBS-oxidized pesticides. These results were in agreement with data obtained with other esterase activities [117]. To avoid deviancy in results, all the measurements were carried out

using a reference enzymatic activity of EST2 in both normal and oxidative (with addition of NBS) conditions.

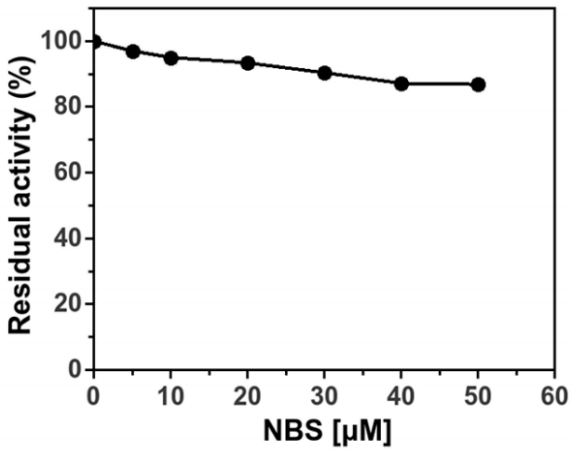

Figure 3.23. **Plot of EST2 residual activity in presence of increasing NBS concentration levels**

EST2 inhibition measurements on in vitro NBS-activated pesticides

The principle of EST2 inhibition by OPs was largely described in literature [118,119]. Briefly, the reactive organophosphorus group reacts with the catalytic serine residue in the active site of enzyme producing a covalent intermediate. This results in the irreversible inhibition of EST2 characterized by a progressive decrease of enzymatic activity over time, until complete inhibition in presence of inhibitor excess. The most interesting thing is that the affinity showed by EST2 toward the paraoxon is so high and the reaction is so far, that the reactive rate cannot be measured by conventional method of pseudo first-order rate-constant for the determination of irreversible inhibition [118,120]. The high interest in bioreceptors showing high affinity irreversible inhibition, is particularly evident in the case of compounds that are highly toxic for living organisms, such as pesticides or never agents. By exploiting the fast inhibition rate of high affinity irreversible inhibitors, it becomes possible to measure the amount of toxic compound independently from the time and the amount of inhibitor, having as its only limit the detection of enzymatic activity. In fact, an increased sensitivity and reproducibility of the enzyme assay increases the possibility to measure small differences in the residual activity of the enzyme with increased sensitivity in the determination of the inhibitor concentrations. Using a fluorescence-based assay, in our previous work we detected 230 fmol of paraoxon at 10% of inhibition, reaching a quantification limit of 125 fmol of pesticide [121]. The same conditions for the assays of thio-OP pesticides were used.

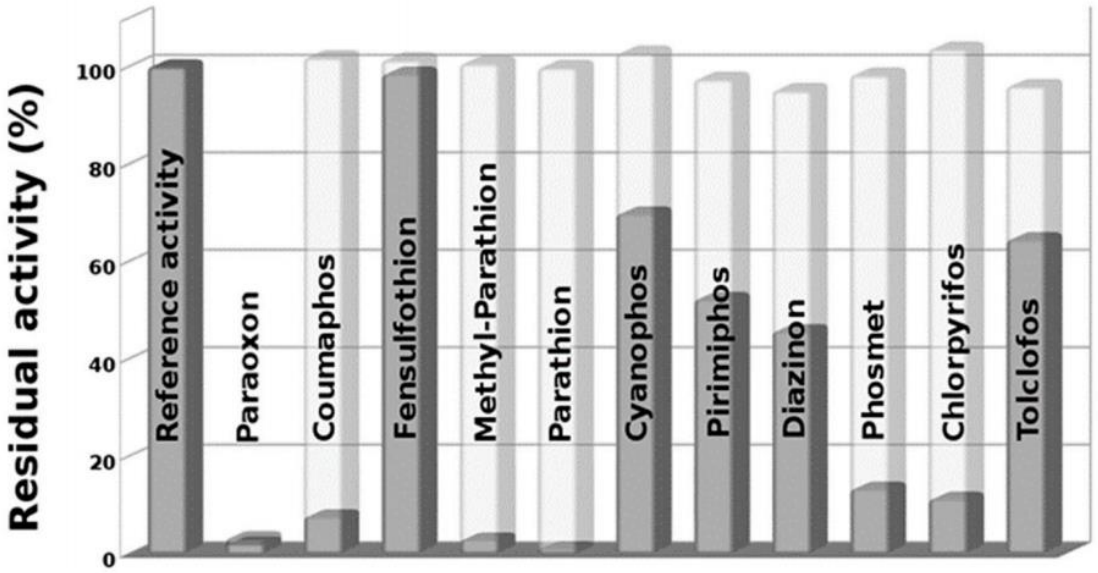

Figure 3.24. **Plot of EST2 residual activity in absence (reference activity) and presence of different pesticides in their native form (light) and oxidized with NBS (dark)**

The plotted data of the residual activity of EST2, with respect to the various pesticides tested (Figure 3.24) in both condition – without and after NBS oxidation – revealed the capability of oxidized thio-OPs to irreversibly inhibit the EST2 activity. As expected, data indicated a complete loss in residual activity for methyl-parathion and parathion pesticides after NBS treatment. In fact, these thio-OP compounds, as demonstrated by mass spectrometry measurements on parathion (Figure 3.24c), are transformed in methyl paraoxon and paraoxon, respectively, which completely inhibit the EST2 activity in very short time [118,119]. Moreover, we observed a significant reduction of EST2 residual activity for chlorpyrifos, coumaphos and phosmet. Also, the oxidized form of diazinon, cyanophos, pirimiphos and tolcofos reduced the enzyme activity of about 30-50% with respect to the same phosphorothionate compounds.

No significant effects were observed for the inhibition measured by assaying fensulfothion after oxidation. The pesticide paraoxon, as expected, showed a total reduction in the enzyme activity without oxidant pre-treatment in this experiment, as an excellent positive control.

In previous research there already has been demonstrated the binding of some thio-OP pesticides, such as parathion, diazinon and chlorpyrifos [75], to the acyl- or alcohol- binding pockets of EST2. This means that the EST2 is already able to bind almost all the OP compounds, including thio-OPs. However, these intermediates were non-covalently bonded to the protein when in the thio-form, because of the low reactivity of sulphur group. Thus, in presence of an excess of colorimetric or fluorescent substrates for this enzyme, the pesticide is displaced from the catalytic site and the enzymatic activity remains unaltered. The obtained data is significant and clearly demonstrates the different between the efficacy of inhibition for the pesticides tested in oxidizing conditions compared

to the original ones. In fact, in the latter conditions, the oxon-OP products irreversibly inhibited the EST2 activity as determined by the decrease in activity over time. Data also confirms the previously proposed hypothesis [122], that the replacement of Sulphur with oxygen bring an increased positive charge density on the central phosphorous atom that allows for a more favorable nucleophilic attack of the -OH group of serine, irreversibly inhibiting the enzyme activity. The oxidative form of tested compounds can be produced during storage and by breakdown products released from microorganisms or through natural exposition to light during application in the external environment. The findings in this study support the hypothesis that mandatory monitoring and analysis is necessary of oxidized forms of thio-OP for a complete risk assessment.

Automatic approach in the pesticide determination by robotic system

In this study, an automatized assay was developed allowing a streamlined, multi-sample analysis process using a biosensing device. The goal was achieved by exploiting an automatized approach on a Microlab® STAR Liquid Handling Workstation equipped with a robotic arm and a VICTOR™ X3 Multi-label Plate Reader. Using the robotic workstation, protocols were developed for a 96-well plate assay using EST2, the pesticide paraoxon as a standard molecule and 4-MUBu as a substrate of the enzymatic reaction that can also provide the fluorescent signal. As a first step, we assessed the existence of a linear relationship between amount of 4-MU used and fluorescence intensity measured. The data obtained demonstrated a good linearity (R^2 = 0.9975) between fluorescence intensity measured by the VICTOR™ plate reader and 4-MU in the assayed range of concentrations (0.4 – 3.2 mM) (Figure 3.25).

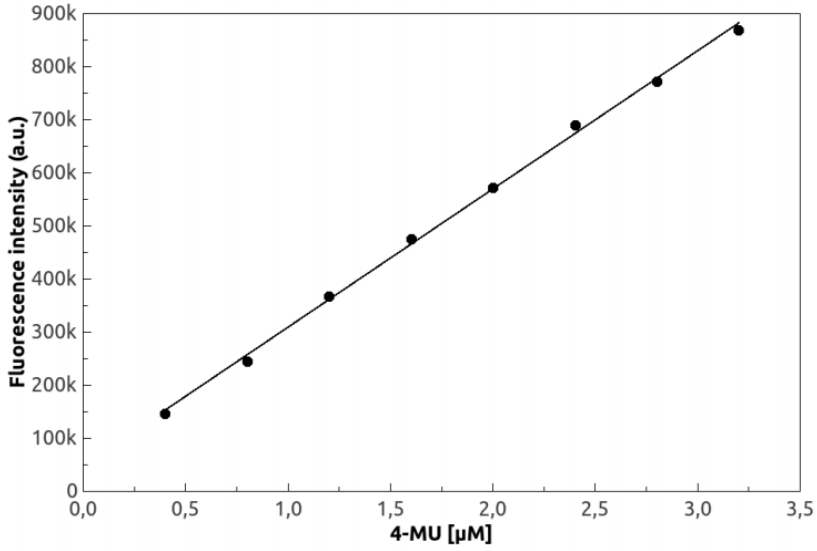

Figure 3.25. **Calibration curve of fluorescence intensity at increasing concentration levels of 4-MU in HEPES buffer, measured using the robotic workstation**

The accuracy of robot for the dispensation of 4-MU aliquots in the plate wells was tested. In agreement with the standard assay for the spectrofluorometer, similar results were observed for the assay of EST2 activity using 4-MUBu as substrate in the plate reader by measuring a linear increase of the signal of fluorescence intensity. Using the fluorescence-based assay, a sensitivity of $4.3 \times 10^{-2} \pm 2.2 \times 10^{-3}$ in the linear range ($R^2 = 0.986$) from 500 to 2000 fmol of paraoxon was obtained (Figure 3.26), mathematically represented by the linear regression, where *x* is the concentration of paraoxon, *y* is the residual activity and b (intercept) is the sensitivity of the biosensor. In these conditions, we calculated a LOD of 205.5 ± 6.98 fmol at 10% of inhibition and a precision within the 5% of standard deviation. The precision, as well as the accuracy in the determination of paraoxon, increases at higher pesticide concentration levels, because the ratio enzyme-inhibitor is closer to 1:1 ratio, as widely explained in our previous works [118,119].

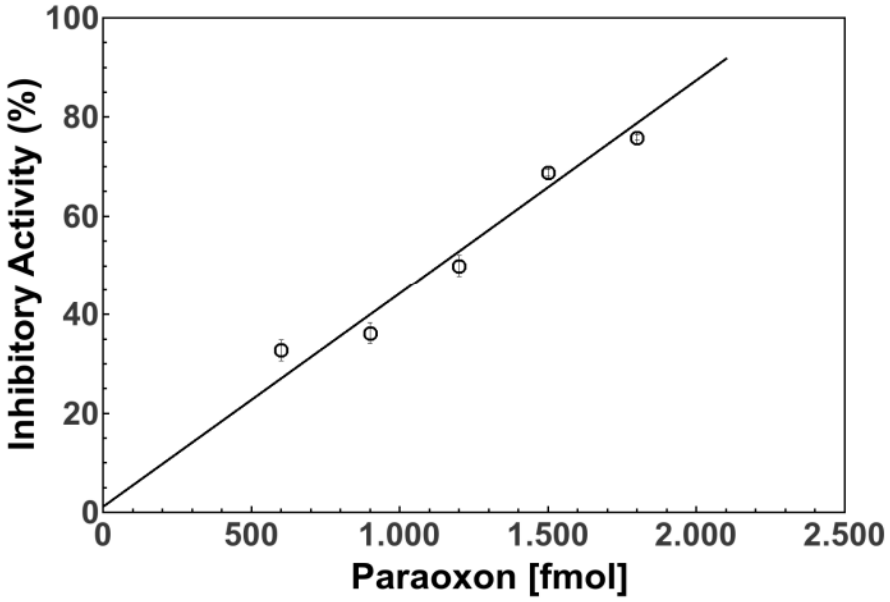

Figure 3.26. **Calibration curve of inhibitory activity at increasing concentration levels of Paraoxon in HEPES buffer in presence of enzyme EST2**

An inhibition pattern similar to the one obtained manually, was also observed by measuring EST2 residual activity in presence of oxidized pesticides by robotic workstation (Figure 3.27a). The observed variability within 20% difference, in the automated assay with respect to non-automated measurements, was prevalently related to differences in the incubation times and in the reproducibility of dispensation. Although manual operations have been conducted under controlled conditions, the reproducibility of assays is conditioned by the ability of operator in combination with instrumental errors. In the automated assay the reproducibility of dispensation is assured by the air displacement pipetting of the Hamilton workstation to achieve superior measurement accuracy. In addition, the pipette channels and tips are designed to fit precisely together to eliminate tip distortion and ensure the

highest accuracy during liquid handling steps (less of 0.1% error). Moreover, anti-droplet control and liquid level detection technologies safeguard samples and results integrity. Furthermore, the automated assay granted high reproducibility in the time of incubation and measuring, because the system is software supervised and all processes of dispensation, incubation, and assay, are scheduled. Also, the automated process allowed to easily collect data at different times in order to obtain a complete inhibition kinetic for each inhibitor.

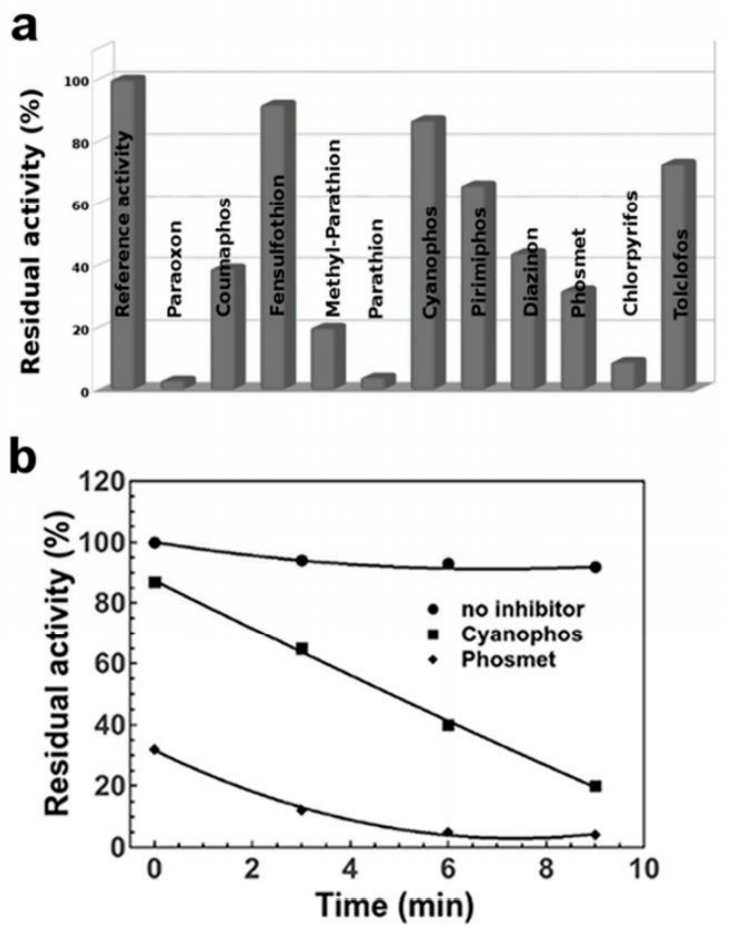

Figure 3.27. **Robotic approach for OP detection in water. (a) Plot of EST2 residual activity in absence (Reference activity) and presence of different pesticides oxidized with NBS, measured using the robotic workstation. (b) Plot of EST2 residual activity measured using the robotic workstation at different inhibition times in absence and in presence of cyanophos and phosmet oxidized with NBS**

In agreement with the irreversible inhibitory action of the enzyme catalytic-site by pesticides, we observed a time dependent inactivation of EST2 activity (Figure 3.27b). Differently from the fast inhibition of EST2 activity in presence of paraoxon, we observed a slowed rate of inhibition for some NBS-treated thio-OPs, requiring from seconds to a few minutes for the complete inhibition of enzyme activity. These differences could also explain the different results obtained in the non-automated assay.

A delay in the assay condition due to the manual operations could give different results in the determination of the residual activity at some time resulting in the lack of synchronization between time and residual activity, reducing the accuracy of the determination.

The time dependent inactivation for each thio-OP cannot extensively describe the EST2 ability to covalently bind these compounds, several parameters can be determined, such as the affinity constants. Thus, this is the start point for a future biochemical characterization of these group of pesticides that in this work we have demonstrated can inhibit the EST2 activity.

Pesticide pseudo fingerprint

The extension of the incubation time of EST2 in presence of oxidized pesticides, revealed differences in the shape of the curves for the residual activity decrease, indicating a distinctive inhibition kinetics for the different pesticides (Figure 3.27b). These differences in the inhibition efficiency are probably related to steric hindrance of different OP molecules, as previously demonstrated for some of them [75]. The differences in the inhibition kinetics could be used for the characterization and identifying of pesticides.

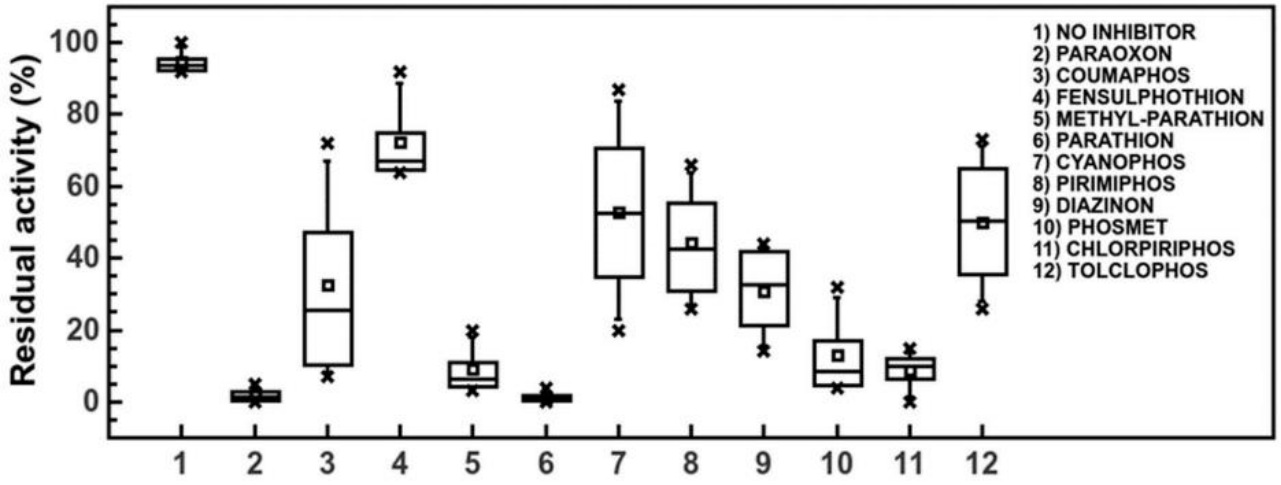

Figure 3.28. **Box-plot of EST2 residual activity in presence of different NBS-oxidized pesticides measured in the range of time from 0 to 9 min by the robotic workstation**

In Figure 3.28, a box-plot of EST2 residual activity in presence of NBS-oxidized pesticides measured by the robotic workstation, is illustrated. Except for paraoxon and parathion, almost all the pesticides show a distinctive distribution of the residual activity permitting a pseudo-fingerprinting of compounds. The identification is still limited to the presence of a single pesticide, but the development of mathematical models in data processing software will help in circumventing such limitation by identifying the key compound features. In addition, the development of multi-enzymatic devices,

carrying bioreceptors with different specificity towards OP compounds, such as EST2 mutants [114], could provide supplementary parameters in order to discriminate between the different pesticides present in a complex solution more similar to real food samples. Moreover, being able to obtain, by the automated approach, lot of data in a very short time, the use of machine learning or deep learning methods for pesticide recognition could be hypothesized. In fact, these techniques usually based on artificial neural networks, require a large amount of data both to be used as "training" data and data for algorithm validation, in order to perform a task, for example, to predict the pesticide composition in a sample.

3.3.2. Determination of organophosphates in urine

4-MUBu Fluorescence Measurements and the Determination of Kinetics Parameters

The sensitivity of fluorescence detection is approximately one thousand times greater than absorption spectrophotometric methods. This has led to greater limits of detection simultaneously using less sample material. In order to develop detection methods able to discriminate smaller amounts of organophosphate (OP) inhibitors, the conditions for the measurements of EST2 activity were set up using 4-MUBu as a fluorogenic substrate. One of the first uses of 4-MUBu as fluorogenic substrate has been described in 1977 to detect mycobacterial esterase easily and rapidly [123]. The use of this substrate has allowed to detect very low lipolytic activity [19], while testing multiple samples simultaneously and maintaining short incubation times. In the study, a suitable resistance of 4-MUBu to the spontaneous hydrolysis (Figure 3.29A) at neutral pH was observed, using 25 mM HEPES pH 7.0 (curve 1 in Figure 3.30A), a zwitterionic organic chemical buffer. All the further experiments were carried out in these conditions. In agreement with an enzyme-substrate reaction, as described in the Figure 3.29B, a linear increase of the signal of fluorescence intensity after the addition of EST2 to the 4-MUBu solution was observed, indicating the release of 4-MU (curve 2 in Figure 3.30A). A coefficient value of 57.16 ± 1.03 fluorescence units for pmol of 4-MU, was determined by using a calibration curve in HEPES (Figure 3.30B). By measuring the amount of 4-MU released by EST2 activity at different 4-MUBu concentrations, determination of the kinetic constant values is possible with this substrate. The K_M and k_{cat} values of 221.6 μM and 30.7×102 s^{-1}, respectively, were determined for the hydrolysis of 4-MUBu by measuring the EST2 activity at 30 °C in 25 mM HEPES buffer pH 7.0.

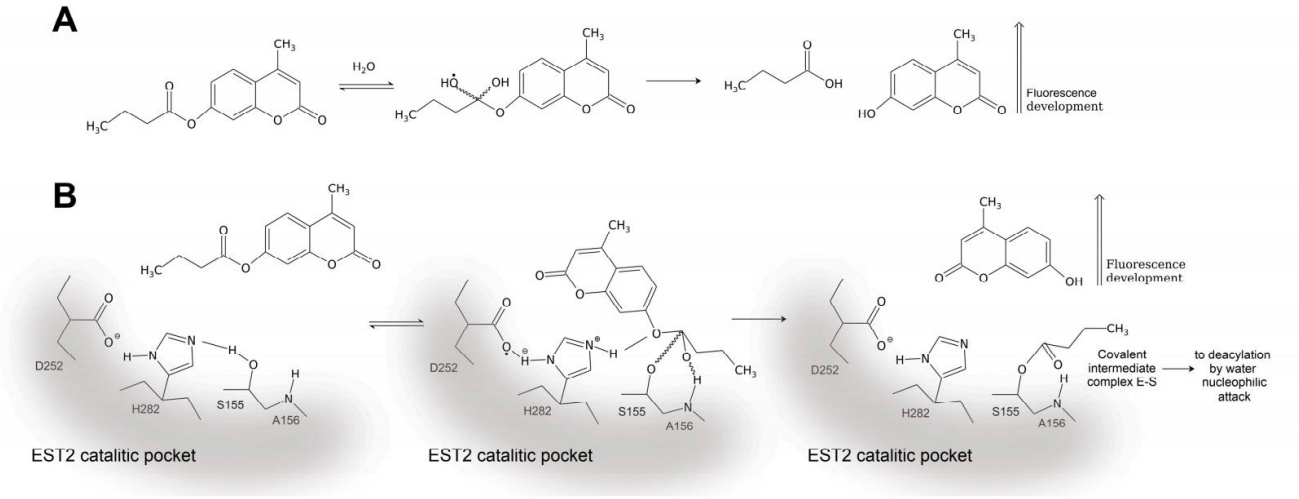

Figure 3.29. **Mechanism of (A) the spontaneous hydrolysis of 4-MUBu, in HEPES buffer and (B) by enzymatic hydrolysis after the addition of EST2; the release of 4-MU results in the increase of fluorescence**

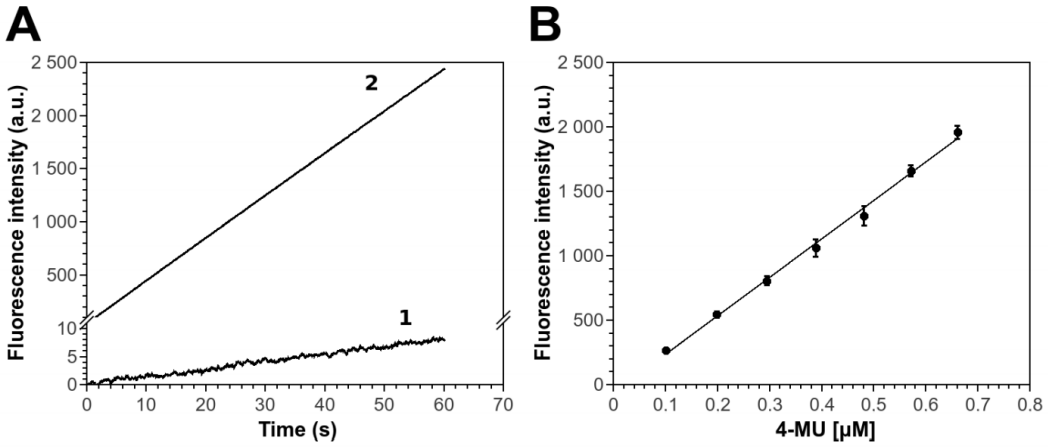

Figure 3.30. **EST2 assay using 4-MUBu. (A) Fluorescence development of 4-MUBu by spontaneous hydrolysis in HEPES buffer (curve 1) and enzymatic hydrolysis after the addition of EST2 (curve 2). (B) Calibration curve of fluorescence intensity at increasing concentrations of 4-MU in HEPES buffer for the calculation of the coefficient value necessary for the determination of the amount of reaction products from the enzymatic hydrolysis (R^2 = 0.996, SD from n=3)**

The EST2 kinetic constants determined using 4-MUBu as a substrate were compared, with the ones determined on p-nitrophenyl butyrate, a chromogenic substrate with the same carbon chain length of the acidic moiety. The values obtained on fluorogenic substrate differ about 2-fold with respect to the kinetic constants previously determined using p-Nitrophenyl butyrate as substrate in 40 mM sodium phosphate pH 7.0 at 70 °C (90 ± 6 µM and 18.5 ± 0.9 × 102 s^{-1}) [124]. The different affinity

could be explained by used an assay temperature of 40 °C lower than the optimal one. This makes the protein structure more rigid to the binding, with the substrate generally decreasing the enzyme affinity. However, the enzyme characterization at 30 °C is justified for its use at room temperature as a biosensing device. Moreover, the greater steric hindrance of the two phenolic rings of 4-MUBu with respect to the single ring of p-nitrophenyl ester in the chromogenic substrates could play a different role in the binding at the active site of the enzyme.

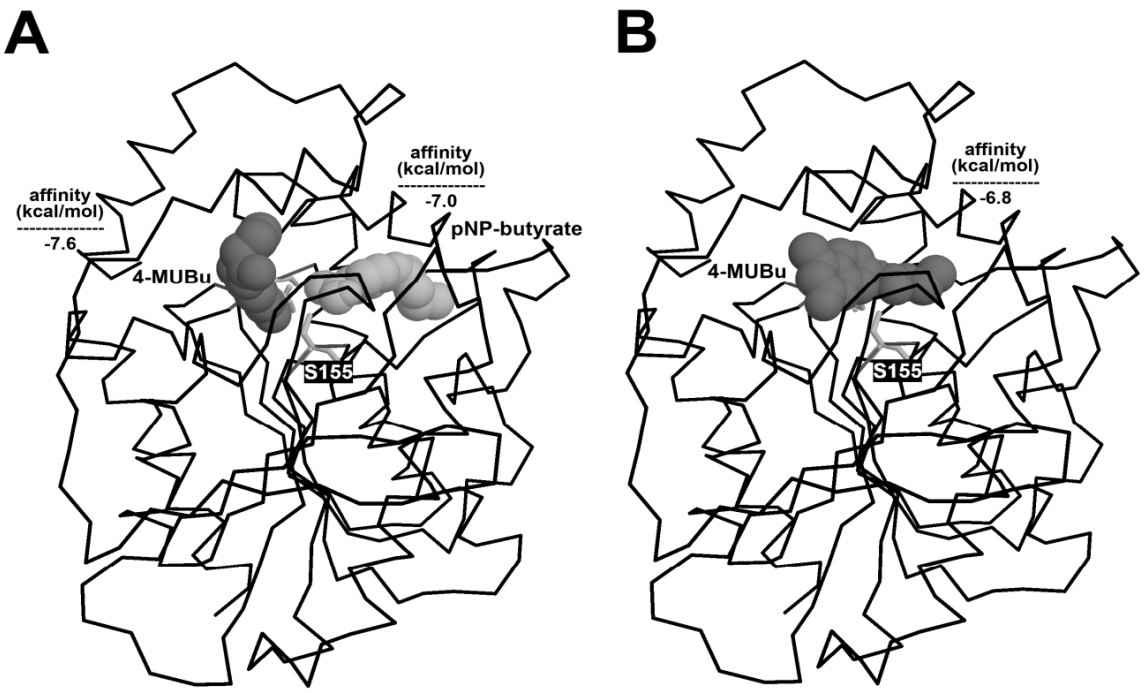

Figure 3.31. **Docking analysis with binding free energies (shown as kcal mol^{-1}) of complexes between EST2 and substrates. Trace representation of EST2 backbone (black), residues in the catalytic site are represented as stick in gray, the substrates MUBu (dark gray) and p-nitrophenyl-butyrate (gray) are depicted as a van der Waals surface (WDV) representation. (A) Accommodation of 4-MUBu in the alcohol pocket of EST2, with respect to the p-nitrophenyl-butyrate bonding to the acyl one; and (B) arrangement of 4-MUBu in the catalytic site with less affinity with respect to the alcohol pocket**

Notably, the poses with the lowest energy of binding, or binding affinity, determined for both substrates by docking simulations, highlights unexpected accommodation of 4-MUBu in the alcohol-binding site of the enzyme, differently from the p-Nitrophenyl butyrate which is accommodated in the acyl pocket one (Figure 3.31A).

This result is in accordance with the substrate-induced switch demonstrated for long chain substrates (with high steric hindrance) in the EST2 reaction mechanism [125]. Further, less binding

free energy (about 1 kcal mol^{-1}), with a distance from the best pose determined by the root-mean-square deviation (RMSD) lower and upper bound of 4.326 and 7.494, respectively, is measured for the binding of the two phenolic rings of 4-MUBu into the acyl-binding pocket of the EST2 catalytic site (Figure 3.31B). The energy released in the formation of noncovalent bonds is only 1−5 kcal mol^{-1}, much less than the bond energies of single covalent bonds; moreover, the average kinetic energy of molecules at room temperature (25 °C) is about 0.6 kcal mol^{-1}. Considering the energies involved in these interactions, the allocation in the alcohol pocket is favorite with respect to the acyl one. Despite the different affinity shown towards the fluorescent substrate by EST2, the catalysis efficiency was almost doubled, and, most importantly, the assay sensitivity for substrate was improved about 20 times. In fact, at room temperature, using colorimetric substrates, measurements with a stable signal for the enzymatic activity were possible by assaying 29.2 pmol of enzyme [118]. Further assays using 1.46 pmol of EST2 were highly reproducible at similar conditions of pH and temperature (30 °C).

EST2 inhibition with paraoxon determined by fluorescence assay

The EST2 inhibition mechanism is proposed in [119], taking into account the widely described reaction mechanism [125] (Figure 3.32A). In summary, the affinity constant towards the inhibitor (K_i) represents the K_M constant for the substrate, while the inhibition rate constant k_i corresponds to the acylation constant k_2. The rate constant of deacylation (k_{cat}) is very high in the enzymatic reaction on the substrate, but on the contrary is very small in the irreversible inhibition kinetics, hence freezing the enzyme-inhibitor intermediately into a very stable complex (Figure 3.32A).

The EST2 affinity towards paraoxon results higher than that of synthetic substrate, meaning that the K_i is not determinable by using the conventional method of pseudo-first-order kinetics [119] for the determination of irreversible inhibition constants. The formation of the covalent bond between the side-chain of serine residue 155, in the catalytic site, and the reactive organophosphate group of paraoxon [119], is favored (Figure 3.32B).

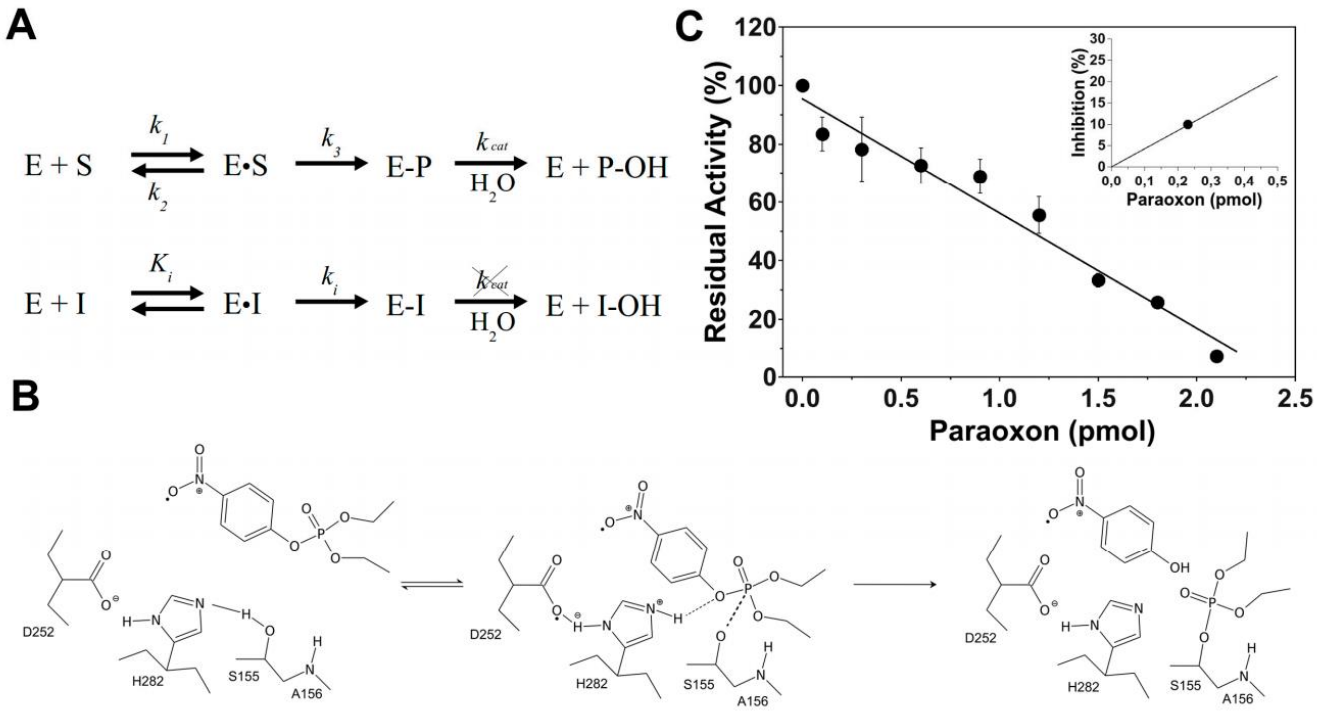

Figure 3.32. **Inhibition of EST2 by diethyl (4-nitrophenyl) phosphate (paraoxon). Description of the kinetic (A) and molecular (B) mechanism of the inhibition of EST2 by paraoxon. The inhibited enzyme is frozen in a stable covalent intermediate with the organophosphate group of pesticide. (C) Plot of EST2 residual activity in presence of an increasing concentration of paraoxon. In the insert, the percentage of the inhibition of EST2 in the presence of this increasing concentration of paraoxon. The error bars represent the standard deviation (SD) from three independent experiments**

This covalent intermediate results in a very stable conformation, that irreversibly inhibits the enzyme, requiring a stronger nucleophilic group, with respect to water, in order to complete the next diacylation step to release the free enzyme [118,119]. In particular, the balance of this reaction is completely shifted towards the formation of the covalent intermediate, in a matter of few seconds, obtaining the full inhibition of an amount of enzyme corresponding to the quantity of paraoxon added in a concentration ratio 1:1 [118,119]. Taking advantage of the high affinity of EST2 towards these compounds, allows to utilize the residual activity of the enzyme after irreversible inhibition for the fast detection and quantification of OPs in human and environmental samples. The fluorometric assay allows us to measure the EST2 residual activity in the presence of very low concentration levels of paraoxon in the range from 100 to 2100 fmol (Figure 3.32C). The coefficient of determination (R^2 > 0.96), determined for the residual activity plotted against paraoxon concentration, indicated a good linear response for the determination of the residual activity.

The calculation of the percentage of inhibition, after incubation with paraoxon in the experimental conditions, allowed to calculate a value of 230 fmol for the tested pesticide at a 10% of inhibition (insert in Figure 3.32C). Compared to previous work [118], the improved the limit of detection for paraoxon using EST2 was about 80-fold, reaching a quantification limit of 125 fmol. The calculated quantification limit is comparable to more sophisticated analytical systems used, such as mass spectrometers.

Paraoxon determination in human fluid samples

The main problem related to the use of a substrate for esterase activity is represented by the presence of lipase activities in human fluids. In fact, the measurements carried out on assay solutions containing serum aliquots from human blood highlight that is it impossible to measure the EST2 activity due to the massive presence of lipase activities in the blood, which hydrolyzes the 4-MUBu. New methodologies need to be developed in order to selectively inhibit the lipase activities, using inhibitors inactive on EST2, or by removing them from the samples using a preliminary protein aggregation/precipitation step, that allows for the measurement of EST2 residual activity in human serum for the detection of OP metabolites in blood. Instead, the low amount of lipase activities, less than 1 unit dl^{-1} in 24-hour urine samples from healthy donors, has made it possible to measure the EST2 activity in samples of this human fluid. In order to verify if urine affects the EST2 activity, enzymatic activity was measured at increasing concentrations of urine (Figure 3.33A).

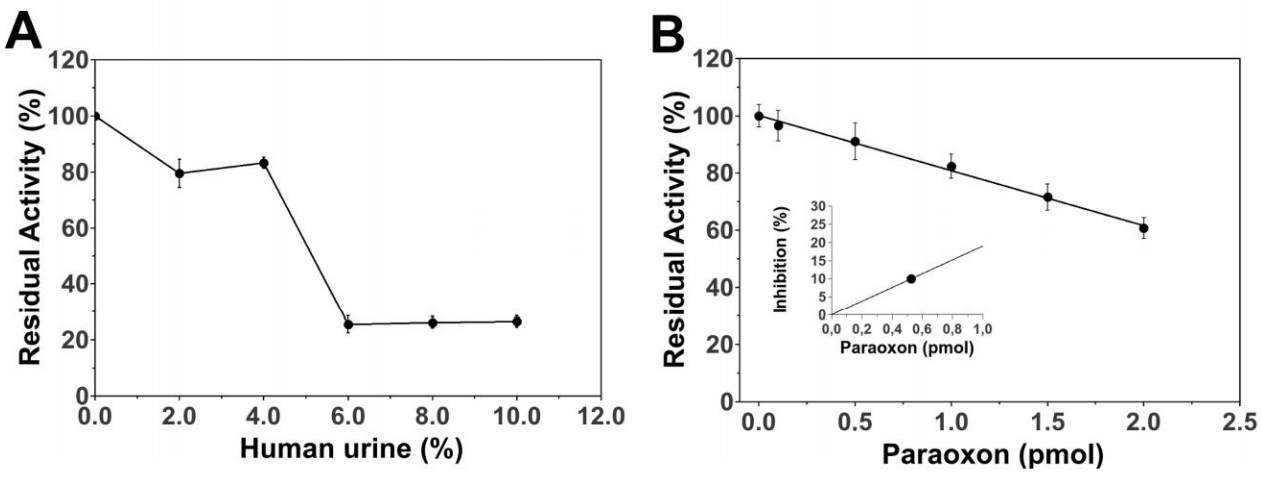

Figure 3.33. **Determination of paraoxon in human urine. (A) Plot of EST2 residual activity in presence of increased amount of urine. (B) Plot of EST2 residual activity in 4% urine, in the presence of the increasing concentration of paraoxon. In the insert, the percentage of inhibition of EST2 in the presence of this increasing concentration of paraoxon. The error bars represent the SD from three independent experiments**

EST2 activity is affected by the addition of urine concentrations higher than 4%, so it was used as an appropriate final concentration for the inhibition measurements. A decrease of enzymatic activity was measured after EST2 incubation in the presence of a mixture containing 4% urine and paraoxon (Figure 3.33B). The enzyme did not appear to be completely inhibited by a stoichiometric amount of paraoxon, in agreement with previous data on complex matrices, such as fruit juices [118].

Probably, as described in the irreversible inhibition kinetics [119], the retained enzyme activity could be explained by the presence of protecting substances that compete with the irreversible inhibitor for the same binding site. Since human urine is a complex solution that reflects the physiological state of an individual, we cannot exclude that in some samples, i.e., from individual following specific diets of under medication, there could be chemicals present which could regenerate the enzyme activity after inhibition or affect the fluorescent emission of 4-MU (by fluorescence quenching or enhancement), thus yielding some false positive or negative samples.

Exploiting the high specificity of EST2 towards paraoxon, the improved sensitivity of the fluorescence assay on the substrate and the low amount of urine (only 4%) required for the measurement, we can reduce the effects coming from the presence of unwanted metabolites in urine samples. Moreover, in order to completely solve the exposed problems, two fast reference tests (quality control samples) could be included in the measurement in order to determine the 100% activity in presence of the urine sample, and the residual activity at a known paraoxon concentration. The equation of linear regression determined for the residual activity against the paraoxon concentrations showed $R^2 > 0.99$, indicating a good linear response for the determination of the residual activity in the presence of 4% urine. From the measurements an amount of 524 ± 14.15 fmol of paraoxon was recognized at 10% inhibition, with a LOQ of 262 ± 8.12 pmol mL^{-1} of paraoxon in urine and the possibility of similar detection limits in other bodily fluids [126]. These values were comparable to the amount determined by LC and GC-MS in urine samples of donors exposed to OPs [127].

CONCLUSIONS

1. The developed analytical method for the determination of multi-class anticoccidial drug residues in poultry and egg matrix using UHPLC-Orbitrap-HRMS with FS-ddMS^2 detection ensures reliable detection of these veterinary drug residues at or below the regulated levels. The method was thoroughly optimized and validated according to the EU Commission Regulation 2002/657/EC to meet the suitability criteria for veterinary drug screening, quality control programs and occurrence studies. The main advantage of the proposed method is the relatively quick and generic sample preparation procedure with indisputable confirmatory abilities.

2. A step by step optimization procedure was employed in our work and represents a systematic approach for the optimization of Orbitrap MS parameters. We have highlighted the significance and influence of a wide range of parameters on the MS response to selected veterinary drugs. Our design of experiments (DoE) approach allowed to find the most suitable values of parameters and to enhance the signal intensity by 10%–99% for 16 out of the 17 analyzed compounds.

3. High selectivity was achieved by the application of FS-ddMS^2 workflow with a suspect inclusion list, acquiring simultaneous full scan and MS^2 spectra. FS detection was chosen over targeted quantification (t-SIM and PRM), to allow for further broadening of the scope of veterinary drugs (suspects) analyzed and to enable the merging of distinct sample preparation methods.

4. The UHPLC-Orbitrap-HRMS methodology developed for the non-targeted suspect screening of potentially hazardous substances in food contact materials made of paper was shown to be useful and adaptable. This study provided evidence about the occurrence of substances of concern, some of which have been identified for the first time in paper materials, and the possibilities for the use of in silico modelling in the confines of rapid, priority-based hazard assessment.

5. Prioritization strategy by suspect mass lists yielded an initial identification of masses of interest and was followed by dedicated fragmentation experiments, which allowed for tentative identification of suspects by mass spectra library search and in silico fragmentation tools. The combination of MetFrag and SIRIUS 4 helped direct identification efforts by adding another layer of confidence in the structures annotated by spectra library search. In total, 27 substances were annotated with library spectra and in silico fragmentation annotation (level 2ab) and 13 substances were annotated solely based on high similarity of in silico fragmentation

spectra (level 2b). The identification criteria were not fulfilled for 34 substances and the confidence level was lowered in those cases.

6. There were no in vivo or in vitro toxicity data available for most of the tentatively identified compounds, consequently, to evaluate the hazardous potential of these substances, the theoretical toxicity was estimated by (Q)SAR predictions. Three and eight substances were determined as possible mutagens and carcinogens, respectively. The two positive mutagens (4,4′-oxydianiline and Michler's ketone) and three carcinogens (1,4-dihydroxybenzene, 4,4′-oxydianiline and Michler's ketone) were in accordance with the experimental results, provided by the OECD Toolbox. Some outliers were indicated as the experimental data showed positive tests, but the mean model scores yielded equivocal assignment for two mutagens (1,4-dihydroxybenzene and dimethoxy ethyl phthalate) and one carcinogen (benzophenone). Vice versa, in some cases (Q)SAR mean model scores predicted borderline positive or equivocal test results while experimental data is available showing no adverse reactions suggestive of toxicity.

7. While providing helpful evidence for hazard identification of "known unknowns", more research is required to continuously improve and experimentally validate mathematical models underlying (Q)SAR predictions. In addition, improved model averaging algorithms must be developed, which better account for cases in which conflicting predictions are obtained by the different tools employed.

8. A fluorescence-based automated robotic system employing esterase-2 from *Alicyclobacillus acidocaldarius* as a bioreceptor was developed for the detection of 11 chemically oxidized thio-organophosphates in aqueous matrices. Low detection limits of 10 pmol of inhibitors were achieved.

9. Differences in the shape of the inhibition curves were determined by measuring the decrease of esterase-2 residual activity over time. These differences could be used for the characterization and identification of thio-organophosphate pesticides, leading to a pseudo fingerprinting for each of these compounds.

10. The developed biosensor method was later adapted for the determination of a single residue (paraoxon) in human urine. Method robustness tests indicated the stability of esterase-2 in a diluted solution of 4% human urine. The determined concentration levels of paraoxon were accurately determined in the range from 0.1 to 2 pmol. The system sensitivity for OP detection is calculated at 524 ± 14.15 fmol of paraoxon recognized at 10% of inhibition, with an estimated limit of quantification of 262 ± 8.12 pmol mL^{-1}.

11. The research performed on biosensors represents a starting point to develop technologies for automated screening of chemical compounds in environmental, food or biological samples

ACKNOWLEDGEMENTS

The research in this thesis was made possible and supported by the European Food Risk Assessment Fellowship Programme (EU-FORA) granted from the European Food Safety Authority (EFSA), number GP/EFSA/AFSCO/2016/02-Ga7.

I would like to express profound gratitude to my thesis supervisors Dr. chem. Vadims Bartkevičs and Dr. chem. Arturs Vīksna for the invaluable professional guidance, inspiration, and support. Particularly grateful I am to Dr. Vadims, for allowing me to pursue my own research ideas. Special appreciation goes to my Italian supervisor Dr. Ferdinando Febbraio. The work on biosensors would not have been possible without his expertise, thoughtful guidance and, most importantly, hospitality.

Many thanks to my colleagues and collaborators from Institute "BIOR", especially to (soon to be) Ph.D. Ingus Pērkons for the valuable (occasionally scientific) discussions over the years. I thank to Dr. chem. Iveta Pugajeva, Dr. chem. Dzintars Začs and Dr. chem. Ingars Reinholds for setting a good example and the provided guidance over the years.

I would like to thank to all the EU-FORA 1st cohort family, especially Stelios Koulouris and Christoph Unger, for being there even when scattered all over Europe. Special thanks to Ph.D. Joseph Daniel Rasinger for the valuable collaboration after the fellowship.

Finally, I would like to thank my Dad and Brother for being an inspiration to undertake this journey.

REFERENCES

[1] B.J.A. Berendsen, T. Meijer, H.G.J. Mol, L. van Ginkel, M.W.F. Nielen, A global inter-laboratory study to assess acquisition modes for multi-compound confirmatory analysis of veterinary drugs using liquid chromatography coupled to triple quadrupole, time of flight and orbitrap mass spectrometry, Anal. Chim. Acta. 962 (2017) 60–72. doi:10.1016/j.aca.2017.01.046.

[2] Ł. Rajski, M. del Mar Gómez Ramos, A.R. Fernández-Alba, Evaluation of MS2 workflows in LC-Q-Orbitrap for pesticide multi-residue methods in fruits and vegetables, Anal. Bioanal. Chem. 409 (2017) 5389–5400. doi:10.1007/s00216-017-0220-2.

[3] L.S. Riter, O. Vitek, K.M. Gooding, B.D. Hodge, R.K. Julian, Statistical design of experiments as a tool in mass spectrometry, J. Mass Spectrom. 40 (2005) 565–579. doi:10.1002/jms.871.

[4] A. Kaufmann, S. Walker, Post-run target screening strategy for ultra high performance liquid chromatography coupled to Orbitrap based veterinary drug residue analysis in animal urine, J. Chromatogr. A. 1292 (2013) 104–110.

[5] European Parliament and Council, REGULATION (EC) No 1935/2004 on materials and articles intended to come into contact with food, Off. J. Eur. Union. 47 (2004) 4–17.

[6] . European Parliament and Council, Regulation (EU) No 10/2011 of the European Parliament and of the Council of 14 January 2011 on on plastic materials and articles intended to come into contact with food, Off. J. Eur. Union. 50 (2011) 1–89.

[7] European Commission, EC/282/2008 on recycled plastic materials and articles intended to come into contact with foods, Off. J. Eur. Communities. L86 (2008) 9–18.

[8] M. Van Bossuyt, E. Van Hoeck, T. Vanhaecke, V. Rogiers, B. Mertens, Printed paper and board food contact materials as a potential source of food contamination, Regul. Toxicol. Pharmacol. 81 (2016) 10–19. doi:10.1016/j.yrtph.2016.06.025.

[9] B. Geueke, C.C. Wagner, J. Muncke, Food contact substances and chemicals of concern: A comparison of inventories, Food Addit. Contam. - Part A Chem. Anal. Control. Expo. Risk Assess. 31 (2014) 1438–1450. doi:10.1080/19440049.2014.931600.

[10] L. Bengtström, A.K. Rosenmai, X. Trier, L.K. Jensen, K. Granby, A.M. Vinggaard, M. Driffield, J. Højslev Petersen, Non-targeted screening for contaminants in paper and board food-contact materials using effect-directed analysis and accurate mass spectrometry, Food Addit. Contam. - Part A Chem. Anal. Control. Expo. Risk Assess. 33 (2016) 1080–1093. doi:10.1080/19440049.2016.1184941.

[11] M. Van Bossuyt, E. Van Hoeck, G. Raitano, S. Manganelli, E. Braeken, G. Ates, T. Vanhaecke, S. Van Miert, E. Benfenati, B. Mertens, V. Rogiers, (Q)SAR tools for priority setting: A case

study with printed paper and board food contact material substances, Food Chem. Toxicol. 102 (2017) 109–119. doi:10.1016/j.fct.2017.02.002.

[12] A.K. Rosenmai, L. Bengtström, C. Taxvig, X. Trier, J.H. Petersen, T. Svingen, M.L. Binderup, van V.L. Barbara Medea Alice, M. Dybdahl, K. Granby, A.M. Vinggaard, An effect-directed strategy for characterizing emerging chemicals in food contact materials made from paper and board, Food Chem. Toxicol. 106 (2017) 250–259. doi:10.1016/j.fct.2017.05.061.

[13] Council of the EU, Council adopts ban on single-use plastics, (2019). https://www.consilium.europa.eu/en/press/press-releases/2019/05/21/council-adopts-ban-on-single-use-plastics/ (accessed August 1, 2020).

[14] N.I. Rousis, R. Bade, L. Bijlsma, E. Zuccato, J. V. Sancho, F. Hernandez, S. Castiglioni, Monitoring a large number of pesticides and transformation products in water samples from Spain and Italy, Environ. Res. 156 (2017) 31–38. doi:10.1016/j.envres.2017.03.013.

[15] R. Meffe, I. de Bustamante, Emerging organic contaminants in surface water and groundwater: A first overview of the situation in Italy, Sci. Total Environ. 481 (2014) 280–295. doi:10.1016/j.scitotenv.2014.02.053.

[16] T. Matsushita, A. Morimoto, T. Kuriyama, E. Matsumoto, Y. Matsui, N. Shirasaki, T. Kondo, H. Takanashi, T. Kameya, Removals of pesticides and pesticide transformation products during drinking water treatment processes and their impact on mutagen formation potential after chlorination, Water Res. 138 (2018) 67–76. doi:10.1016/j.watres.2018.01.028.

[17] G.K. Sidhu, S. Singh, V. Kumar, D.S. Dhanjal, S. Datta, J. Singh, Toxicity, monitoring and biodegradation of organophosphate pesticides: A review, Crit. Rev. Environ. Sci. Technol. 49 (2019) 1135–1187. doi:10.1080/10643389.2019.1565554.

[18] A. Sarkar, K.D. Sarkar, V. Amrutha, K. Dutta, An overview of enzyme-based biosensors for environmental monitoring, Elsevier Inc., 2019. doi:10.1016/B978-0-12-814679-8.00015-7.

[19] I.M. Roberts, Hydrolysis of 4-methylumbelliferyl butyrate: A convenient and sensitive fluorescent assay for lipase activity, Lipids. 20 (1985) 243–247. doi:10.1007/BF02534195.

[20] E.L. Schymanski, H.P. Singer, J. Slobodnik, I.M. Ipolyi, P. Oswald, M. Krauss, T. Schulze, P. Haglund, T. Letzel, S. Grosse, N.S. Thomaidis, A. Bletsou, C. Zwiener, M. Ibáñez, T. Portolés, R. De Boer, M.J. Reid, M. Onghena, U. Kunkel, W. Schulz, A. Guillon, N. Noyon, G. Leroy, P. Bados, S. Bogialli, D. Stipaničev, P. Rostkowski, J. Hollender, Non-target screening with high-resolution mass spectrometry: Critical review using a collaborative trial on water analysis, Anal. Bioanal. Chem. 407 (2015) 6237–6255. doi:10.1007/s00216-015-8681-7.

[21] J. Hollender, B. van Bavel, V. Dulio, E. Farmen, K. Furtmann, J. Koschorreck, U. Kunkel, M. Krauss, J. Munthe, M. Schlabach, J. Slobodnik, G. Stroomberg, T. Ternes, N.S. Thomaidis, A. Togola, V. Tornero, High resolution mass spectrometry-based non-target screening can support

regulatory environmental monitoring and chemicals management, Environ. Sci. Eur. 31 (2019). doi:10.1186/s12302-019-0225-x.

[22] E.L. Schymanski, J. Jeon, R. Gulde, K. Fenner, M. Ruff, H.P. Singer, J. Hollender, Identifying small molecules via high resolution mass spectrometry: Communicating confidence, Environ. Sci. Technol. 48 (2014) 2097–2098. doi:10.1021/es5002105.

[23] B.Y.L. Peisl, E.L. Schymanski, P. Wilmes, Dark matter in host-microbiome metabolomics: Tackling the unknowns–A review, Anal. Chim. Acta. 1037 (2018) 13–27. doi:10.1016/j.aca.2017.12.034.

[24] M.S. Filigenzi, N. Ehrke, L.S. Aston, R.H. Poppenga, Evaluation of a rapid screening method for chemical contaminants of concern in four food-related matrices using QuEChERS extraction, UHPLC and high resolution mass spectrometry, Food Addit. Contam. - Part A Chem. Anal. Control. Expo. Risk Assess. 28 (2011) 1324–1339. doi:10.1080/19440049.2011.604796.

[25] A.M. Knolhoff, C.N. Kneapler, T.R. Croley, Optimized chemical coverage and data quality for non-targeted screening applications using liquid chromatography/high-resolution mass spectrometry, Anal. Chim. Acta. 1066 (2019) 93–101. doi:10.1016/j.aca.2019.03.032.

[26] G. Aichinger, N. Živná, E. Varga, F. Crudo, B. Warth, D. Marko, Microfiltration results in the loss of analytes and affects the in vitro genotoxicity of a complex mixture of Alternaria toxins, Mycotoxin Res. (2020). doi:10.1007/s12550-020-00405-9.

[27] M. Rychlik, H. Lepper, C. Weidner, S. Asam, Risk evaluation of the Alternaria mycotoxin tenuazonic acid in foods for adults and infants and subsequent risk management, Food Control. 68 (2016) 181–185. doi:10.1016/j.foodcont.2016.03.035.

[28] A. Furey, M. Moriarty, V. Bane, B. Kinsella, M. Lehane, Ion suppression; A critical review on causes, evaluation, prevention and applications, Talanta. 115 (2013) 104–122. doi:10.1016/j.talanta.2013.03.048.

[29] M. Hu, M. Krauss, W. Brack, T. Schulze, Optimization of LC-Orbitrap-HRMS acquisition and MZmine 2 data processing for nontarget screening of environmental samples using design of experiments, Anal. Bioanal. Chem. 408 (2016) 7905–7915. doi:10.1007/s00216-016-9919-8.

[30] J. Pezzatti, J. Boccard, S. Codesido, Y. Gagnebin, A. Joshi, D. Picard, V. González-Ruiz, S. Rudaz, Implementation of liquid chromatography–high resolution mass spectrometry methods for untargeted metabolomic analyses of biological samples: A tutorial, Anal. Chim. Acta. 1105 (2020) 28–44. doi:10.1016/j.aca.2019.12.062.

[31] T. Pluskal, S. Castillo, A. Villar-Briones, M. Orešič, MZmine 2: Modular framework for processing, visualizing, and analyzing mass spectrometry-based molecular profile data, BMC Bioinformatics. 11 (2010). doi:10.1186/1471-2105-11-395.

[32] C.A. Smith, E.J. Want, G. O'Maille, R. Abagyan, G. Siuzdak, XCMS: Processing Mass Spectrometry Data for Metabolite Profiling Using Nonlinear Peak Alignment, Matching, and Identification, Anal. Chem. 78 (2006) 779–787. doi:10.1021/ac051437y.

[33] C.A. Chamberlain, V.Y. Rubio, T.J. Garrett, Impact of matrix effects and ionization efficiency in non - quantitative untargeted metabolomics, Metabolomics. (2019) 1–9. doi:10.1007/s11306-019-1597-z.

[34] R. Di Guida, J. Engel, J.W. Allwood, R.J.M. Weber, M.R. Jones, U. Sommer, M.R. Viant, W.B. Dunn, Non-targeted UHPLC-MS metabolomic data processing methods: a comparative investigation of normalisation, missing value imputation, transformation and scaling, Metabolomics. 12 (2016). doi:10.1007/s11306-016-1030-9.

[35] R. Goodacre, D. Broadhurst, A.K. Smilde, B.S. Kristal, J.D. Baker, R. Beger, C. Bessant, S. Connor, G. Capuani, A. Craig, Proposed minimum reporting standards for data analysis in metabolomics, Metabolomics. 3 (2007) 231–241.

[36] D. Broadhurst, R. Goodacre, S.N. Reinke, J. Kuligowski, I.D. Wilson, M.R. Lewis, W.B. Dunn, Guidelines and considerations for the use of system suitability and quality control samples in mass spectrometry assays applied in untargeted clinical metabolomic studies, Metabolomics. 14 (2018) 0. doi:10.1007/s11306-018-1367-3.

[37] B. Ng, N. Quinete, P.R. Gardinali, Assessing accuracy, precision and selectivity using quality controls for non-targeted analysis, Sci. Total Environ. 713 (2020) 136568. doi:10.1016/j.scitotenv.2020.136568.

[38] J.A. Kirwan, D.I. Broadhurst, R.L. Davidson, M.R. Viant, Characterising and correcting batch variation in an automated direct infusion mass spectrometry (DIMS) metabolomics workflow, Anal. Bioanal. Chem. 405 (2013) 5147–5157. doi:10.1007/s00216-013-6856-7.

[39] J.J.J. van der Hooft, R.C.H. de Vos, L. Ridder, J. Vervoort, R.J. Bino, Structural elucidation of low abundant metabolites in complex sample matrices, Metabolomics. 9 (2013) 1009–1018. doi:10.1007/s11306-013-0519-8.

[40] K. Dührkop, M. Fleischauer, M. Ludwig, A.A. Aksenov, A. V. Melnik, M. Meusel, P.C. Dorrestein, J. Rousu, S. Böcker, SIRIUS 4: a rapid tool for turning tandem mass spectra into metabolite structure information, Nat. Methods 2019. (2019) 1. doi:10.1038/s41592-019-0344-8.

[41] Y. Djoumbou-Feunang, A. Pon, N. Karu, J. Zheng, C. Li, D. Arndt, M. Gautam, F. Allen, D.S. Wishart, Cfm-id 3.0: Significantly improved esi-ms/ms prediction and compound identification, Metabolites. 9 (2019) 1–23. doi:10.3390/metabo9040072.

[42] S. Neumann, C. Ruttkies, J. Hollender, E.L. Schymanski, S. Wolf, MetFrag relaunched: incorporating strategies beyond in silico fragmentation, J. Cheminform. 8 (2016) 1–16.

doi:10.1186/s13321-016-0115-9.

[43] L. Moruz, L. Käll, Peptide retention time prediction, Mass Spectrom. Rev. 36 (2017) 615–623. doi:10.1002/mas.21488.

[44] R. Aalizadeh, M.C. Nika, N.S. Thomaidis, Development and application of retention time prediction models in the suspect and non-target screening of emerging contaminants, Elsevier B.V., 2019. doi:10.1016/j.jhazmat.2018.09.047.

[45] N. Bhalla, P. Jolly, N. Formisano, P. Estrela, Introduction to biosensors, Essays Biochem. 60 (2016) 1–8. doi:10.1042/EBC20150001.

[46] S. Liébana, G.A. Drago, Bioconjugation and stabilisation of biomolecules in biosensors, Essays Biochem. 60 (2016) 59–68. doi:10.1042/EBC20150007.

[47] I.Y. Jung, E.H. Lee, A.Y. Suh, S.J. Lee, H. Lee, Oligonucleotide-based biosensors for in vitro diagnostics and environmental hazard detection, Anal. Bioanal. Chem. 408 (2016) 2383–2406. doi:10.1007/s00216-015-9212-2.

[48] J.W. Lim, D. Ha, J. Lee, S.K. Lee, T. Kim, Review of micro/nanotechnologies for microbial biosensors, Front. Bioeng. Biotechnol. 3 (2015) 1–13. doi:10.3389/fbioe.2015.00061.

[49] P.K. Ferrigno, Non-antibody protein-based biosensors, Essays Biochem. 60 (2016) 19–25. doi:10.1042/EBC20150003.

[50] J.H. Kim, S.G. Hong, H.J. Sun, S. Ha, J. Kim, Precipitated and chemically-crosslinked laccase over polyaniline nanofiber for high performance phenol sensing, Chemosphere. 143 (2016) 142–147. doi:10.1016/j.chemosphere.2015.08.011.

[51] A. Sharma, G. Catanante, A. Hayat, G. Istamboulie, I. Ben Rejeb, S. Bhand, J.L. Marty, Development of structure switching aptamer assay for detection of aflatoxin M1 in milk sample, Talanta. 158 (2016) 35–41. doi:10.1016/j.talanta.2016.05.043.

[52] N.R. Shanmugam, S. Muthukumar, A.P. Selvam, S. Prasad, Electrochemical nanostructured ZnO biosensor for ultrasensitive detection of cardiac troponin-T, Nanomedicine. 11 (2016) 1345–1358. doi:10.2217/nnm-2016-0048.

[53] Y. Tang, F. Long, C. Gu, C. Wang, S. Han, M. He, Reusable split-aptamer-based biosensor for rapid detection of cocaine in serum by using an all-fiber evanescent wave optical biosensing platform, Anal. Chim. Acta. 933 (2016) 182–188. doi:10.1016/j.aca.2016.05.021.

[54] P. Damborský, J. Švitel, J. Katrlík, Optical biosensors, Essays Biochem. 60 (2016) 91–100. doi:10.1042/EBC20150010.

[55] J.L. Hammond, N. Formisano, P. Estrela, S. Carrara, J. Tkac, Electrochemical biosensors and nanobiosensors, Essays Biochem. 60 (2016) 69–80. doi:10.1042/EBC20150008.

[56] M.C. Lim, Y.R. Kim, Analytical applications of nanomaterials in monitoring biological and chemical contaminants in food, J. Microbiol. Biotechnol. 26 (2016) 1505–1516.

doi:10.4014/jmb.1605.05071.

[57] G. Rocchitta, A. Spanu, S. Babudieri, G. Latte, G. Madeddu, G. Galleri, S. Nuvoli, P. Bagella, M.I. Demartis, V. Fiore, R. Manetti, P.A. Serra, Enzyme biosensors for biomedical applications: Strategies for safeguarding analytical performances in biological fluids, Sensors (Switzerland). 16 (2016). doi:10.3390/s16060780.

[58] I. Palchetti, New trends in the design of enzyme-based biosensors for medical applications, Mini Rev. Med. Chem. 16 (2016) 1125–1133.

[59] J. Lee, J. Kim, S. Kim, D.H. Min, Biosensors based on graphene oxide and its biomedical application, Adv. Drug Deliv. Rev. 105 (2016) 275–287. doi:10.1016/j.addr.2016.06.001.

[60] C.S. Bever, J.X. Dong, N. Vasylieva, B. Barnych, Y. Cui, Z.L. Xu, B.D. Hammock, S.J. Gee, VHH antibodies: emerging reagents for the analysis of environmental chemicals, Anal. Bioanal. Chem. 408 (2016) 5985–6002. doi:10.1007/s00216-016-9585-x.

[61] W. He, S. Yuan, W.H. Zhong, M.A. Siddikee, C.C. Dai, Application of genetically engineered microbial whole-cell biosensors for combined chemosensing, Appl. Microbiol. Biotechnol. 100 (2016) 1109–1119. doi:10.1007/s00253-015-7160-6.

[62] X. Liang, C. Li, J. Zhu, X. Song, W. Yu, J. Zhang, S. Zhang, J. Shen, Z. Wang, Dihydropteroate synthase based sensor for screening multi-sulfonamides residue and its comparison with broad-specific antibody based immunoassay by molecular modeling analysis, Anal. Chim. Acta. 1050 (2019) 139–145. doi:10.1016/j.aca.2018.11.005.

[63] Q.T. Hua, N. Ruecha, Y. Hiruta, D. Citterio, Disposable electrochemical biosensor based on surface-modified screen-printed electrodes for organophosphorus pesticide analysis, Anal. Methods. 11 (2019) 3439–3445. doi:10.1039/c9ay00852g.

[64] J. Rusko, F. Febbraio, Development of an automated multienzymatic biosensor for risk assessment of pesticide contamination in water and food, EFSA J. 16 (2018). doi:10.2903/j.efsa.2018.e16084.

[65] S. Andreescu, J.L. Marty, Twenty years research in cholinesterase biosensors: From basic research to practical applications, Biomol. Eng. 23 (2006) 1–15. doi:10.1016/j.bioeng.2006.01.001.

[66] N. Jaffrezic-Renault, New trends in biosensors for organophosphorus pesticides, Sensors. 1 (2001) 60–74. doi:10.3390/s10100060.

[67] B. Prieto-Simón, M. Campàs, S. Andreescu, J.L. Marty, Trends in flow-based biosensing systems for pesticide assessment, Sensors. 6 (2006) 1161–1186. doi:10.3390/s6101161.

[68] Y. Chen, Organophosphate-induced brain damage: Mechanisms, neuropsychiatric and neurological consequences, and potential therapeutic strategies, Neurotoxicology. 33 (2012) 391–400. doi:10.1016/j.neuro.2012.03.011.

[69] G. Manco, R. Nucci, F. Febbraio, Use of Esterase Activities for the Detection of Chemical Neurotoxic Agents, Protein Pept. Lett. 16 (2009) 1225–1234. doi:10.2174/092986609789071252.

[70] C.S. Pundir, N. Chauhan, Acetylcholinesterase inhibition-based biosensors for pesticide determination: A review, Anal. Biochem. 429 (2012) 19–31. doi:10.1016/j.ab.2012.06.025.

[71] E.A. Songa, J.O. Okonkwo, Recent approaches to improving selectivity and sensitivity of enzyme-based biosensors for organophosphorus pesticides: A review, Talanta. 155 (2016) 289–304. doi:10.1016/j.talanta.2016.04.046.

[72] S. Sotiropoulou, D. Fournier, N.A. Chaniotakis, Genetically engineered acetylcholinesterase-based biosensor for attomolar detection of dichlorvos, Biosens. Bioelectron. 20 (2005) 2347–2352. doi:10.1016/j.bios.2004.08.026.

[73] C. Durrieu, Y. Ferro, M. Perullini, A. Gosset, M. Jobbágy, S.A. Bilmes, Feasibility of using a translucid inorganic hydrogel to build a biosensor using immobilized algal cells, Environ. Sci. Pollut. Res. 23 (2016) 9–13. doi:10.1007/s11356-015-5023-4.

[74] P. Jolly, P. Estrela, M. Ladomery, Oligonucleotide-based systems: DNA, microRNAs, DNA/RNA aptamers, Essays Biochem. 60 (2016) 27–35. doi:10.1042/EBC20150004.

[75] P. Carullo, G.P. Cetrangolo, L. Mandrich, G. Manco, F. Febbraio, Fluorescence spectroscopy approaches for the development of a real-time organophosphate detection system using an enzymatic sensor, Sensors (Switzerland). 15 (2015) 3932–3951. doi:10.3390/s150203932.

[76] C. Yan, F. Qi, S. Li, J. Xu, C. Liu, Z. Meng, L. Qiu, M. Xue, W. Lu, Z. Yan, Functionalized photonic crystal for the sensing of Sarin agents, Talanta. 159 (2016) 412–417. doi:10.1016/j.talanta.2016.06.045.

[77] 96/23/Ec Commission Decision, 96/23/EC COMMISSION DECISION of 12 August 2002 implementing Council Directive 96/23/EC concerning the performance of analytical methods and the interpretation of results (notified under document number C(2002) 3044)(Text withEEA relevance) (2002/657/EC), 96/23/Ec Comm. Decis. (2002) 29. doi:10.1017/CBO9781107415324.004.

[78] S. Croubels, S. De Baere, P. De Backer, Practical approach for the stability testing of veterinary drugs in solutions and in biological matrices during storage, Anal. Chim. Acta. 483 (2003) 419–427.

[79] A.D. McEachran, K. Mansouri, C. Grulke, E.L. Schymanski, C. Ruttkies, A.J. Williams, "MS-Ready" structures for non-targeted high-resolution mass spectrometry screening studies, J. Cheminform. 10 (2018) 1–16. doi:10.1186/s13321-018-0299-2.

[80] J. Rusko, Data for: Non-target and suspected-target screening for potentially hazardous chemicals in food contact materials: investigation of paper straws, (2019).

doi:doi/10.7910/DVN/MNY13S.

[81] J. Rusko, M. Jansons, I. Pugajeva, D. Zacs, V. Bartkevics, Development and optimization of confirmatory liquid chromatography—Orbitrap mass spectrometry method for the determination of 17 anticoccidials in poultry and eggs, J. Pharm. Biomed. Anal. 164 (2019) 402–412. doi:10.1016/j.jpba.2018.10.056.

[82] OECD QSAR Toolbox v4.3, (2019). http://www.oecd.org/env/ehs/risk-assessment/theoecdqsartoolbox.htm.

[83] F. Frenzel, T. Buhrke, I. Wenzel, J. Andrack, J. Hielscher, A. Lampen, Use of in silico models for prioritization of heat-induced food contaminants in mutagenicity and carcinogenicity testing, Arch. Toxicol. 91 (2017) 3157–3174. doi:10.1007/s00204-016-1924-3.

[84] E. Benfenati, A. Manganaro, G. Gini, VEGA-QSAR: AI inside a platform for predictive toxicology, CEUR Workshop Proc. 1107 (2013) 21–28.

[85] A. Maunz, M. Gütlein, M. Rautenberg, D. Vorgrimmler, D. Gebele, C. Helma, Lazar: A modular predictive toxicology framework, Front. Pharmacol. 4 APR (2013) 1–10. doi:10.3389/fphar.2013.00038.

[86] G. Manco, E. Adinolfi, F.M. Pisani, G. Ottolina, G. Carrea, M. Rossi, Overexpression and properties of a new thermophilic and thermostable esterase from Bacillus acidocaldarius with sequence similarity to hormone-sensitive lipase subfamily, Biochem. J. 332 (1998) 203–212. doi:10.1042/bj3320203.

[87] O. Trott, A.J. Olson, AutoDock Vina: Improving the speed and accuracy of docking with a new scoring function, efficient optimization, and multithreading, J. Comput. Chem. 32 (2009) NA-NA. doi:10.1002/jcc.21334.

[88] Schrödinger, LLC, The {PyMOL} Molecular Graphics System, Version~1.8, 2015.

[89] L. Clarke, M. Moloney, J. O'Mahony, R. O'Kennedy, M. Danaher, Determination of 20 coccidiostats in milk, duck muscle and non-avian muscle tissue using UHPLC-MS/MS, Food Addit. Contam. Part A. 30 (2013) 958–969. doi:10.1080/19440049.2013.794306.

[90] F. Barreto, C. Ribeiro, R.B. Hoff, T.D. Costa, A simple and high-throughput method for determination and confirmation of 14 coccidiostats in poultry muscle and eggs using liquid chromatography – quadrupole linear ion trap - tandem mass spectrometry (HPLC–QqLIT-MS/MS): Validation according to European , Talanta. 168 (2017) 43–51. doi:10.1016/j.talanta.2017.02.007.

[91] M. Moloney, L. Clarke, J. O'Mahony, A. Gadaj, R. O'Kennedy, M. Danaher, Determination of 20 coccidiostats in egg and avian muscle tissue using ultra high performance liquid chromatography–tandem mass spectrometry, J. Chromatogr. A. 1253 (2012) 94–104.

[92] S.M. Goulart, M.E.L.R. de Queiroz, A.A. Neves, J.H. de Queiroz, Low-temperature clean-up

method for the determination of pyrethroids in milk using gas chromatography with electron capture detection, Talanta. 75 (2008) 1320–1323.

[93] G. Rübensam, F. Barreto, R.B. Hoff, T.L. Kist, T.M. Pizzolato, A liquid–liquid extraction procedure followed by a low temperature purification step for the analysis of macrocyclic lactones in milk by liquid chromatography–tandem mass spectrometry and fluorescence detection, Anal. Chim. Acta. 705 (2011) 24–29.

[94] B. Shao, X. Wu, J. Zhang, H. Duan, X. Chu, Y. Wu, Development of a rapid LC–MS–MS method for multi-class determination of 14 coccidiostat residues in eggs and chicken, Chromatographia. 69 (2009) 1083–1088.

[95] B.F. Spisso, R.G. Ferreira, M.U. Pereira, M.A. Monteiro, T.Á. Cruz, R.P. Da Costa, A.M.B. Lima, A.W. Da Nobrega, Simultaneous determination of polyether ionophores, macrolides and lincosamides in hen eggs by liquid chromatography–electrospray ionization tandem mass spectrometry using a simple solvent extraction, Anal. Chim. Acta. 682 (2010) 82–92.

[96] K. George, U. Vincent, C. von Holst, Analysis of antimicrobial agents in pig feed by liquid chromatography coupled to orbitrap mass spectrometry, J. Chromatogr. A. 1293 (2013) 60–74. doi:10.1016/j.chroma.2013.03.078.

[97] M.U. Pereira, B.F. Spisso, S. do Couto Jacob, M.A. Monteiro, R.G. Ferreira, B. de Souza Carlos, A.W. da Nóbrega, Validation of a liquid chromatography–electrospray ionization tandem mass spectrometric method to determine six polyether ionophores in raw, UHT, pasteurized and powdered milk, Food Chem. 196 (2016) 130–137.

[98] P. Herrero, N. Cortés-Francisco, F. Borrull, J. Caixach, E. Pocurull, R.M. Marcé, Comparison of triple quadrupole mass spectrometry and Orbitrap high-resolution mass spectrometry in ultrahigh performance liquid chromatography for the determination of veterinary drugs in sewage: Benefits and drawbacks, J. Mass Spectrom. 49 (2014) 585–596. doi:10.1002/jms.3377.

[99] A. Martínez-Villalba, E. Moyano, C.P.B. Martins, M.T. Galceran, Fast liquid chromatography/tandem mass spectrometry (highly selective selected reaction monitoring) for the determination of toltrazuril and its metabolites in food, Anal. Bioanal. Chem. 397 (2010) 2893–2901.

[100] N. Lemonakis, A.L. Skaltsounis, A. Tsarbopoulos, E. Gikas, Optimization of parameters affecting signal intensity in an LTQ-orbitrap in negative ion mode: A design of experiments approach, Talanta. 147 (2016) 402–409. doi:10.1016/j.talanta.2015.10.009.

[101] P. Kumar, A. Rúbies, F. Centrich, M. Granados, N. Cortés-Francisco, J. Caixach, R. Companyó, Targeted analysis with benchtop quadrupole–orbitrap hybrid mass spectrometer: Application to determination of synthetic hormones in animal urine, Anal. Chim. Acta. 780 (2013) 65–73.

[102] J. Rusko, I. Perkons, J. Rasinger, V. Bartkevics, Non-target and suspected-target screening for

potentially hazardous chemicals in food contact materials: investigation of paper straws, Food Addit. Contam. Part A. (2020). doi:10.1080/19440049.2020.1711969.

[103] M.A. Lago, L.K. Ackerman, Identification of print-related contaminants in food packaging, Food Addit. Contam. - Part A Chem. Anal. Control. Expo. Risk Assess. 33 (2016) 518–529. doi:10.1080/19440049.2015.1136435.

[104] Q.B. Lin, T.J. Wang, H. Song, B. Li, Analysis of isothiazolinone biocides in paper for food packaging by ultra-high-performance liquid chromatography-tandem mass spectrometry, Food Addit. Contam. - Part A Chem. Anal. Control. Expo. Risk Assess. 27 (2010) 1775–1781. doi:10.1080/19440049.2010.521896.

[105] Y. Sanchis, C. Coscollà, M. Roca, V. Yusà, Target analysis of primary aromatic amines combined with a comprehensive screening of migrating substances in kitchen utensils by liquid chromatography-high resolution mass spectrometry, Talanta. 138 (2015) 290–297. doi:10.1016/j.talanta.2015.03.026.

[106] T. Jung, T.J. Simat, Multi-analyte methods for the detection of photoinitiators and amine synergists in food contact materials and foodstuffs - Part II: UHPLC-MS/MS analysis of materials and dry foods, Food Addit. Contam. - Part A Chem. Anal. Control. Expo. Risk Assess. 31 (2014) 743–766. doi:10.1080/19440049.2014.882519.

[107] A. Sanches-Silva, C. Andre, I. Castanheira, J.M. Cruz, S. Pastorelli, C. Simoneau, P. Paseiro-Losada, Study of the migration of photoinitiators used in printed food-packaging materials into food simulants, J. Agric. Food Chem. 57 (2009) 9516–9523. doi:10.1021/jf8035758.

[108] A. Vavrouš, L. Vápenka, J. Sosnovcová, K. Kejlová, K. Vrbík, D. Jírová, Method for analysis of 68 organic contaminants in food contact paper using gas and liquid chromatography coupled with tandem mass spectrometry, Food Control. 60 (2016) 221–229. doi:10.1016/j.foodcont.2015.07.043.

[109] A. Zülch, O. Piringer, Measurement and modelling of migration from paper and board into foodstuffs and dry food simulants, Food Addit. Contam. - Part A Chem. Anal. Control. Expo. Risk Assess. 27 (2010) 1306–1324. doi:10.1080/19440049.2010.483693.

[110] Y.S. Song, H.J. Park, V. Komolprasert, Analytical procedure for quantifying five compounds suspected as possible contaminants in recycled paper/paperboard for food packaging, J. Agric. Food Chem. 48 (2000) 5856–5859. doi:10.1021/jf000512x.

[111] B. Geueke, Dossier - Non-intentionally added substances (NIAS), Food Packag. Forum. (2018) 7. doi:10.5281/zenodo.1265331.

[112] A.M. Brunner, M.M.L. Dingemans, K.A. Baken, A.P. van Wezel, Prioritizing anthropogenic chemicals in drinking water and sources through combined use of mass spectrometry and ToxCast toxicity data, J. Hazard. Mater. 364 (2019) 332–338.

doi:10.1016/j.jhazmat.2018.10.044.

[113] J. Muncke, T. Backhaus, B. Geueke, M. V. Maffini, O.V. Martin, J.P. Myers, A.M. Soto, L. Trasande, X. Trier, M. Scheringer, Scientific challenges in the risk assessment of food contact materials, Environ. Health Perspect. 125 (2017) 1–9. doi:10.1289/EHP644.

[114] P. Carullo, M. Chino, G.P. Cetrangolo, S. Terreri, A. Lombardi, G. Manco, A. Cimmino, F. Febbraio, Direct detection of organophosphate compounds in water by a fluorescence-based biosensing device, Sensors Actuators, B Chem. 255 (2018) 3257–3266. doi:10.1016/j.snb.2017.09.152.

[115] M. Del Carlo, A. Pepe, M. Sergi, M. Mascini, A. Tarentini, D. Compagnone, Detection of coumaphos in honey using a screening method based on an electrochemical acetylcholinesterase bioassay, Talanta. 81 (2010) 76–81. doi:10.1016/j.talanta.2009.11.038.

[116] M.B. Kralj, P. Trebše, M. Franko, Oxidation as a pre-step in determination of organophosphorus compounds by the AChE-TLS bioassay, Acta Chim. Slov. 53 (2006) 43–51.

[117] C. jun Hou, K. He, L. min Yang, D. qun Huo, M. Yang, S. Huang, L. Zhang, C. hong Shen, Catalytic characteristics of plant-esterase from wheat flour, World J. Microbiol. Biotechnol. 28 (2012) 541–548. doi:10.1007/s11274-011-0845-9.

[118] F. Febbraio, L. Merone, G.P. Cetrangolo, M. Rossi, R. Nucci, G. Manco, Thermostable esterase 2 from Alicyclobacillus acidocaldarius as biosensor for the detection of organophosphate pesticides, Anal. Chem. 83 (2011) 1530–1536. doi:10.1021/ac102025z.

[119] F. Febbraio, S.E. D'Andrea, L. Mandrich, L. Merone, M. Rossi, R. Nucci, G. Manco, Irreversible inhibition of the thermophilic esterase EST2 from Alicyclobacillus acidocaldarius, Extremophiles. 12 (2008) 719–728. doi:10.1007/s00792-008-0179-1.

[120] M. Dixon, E.C. Webb, Enzymes, 3rd ed., Longman Group Limited London: New York, NY, USA, 1979.

[121] G.P. Cetrangolo, C. Gori, J. Rusko, S. Terreri, G. Manco, A. Cimmino, F. Febbraio, Determination of picomolar concentrations of paraoxon in human urine by fluorescence-based enzymatic assay, Sensors (Switzerland). 19 (2019) 4852. doi:10.3390/s19224852.

[122] D. Krstić, M. Colović, K. Krinulović, D. Djurić, V. Vasić, Inhibition of AChE by single and simultaneous exposure to malathion and its degradation products., Gen. Physiol. Biophys. 26 (2007) 247–253.

[123] J.M. Grange, A fluorigenic substrate for the rapid differentiation of Mycobacterium fortuitum from Mycobacterium chelonei on the basis of heat stable esterase activity, Tubercle. 58 (1977) 147–150.

[124] L. Mandrich, V. Menchise, V. Alterio, G. De Simone, C. Pedone, M. Rossi, G. Manco, Functional and structural features of the oxyanion hole in a thermophilic esterase from

Alicyclobacillus acidocaldarius, Proteins Struct. Funct. Genet. 71 (2008) 1721–1731. doi:10.1002/prot.21877.

[125] G. De Simone, L. Mandrich, V. Menchise, V. Giordano, F. Febbraio, M. Rossi, C. Pedone, G. Manco, A substrate-induced switch in the reaction mechanism of a thermophilic esterase: Kinetic evidences and structural basis, J. Biol. Chem. 279 (2004) 6815–6823. doi:10.1074/jbc.M307738200.

[126] S. Dulaurent, C. Moesch, P. Marquet, J.M. Gaulier, G. Lachâtre, Screening of pesticides in blood with liquid chromatography-linear ion trap mass spectrometry, Anal. Bioanal. Chem. 396 (2010) 2235–2249. doi:10.1007/s00216-009-3443-z.

[127] T. Berman, R. Goldsmith, T. Göen, J. Spungen, L. Novack, H. Levine, Y. Amitai, T. Shohat, I. Grotto, Urinary concentrations of organophosphate pesticide metabolites in adults in Israel: Demographic and dietary predictors, Environ. Int. 60 (2013) 183–189. doi:10.1016/j.envint.2013.08.008.

ANNEXES

Annex 1

The tolerance limits for anticoccidial drugs residues in poultry muscle and eggs and the working standard concentrations

	Tolerance limit (μg kg^{-1})		Mixed working standard concentration (μg mL^{-1})	
	Poultry muscle	Eggs	Poultry muscle	Eggs
APL	Not listed	Not listed	12.5	2.5
CLOP	Not listed	Not listed	12.5	2.5
DEC	500 [a]	20 [b]	125	5
DCZ	500 [c]	2 [d]	125	0.5
HAL	Not listed	6 [b]	2.5	1.5
LAS	60 [e]	150 [e]	15	37.5
MAD	30/2 [d,f]	12 [d]	0.5	3
MON	8 [g]	2 [h]	2	0.5
NAR	50 [i]	2 [b]	12.5	0.5
NEQ	Not listed	Not listed	2.5	2.5
DNC	50 [d]	300 [d]	12.5	75
ROB	200 [j]	25 [b]	50	6.25
SAL	5 [b]	3 [b]	1.25	0.75
SEM	Not listed	2 [b]	2.5	0.5
TOL	100 [k]	Not permitted [k]	25	2.5
TOLS	100 [k]	Not permitted [k]	25	2.5
TOLX	100 [k]	Not permitted [k]	25	2.5
DEC-d_5	ISTDs		5	5
DNC-d_8			12.5	12.5
HAL-$^{13}C_6$			5	5
NIG			5	5
ROB-d_8			5	5
TOL-d_3			5	5

[a] Commission Implementing Regulation No. 291/2014.
[b] Commission Regulation No. 124/2009.
[c] Commission Implementing Regulation No. 115/2013.
[d] Commission Regulation No. 610/2012.
[e] Commission Implementing Regulation No. 1277/2014.
[f] Commission Implementing Regulation No. 388/2011.
[g] Commission Implementing Regulation No. 495/2011.
[h] Commission Implementing Regulation No. 59/2013.
[i] Commission Regulation No. 885/2010.
[j] Commission Regulation No. 101/2009.
[k] Commission Regulation No. 37/2010.

Experimental design results for the optimization of source parameters. Values are normalized to the observed maximum (in green font, bold)

Runs	Center point levels					Analyte														Signal intensity score [a]
	A	B	C	D	E	APL	CLOP	DCZ	DEC	DNC	HAL	LAS	MAD	MON	NAR	NEQ	ROB	SAL	SEM	TOL	TOLS	TOLX	
1	0	0	0	-1	-1	59	49	44	4	31	73	8	2	2	2	61	71	3	3	26	36	42	516
2	0	0	-1	0	-1	42	39	22	1	28	63	2	1	1	1	44	55	1	1	10	16	10	337
3	0	-1	0	0	-1	78	72	51	28	60	63	47	46	34	20	71	75	30	41	37	62	64	879
4	-1	0	0	0	-1	74	68	83	59	35	70	73	27	33	22	76	72	37	42	80	76	65	992
5	1	0	0	0	-1	33	24	17	1	39	54	2	1	0	0	32	40	1	2	14	20	25	305
6	0	1	0	0	-1	40	34	44	2	40	67	2	1	1	0	41	63	1	1	34	44	35	450
7	0	0	1	0	-1	67	52	78	18	42	81	20	23	6	17	63	60	13	11	66	68	66	751
8	0	0	0	1	-1	31	37	54	5	36	56	9	2	2	2	50	54	3	5	40	49	36	471
9	0	0	-1	-1	0	57	47	22	1	35	83	1	1	1	1	48	54	1	1	11	18	15	397
10	0	-1	0	-1	0	87	77	58	18	67	95	22	14	11	7	94	90	13	18	46	61	76	854
11	-1	0	0	-1	0	91	80	91	32	58	88	47	11	12	11	95	78	25	27	75	96	99	1016
12	1	0	0	-1	0	44	36	40	1	36	69	2	1	1	0	43	59	1	1	28	33	37	432
13	0	1	0	-1	0	53	44	22	1	48	79	3	1	1	1	50	66	1	2	13	25	15	425
14	0	0	1	-1	0	77	63	77	14	48	99	15	34	16	20	77	85	10	14	67	81	79	876
15	0	-1	-1	0	0	69	57	41	14	80	81	19	22	9	14	60	84	6	13	23	27	35	654
16	-1	0	-1	0	0	61	67	43	12	63	80	18	18	10	9	64	69	18	12	38	62	43	687
17	1	0	-1	0	0	32	31	8	0	28	56	0	1	0	0	24	48	0	0	6	10	7	251
18	0	1	-1	0	0	30	33	3	0	24	64	0	0	0	0	22	54	0	0	2	5	2	239
19	-1	-1	0	0	0	**100**	**100**	54	**100**	88	81	**100**	**100**	**100**	**100**	94	89	**100**	**100**	47	73	94	1520
20	1	-1	0	0	0	67	58	72	33	43	69	23	27	19	16	64	73	22	24	57	53	43	763
21	0	0	0	0	0	66	58	50	29	79	88	12	6	6	3	70	59	5	11	34	60	62	698
22	0	0	0	0	0	62	53	58	20	60	83	12	5	4	3	66	82	6	8	47	65	59	693
23	0	0	0	0	0	57	50	69	10	69	77	8	2	3	2	65	75	4	5	54	68	63	681
24	0	0	0	0	0	54	50	28	3	83	83	5	1	1	1	66	84	2	2	23	36	53	575
25	0	0	0	0	0	51	48	40	6	79	78	7	2	2	1	65	80	3	3	32	50	59	606
26	0	0	0	0	0	52	42	59	4	54	80	11	2	2	2	50	65	4	5	43	53	51	579
27	-1	1	0	0	0	55	61	61	5	54	90	11	2	2	2	81	88	3	7	54	70	59	705
28	1	1	0	0	0	26	25	23	1	33	55	1	0	0	0	26	41	0	0	12	19	12	274
29	0	-1	1	0	0	96	83	84	43	77	93	43	86	42	43	86	93	74	44	77	91	**100**	1255
30	-1	0	1	0	0	88	89	**100**	93	70	97	80	63	45	58	96	**100**	44	77	**100**	**100**	92	1392
31	1	0	1	0	0	44	40	58	8	40	70	10	20	4	7	39	49	5	6	48	54	39	541
32	0	1	1	0	0	54	47	73	13	42	83	12	12	5	7	59	69	5	6	59	74	62	682
33	0	0	-1	1	0	27	39	13	1	49	67	1	1	1	0	45	58	0	1	10	17	10	340
34	0	-1	0	1	0	60	70	73	48	63	72	23	25	17	22	74	70	26	22	60	62	59	846
35	-1	0	0	1	0	48	58	89	32	45	72	51	26	17	20	52	60	17	35	92	79	77	870
36	1	0	0	1	0	22	29	28	3	24	51	3	1	1	1	37	45	1	1	19	30	18	314
37	0	1	0	1	0	20	29	33	1	35	60	2	0	0	0	31	45	1	1	22	34	23	337
38	0	0	1	1	0	41	50	85	17	53	74	16	28	13	20	66	72	19	12	78	80	77	801
39	0	0	0	-1	1	77	63	32	18	95	**100**	12	4	3	3	78	88	4	9	26	39	45	696
40	0	0	-1	0	1	50	50	18	1	67	86	1	1	1	1	53	70	1	1	11	21	20	453
41	0	-1	0	0	1	92	75	79	44	88	94	34	43	29	17	69	79	24	28	70	76	64	1005
42	-1	0	0	0	1	74	84	52	33	**100**	93	43	19	17	10	**100**	85	30	31	50	88	91	1000
43	1	0	0	0	1	35	38	44	6	66	64	2	1	1	1	48	53	2	1	31	39	35	467
44	0	1	0	0	1	40	42	39	1	74	77	1	0	0	0	49	64	1	1	30	53	49	521
45	0	0	1	0	1	66	65	94	52	78	90	17	42	14	25	80	81	24	14	89	93	83	1007
46	0	0	0	1	1	33	41	63	9	47	78	8	3	3	2	49	57	4	4	46	52	35	534

[a] Signal intensity score calculated as sum of relative intensities of all analytes acquired for corresponding method. Higher score is better. (n=5)

RSD figures for the data acquired from the optimization of source parameters. Values were normalized to the observed maximum intensities for corresponding analytes

Runs	Center point levels					Analyte														RSD score[a]
	A	B	C	D	E	APL	CLOP	DCZ	DEC	DNC	HAL	LAS	MAD	MON	NAR	NEQ	ROB	SAL	SEM	TOL	TOLS	TOLX	
1	0	0	0	-1	-1	4	7	12	6	51	28	77	61	48	78	3	7	72	80	42	40	55	671
2	0	0	-1	0	-1	10	4	25	27	12	12	75	47	49	93	12	19	93	55	57	44	35	669
3	0	-1	0	0	-1	6	4	54	13	19	11	34	18	8	6	8	19	6	24	44	8	5	287
4	-1	0	0	0	-1	4	6	9	18	18	11	3	28	19	18	1	21	17	28	7	18	12	238
5	1	0	0	0	-1	16	28	79	26	10	17	19	16	81	29	4	18	73	50	27	3	75	571
6	0	1	0	0	-1	13	6	12	35	21	6	10	84	93	20	10	9	46	41	14	12	11	443
7	0	0	1	0	-1	2	2	12	17	26	9	27	23	19	19	1	15	62	11	18	27	14	304
8	0	0	0	1	-1	9	1	29	33	9	9	39	17	17	20	3	4	17	54	57	58	11	387
9	0	0	-1	-1	0	7	14	18	20	48	19	27	13	11	31	22	64	29	16	63	40	57	499
10	0	-1	0	-1	0	2	2	58	21	29	7	39	42	62	11	4	8	16	46	56	9	36	448
11	-1	0	0	-1	0	5	8	25	13	4	22	48	41	53	60	9	14	99	76	21	8	15	521
12	1	0	0	-1	0	2	2	36	13	13	5	62	55	91	61	3	10	109	138	45	27	22	694
13	0	1	0	-1	0	7	3	36	24	38	5	79	79	72	66	9	16	66	76	23	37	56	692
14	0	0	1	-1	0	4	4	30	30	14	6	20	51	16	48	6	4	28	78	31	7	5	382
15	0	-1	-1	0	0	8	15	37	23	16	11	59	28	15	19	51	7	42	57	32	54	57	531
16	-1	0	-1	0	0	15	15	39	26	17	7	28	103	70	27	52	4	121	20	83	65	27	719
17	1	0	-1	0	0	5	4	61	19	20	5	21	50	68	4	19	20	1	65	71	85	77	595
18	0	1	-1	0	0	1	4	34	17	32	5	18	35	39	14	11	22	38	20	43	36	52	421
19	-1	-1	0	0	0	8	10	51	18	12	17	19	31	25	19	2	16	24	41	23	39	63	418
20	1	-1	0	0	0	5	2	14	13	6	7	17	44	71	55	0	8	71	50	16	5	6	390
21	0	0	0	0	0	0	2	20	10	3	8	68	8	7	25	2	6	27	34	15	6	11	252
22	0	0	0	0	0	5	4	43	17	8	1	33	52	14	34	3	14	44	42	45	11	5	375
23	0	0	0	0	0	2	2	7	34	4	6	24	61	38	48	1	4	117	49	3	4	1	405
24	0	0	0	0	0	1	0	25	6	6	5	29	13	9	32	1	3	51	43	19	7	30	280
25	0	0	0	0	0	1	2	30	61	3	18	28	27	69	44	5	1	75	17	44	12	21	458
26	0	0	0	0	0	6	19	9	10	23	10	25	22	18	32	41	19	60	52	17	5	7	375
27	-1	1	0	0	0	3	4	50	82	28	14	54	47	92	69	7	27	59	92	66	68	28	790
28	1	1	0	0	0	16	9	38	136	35	14	85	75	101	71	18	10	47	57	62	75	63	912
29	0	-1	1	0	0	3	4	17	12	14	4	15	23	11	28	7	7	22	42	8	13	10	240
30	-1	0	1	0	0	7	14	53	85	30	4	29	26	45	72	7	18	43	47	63	28	24	595
31	1	0	1	0	0	9	8	31	85	3	5	58	46	11	67	52	23	24	75	57	59	31	644
32	0	1	1	0	0	7	4	3	68	28	14	55	43	57	54	2	28	52	67	19	24	14	539
33	0	0	-1	1	0	2	3	54	17	12	12	39	14	38	7	2	4	22	46	39	96	66	473
34	0	-1	0	1	0	12	19	23	53	35	9	14	97	29	72	6	23	27	22	31	47	34	553
35	-1	0	0	1	0	8	17	11	105	13	6	27	54	50	20	86	72	133	27	23	3	7	662
36	1	0	0	1	0	10	2	51	94	16	6	22	27	24	76	5	21	93	25	76	58	25	631
37	0	1	0	1	0	9	15	50	31	32	18	34	17	33	47	39	20	58	47	71	58	49	628
38	0	0	1	1	0	11	5	21	15	33	7	32	17	20	60	7	18	15	22	30	18	8	339
39	0	0	0	-1	1	3	2	35	58	4	10	48	65	59	77	2	17	30	54	27	31	61	583
40	0	0	-1	0	1	4	2	69	1	40	16	30	36	29	22	3	25	36	28	24	56	24	445
41	0	-1	0	0	1	11	17	23	44	45	8	20	16	47	37	56	28	49	27	24	36	24	512
42	-1	0	0	0	1	5	4	79	50	21	16	49	63	77	46	7	18	46	35	75	21	22	634
43	1	0	0	0	1	28	11	36	86	48	17	58	55	70	46	10	12	75	54	31	48	35	720
44	0	1	0	0	1	6	4	68	39	15	7	47	25	27	68	2	24	78	72	47	4	15	548
45	0	0	1	0	1	18	15	16	42	44	25	42	56	69	57	10	12	68	34	23	35	15	581
46	0	0	0	1	1	15	28	14	47	29	12	22	43	26	44	51	59	25	41	18	58	13	545

[a] Score calculated as a sum of relative intensity standard deviations of all analytes aquired for corresponding method. Lower score is better. (n=5)

Experimental design results for the optimization of Orbitrap parameters. Values were normalized to the observed maximum intensities for corresponding analytes

Runs	Center point levels				Analyte																
	F	G	H		APL	CLOP	DEC	DCZ	HAL	LAS	MAD	MON	NAR	NEQ	DNC	ROB	SAL	SEM	TOL	TOLS	TOLX	RSD Score [a]	Signal intensity score [b]
1	0	-1	-1	RSD%	12	4	3	11	2	11	13	14	6	3	9	2	17	16	10	10	10	153	1369
				Max%	62	70	81	87	76	85	89	87	91	74	78	68	87	74	87	83	90		
2	-1	0	-1	RSD%	3	1	2	2	1	4	5	6	6	1	4	2	2	7	5	7	5	63	1575
				Max%	83	80	96	100	87	93	95	92	93	88	97	81	100	94	98	99	99		
3	1	0	-1	RSD%	3	1	1	7	2	3	7	9	11	2	1	4	19	4	3	7	3	84	1243
				Max%	62	64	64	90	68	67	70	65	67	62	90	66	80	64	84	87	93		
4	0	1	-1	RSD%	2	5	4	6	4	12	6	9	13	5	6	4	11	14	4	8	4	117	1603
				Max%	90	88	89	91	98	100	100	98	99	96	98	96	99	86	92	94	89		
5	-1	-1	0	RSD%	5	3	6	7	3	12	6	3	7	1	3	1	3	23	6	7	8	105	1412
				Max%	60	73	79	93	80	83	94	88	89	78	82	73	92	77	87	88	96		
6	1	-1	0	RSD%	4	4	5	3	5	3	17	13	6	3	5	4	20	7	5	6	6	114	1202
				Max%	56	58	66	83	62	66	75	73	78	61	72	55	78	69	87	81	82		
7	0	0	0	RSD%	1	2	2	2	3	7	10	8	20	1	5	1	12	16	1	5	2	98	1498
				Max%	72	72	85	94	81	95	96	92	96	81	88	79	95	100	90	91	91		
8	0	0	0	RSD%	4	5	3	1	5	4	4	2	8	2	3	2	2	3	5	5	4	60	1476
				Max%	75	71	84	96	79	90	88	91	87	80	92	78	93	88	92	97	95		
9	0	0	0	RSD%	2	0	3	1	2	6	3	3	11	1	3	1	5	17	8	1	3	69	1489
				Max%	76	76	88	97	81	87	88	86	87	80	94	79	94	94	92	96	94		
10	-1	1	0	RSD%	2	3	6	5	4	13	5	6	6	3	7	3	13	18	5	8	6	114	1652
				Max%	100	100	100	99	100	98	99	86	96	100	100	100	92	86	100	100	96		
11	1	1	0	RSD%	2	2	3	2	2	4	8	8	17	3	2	2	8	5	4	2	3	77	1371
				Max%	77	86	71	93	79	75	75	70	78	78	96	87	77	56	92	93	88		
12	0	-1	1	RSD%	3	3	4	8	2	7	6	9	27	2	9	5	8	10	10	12	8	132	1415
				Max%	64	69	78	95	73	86	100	87	100	72	84	69	83	73	97	85	100		
13	-1	0	1	RSD%	2	3	3	2	3	5	1	3	9	2	4	3	2	5	9	5	4	63	1569
				Max%	82	79	98	98	88	96	93	100	94	88	94	82	92	93	98	98	96		
14	1	0	1	RSD%	8	1	4	4	3	11	7	11	10	2	13	6	17	11	11	19	6	144	1226
				Max%	61	63	63	86	67	67	69	70	79	62	83	65	75	62	85	81	88		
15	0	1	1	RSD%	1	7	6	19	8	15	6	12	11	6	17	7	5	18	19	18	20	195	1534
				Max%	91	97	91	90	97	93	87	82	87	94	95	97	90	73	92	92	86		

[a] Score calculated as sum of relative intensity standard deviations of all analytes aquired for corresponding method. Lower score is better. (n=3)

[b] Signal intensity score calculated as sum of relative intensities of all analytes aquired for corresponding method. Higher score is better. (n=3)

Annex 5

Characteristics of samples used in non-target FCM study

No.	Sample	Outlet	Country of origin	Date purchased	Dimensions (mm)	Description
1	Black	Gemoss	Germany	November 16, 2018	255 × 8	White with colorful, thick stripes
2	Purple					
3	Red					
4	Green					
5	Flower			January 8, 2019		White, with flower pattern print
6	Plastic		Sweden	November 16, 2018	150 × 6	Biodegradable
7	Bamboo print		United Kingdom	January 8, 2019	200 × 6	Bamboo resembling print
8	Silver print					Glossy silver resembling print
9	Copper print					Glossy copper resembling print
10	Red	Flying Tiger	China		185 × 6	Single color straws
11	Pink					
12	Teal					
13	Dark blue					
14	Green	Party supplies store	USA		190 × 6	White with colorful stripes
15	Yellow					
16	Orange					
17	Gold print					White straws with glossy gold print stripes

VBA code for ChemRegex module.

```
Option Explicit

Public Function ChemRegex(ChemFormula As String, Element As String) As Long
   Dim strPattern As String
   strPattern = "([A][cglmrstu]|[B][aehikr]?|[C][adeflmnorsu]?|[D][bsy]|[E][rsu]|[F][elmr]?|[G][ade]|[H][efgos]?|[I][nr]?|[K][r]?|[L][airuv]|[M][cdgnot]|[N][abdehiop]?|[O][gs]?|[P][abdmortu]?|[R][abefghnu]|[S][bcegimnr]?|[T][abcehilms]|[U]|[V]|[W]|[X][e]|[Y][b]?|[Z][nr])([0-9]*)"
   Dim regEx As New RegExp

   Dim Matches As MatchCollection, m As Match

   If strPattern <> "" Then
      With regEx
         .Global = True
         .MultiLine = True
         .IgnoreCase = False
         .Pattern = strPattern
      End With

      Set Matches = regEx.Execute(ChemFormula)
      For Each m In Matches
         If m.SubMatches(0) = Element Then
            ChemRegex = IIf(Not m.SubMatches(1) = vbNullString, m.SubMatches(1), 1)
            Exit For
         End If
      Next m
   End If
End Function
```

Processing settings used in Compound Discoverer 2.1 for peak detection, alignment, and identification

Node and parameters	Setting
1. Select spectra	
- Lower RT Limit	0.3
- Upper RT Limit	11.7
- Min. Precursor Mass	100
- Max. Precursor Mass	1200
- Total Intensity Threshold	5000
2. Align Retention Times	
- Alignment Model	Adaptive curve
- Maximum Shift [min]	0.5
- Mass Tolerance	5 ppm
3. Detect Unkown Compounds	
General Settings	
- Mass Tolerance	5 ppm
- Intensity Tolerance [%]	30
- S/N Threshold	3
- Min. Peak Intensity	100000
- Ions	[M+H]+1
- Min. Element Counts	C H
- Max. Element Counts	C80 H140 O30 N15 S4 P4 Cl8 Br6 F30 I1 Si4 Sn1
- Peak detection	
- Filter Peaks	True
- Max. Peak Width [min]	0.75
- Remove Singlets	True
- Min. # Scans per Peak	5
- Min. # Isotopes	2
4. Group Unknown Compounds	
Compound Consolidation	
- Mass Tolerance	5 ppm
- RT Tolerance [min]	0.2
Fragment Data Selection	
- Preferred Ions	[M+H]+1
5. Fill Gaps	
- Mass Tolerance	5 ppm
- S/N Threshold	3
- Use Real Peak Detection	True
6. Mark Background Compounds	
- Max. Sample/Blank	5
- Hide Background	True
7. Predict Compositions	
Prediction Settings	
- Mass Tolerance	5 ppm

- Min. Element Counts	C H
- Max. Element Counts	C80 H140 O30 N15 S4 P4 Cl8 Br6 F30 I1 Si4 Sn1
- Min. RDBE	0
- Max. RDBE	60
- Min. H/C	0.1
- Max. H/C	3.2
- Max. # Candidates	10
Pattern Matching	
- Intensity Tolerance [%]	30
- Intensity Threshold [%]	0.1
- S/N Threshold	3
- Min. Spectral Fit [%]	30
- Min. Pattern Cov. [%]	90
- Use Dynamic Recalibration	True
Fragments Matching	
- Use Fragments matching	True
- Mass Tolerance	5 ppm
- S/N Threshold	3
8. Search Mass Lists	
- Input databases	ESCO list (Silicones, Coatings, Rubber, Printing Inks, Paper and Board, Cork and Wood, Colorants); FDA SCOGS list; FDA Indirect Additives list; SVHC list; SIN list; SVHC list; Extractables and Leachables HRAM Compound Database; EFS HRAM Compound Database; Union list
- Consider Retention	False
- Mass Tolerance	5 ppm
9. Search ChemSpider	
- Databases	ACToR: Aggregated Computation Toxicology Resources; FDA UNII – NLM; FooDB
- Mass Tolerance	5 ppm
- Max. # of results per compound	100
- Max. # of Predicted Compositions to be searched per Compound	3
10. Search mzCloud	
- Compound Classes	All
- Match Ion Activation Type	False
- Match Ion Activation Energy	Match with Tolerance
- Ion Activation Energy Tolerance	40
- Apply Intensity Threshold	True
- Precursor Mass Tolerance	5 ppm
- FT Fragment Mass Tolerance	5 ppm
- IT Fragment Mass Tolerance	0.4 Da
- Identity Search	HighChem HighRes

- Similarity Search	None
- Library	Reference
- Post Processing	Recalibrated
- Match Factor Threshold	50
- Max. # Results	10
11. Search mzVault	
- mzVault Library	/mzVault February 2017.db; /EFS_HRAM_Spectra_Library.db
- Compound Classes	All
- Match Ion Activation Type	False
- Match Ion Activation Energy	Match with Tolerance
- Ion Activation Energy Tolerance	40
- Match Ionization Method	True
- Apply Intensity Threshold	True
- Remove Precursor Ion	True
- Precursor Mass Tolerance	5 ppm
- FT Fragment Mass Tolerance	5 ppm
- IT Fragment Mass Tolerance	0.4 Da
- Match Analyzer Type	True
- Search Algorith	HighChem HighRes
- Match Factor Threshold	50
- Max. # Results	10
12. Assign Compound Annotations	
- Mass Tolerance	5 ppm
- Data Source #1	MassList Match
- Data Source #2	mzCloud Search
- Data Source #3	mzVault Search
- Data Source #4	ChemSpider Search

In silico analysis of:

Combination of toxicological outputs according to Frenzel et al. 2017

Libraries

```
library(tidyverse)
library(dbplyr)
library(scales)
library(matrixStats)
library(DT)
library(data.table)
```

The QSAR predictions were processed and combined as described in Frenzel et al. 2017.

In the table below the data transformations are summarized.

Data preparation of mutagenic predictions for each analysis

Tool	**Test**	**Negative**	**Positive**	**Notes**
TEST	*Mutagenicity Consensus*	0	1	Take output as is
LAZAR	*Mutagenicity (Salmonella typhimurium)*	mutagenic	non-mutagenic	Footnote 1
VEGA	*Mutagenicity consensus model*	0	1	Take output as is

Data preparation of carcinogenic predictions for each analysis

Tool	**Test**	**Negative**	**Positive**	**Notes**
VEGA	*Carcinogenicity model (CAESAR) - assessment*	NON-Carcinogen	Carcinogen	Conversion as in Frenzel et al.
VEGA	*Carcinogenicity model (ISS) - assessment*	NON-Carcinogen	Carcinogen	Conversion as in Frenzel et al.
VEGA	*Carcinogenicity model (IRFMN/Antares) - assessment*	NON-Carcinogen	Carcinogen	Conversion as in Frenzel et al.
VEGA	*Carcinogenicity model (IRFMN/ISSCAN-CGX) - assessment*	NON-Carcinogen	Carcinogen	Conversion as in Frenzel et al.
LAZAR	*Rodents multiple species*	carcinogenic	non-carcinogenic	Footnote 1
LAZAR	*Rat*	carcinogenic	non-carcinogenic	Footnote 1
LAZAR	*Mouse*	carcinogenic	non-carcinogenic	Footnote 1

Footnote 1: In LAZAR additional probability score of pos/neg prediction is provided which indicate the probabilities that the prediction belongs to one of the two classes. The approach described in Frenzel et al was adapted for use with this new output. In essence, the difference between the two

probabilities was calculated and then re-scaled on a scale from 0-1. If a compound was in the training set, 1 and 0 were assigned for experimentally tested compounds which showed (1) or did not show (0) mutagenic (carcinogenic) activities. If no result was obtained the score was set to 0.5.

Table 1. Frenzel et al, 2017

Prediction	**Reliability**	**Carcinogenic score**
Carcinogen	Experimental activity	1
Good reliability	0.9	
Moderate reliability	0.7	
Low reliability	0.5	
Non-carcinogen	Low reliability	0.5
Moderate reliability	0.3	
Good reliability	0.1	
Experimental activity	0	

#Mutagenicity

Retrieve data required for this analysis.

##TEST

# <dbl>	**ID** <dbl>	**Exp** <chr>	**Compound** <chr>	**CASRN** <chr>	**SMILES** <chr>
1	1	0	1,4-Dihydroxybenzene	123-31-9	C1=CC(=CC=C1O)O
2	2	N/A	2-Methyl-4-isothiazolin-3-one	2682-20-4	CN1C(=O)C=CS1
3	3	0	Indole	120-72-9	C1=CC=C2C(=C1)C=CN2
4	4	N/A	3-Methylstyrene	100-80-1	CC1=CC=CC(=C1)C=C
5	5	N/A	N-Methylcaprolactam	2556-73-2	CN1CCCCCC1=O
6	6	0	N-Isopropylaniline	768-52-5	CC(C)NC1=CC=CC=C1

6 rows | 1-6 of 10 columns

##TEST

Pred_Hierarchical clustering <chr>	**Pred_FDA** <chr>	**Pred_Nearest neighbor** <chr>	**Pred_Consensus** <dbl>
0.19	0.06	0	0.08
0.25	0.51	0	0.25
0.3	0.43	0.33	0.35
N/A	0.02	0	0.01
0.03	-0.06	0	-0.01
0.23	-7.0000000000000007E-2	0	0.05

6 rows | 7-10 of 10 columns

##LAZAR

```
lazar_muta_out <- readxl::read_excel("./Compiled_tox_output.xlsx", sheet = "Tox - LAZAR muta out")
```

```
lazar_muta <- lazar_muta_out %>%
  mutate(mutagen_lazar = case_when(
    is.na(.$`Lazar Prediction`) ~ 0.5,
    .$Measurements == "mutagenic" ~ 1,
    .$Measurements == "non-mutagenic" ~ 0,
   .$`Lazar Prediction` == "mutagenic" ~ rescale(
     .$`Lazar predProbability mutagenic` / .$`Lazar predProbability non-mutagenic`,to=c(0.5,1)),
   .$`Lazar Prediction` == "non-mutagenic" ~ rescale(
     .$`Lazar predProbability non-mutagenic` / .$`Lazar predProbability mutagenic`, to=c(0.5,0))))
```

##VEGA

```
vega_out <- readxl::read_excel("./Compiled_tox_output.xlsx", sheet = "Tox - VEGA out")
vega_out$ID <- as.numeric(gsub("#", "", vega_out$ID))
```

```
eq_vega_mut <- vega_out %>% select("ID", starts_with("Muta")) %>%
  select("ID", contains("CONSENSUS")) %>%
  select("ID", contains("assessment")) %>%
  separate("Mutagenicity (Ames test) CONSENSUS model - assessment", into =c ("CMP", "ADI"), sep="[(]Consensus
score:") %>%
  mutate(ADI = as.numeric(str_replace(ADI, "[)]", ""))) %>%
  mutate(mutagen_vega = case_when(
    .$CMP == "Mutagenic " ~  rescale(.$ADI, to=c(0.5,1)),
    .$CMP == "NON-Mutagenic " ~ rescale(.$ADI, to=c(0.5, 0))))
```

#Carcinogenicity

Retrieve data required for this analysis.

##LAZAR

```
#Connection to SQlite
lazar_carc_rodent_out <- readxl::read_excel("./Compiled_tox_output.xlsx", sheet = "Tox - LAZAR carc out1", skip = 1)
%>% type.convert()

lazar_carc_rat_out <- readxl::read_excel("./Compiled_tox_output.xlsx", sheet = "Tox - LAZAR carc output2", skip = 2)
%>% type.convert()

lazar_carc_mouse_out <- readxl::read_excel("./Compiled_tox_output.xlsx", sheet = "Tox - LAZAR carc output3", skip =
2) %>% type.convert()
```

```
lazar_carc_rodent <- lazar_carc_rodent_out %>%
  mutate(carci_lazar_rod = case_when(
    is.na(.$`Lazar Prediction`) ~ 0.5,
    .$Measurements == "carcinogenic" ~ 1,
    .$Measurements == "non-carcinogenic" ~ 0,
   .$`Lazar Prediction` == "carcinogenic" ~ rescale(
```

```
    .$`Lazar predProbability carcinogenic` / .$`Lazar predProbability non-carcinogenic`,to=c(0.5,1)),
   .$`Lazar Prediction` == "non-carcinogenic" ~ rescale(
    .$`Lazar predProbability non-carcinogenic` / .$`Lazar predProbability carcinogenic`, to=c(0.5,0))))
```

```
lazar_carc_rat <- lazar_carc_rat_out %>%
  mutate(carci_lazar_rat = case_when(
    is.na(.$`Lazar Prediction`) ~ 0.5,
    .$Measurements == "carcinogenic" ~ 1,
    .$Measurements == "non-carcinogenic" ~ 0,
   .$`Lazar Prediction` == "carcinogenic" ~ rescale(
    .$`Lazar predProbability carcinogenic` - .$`Lazar predProbability non-carcinogenic`,to=c(0.5,1)),
   .$`Lazar Prediction` == "non-carcinogenic" ~ rescale(
    .$`Lazar predProbability non-carcinogenic` - .$`Lazar predProbability carcinogenic`, to=c(0.5,0))))
```

```
lazar_carc_mouse <- lazar_carc_mouse_out %>%
  mutate(carci_lazar_mus = case_when(
    is.na(.$`Lazar Prediction`) ~ 0.5,
    .$Measurements == "carcinogenic" ~ 1,
    .$Measurements == "non-carcinogenic" ~ 0,
   .$`Lazar Prediction` == "carcinogenic" ~ rescale(
    .$`Lazar predProbability carcinogenic` - .$`Lazar predProbability non-carcinogenic`,to=c(0.5,1)),
   .$`Lazar Prediction` == "non-carcinogenic" ~ rescale(
    .$`Lazar predProbability non-carcinogenic` - .$`Lazar predProbability carcinogenic`, to=c(0.5,0))))
```

##VEGA

```
vega_carc <- vega_out %>% select("ID", starts_with("Carci")) %>%
  select("ID", contains("assessment"))

vega_carc_ceasar <- vega_carc %>% select("ID", contains("CAESAR")) %>%
  separate("Carcinogenicity model (CAESAR) - assessment", into =c ("CMP_CAESAR", "ADI_CAESAR"), sep="[(]")
%>%
  mutate(ADI_CAESAR = str_replace(ADI_CAESAR, "[)]", "")) %>%
  mutate(vega_carci_caesar = case_when(
    (.$CMP_CAESAR == "Carcinogen " | .$CMP_CAESAR == "Possible Carcinogen ")  & ADI_CAESAR ==
"EXPERIMENTAL value" ~ 1.0,
    (.$CMP_CAESAR == "Carcinogen " | .$CMP_CAESAR == "Possible Carcinogen ")  & ADI_CAESAR == "good
reliability" ~ 0.9,
    (.$CMP_CAESAR == "Carcinogen " | .$CMP_CAESAR == "Possible Carcinogen ")  & ADI_CAESAR == "moderate
reliability" ~ 0.7,
    (.$CMP_CAESAR == "Carcinogen " | .$CMP_CAESAR == "Possible Carcinogen ")  & ADI_CAESAR == "low
reliability" ~ 0.5,
    (.$CMP_CAESAR == "NON-Carcinogen "  | .$CMP_CAESAR == "Possible NON-Carcinogen ") & ADI_CAESAR ==
"low reliability" ~ 0.5,
    (.$CMP_CAESAR == "NON-Carcinogen "  | .$CMP_CAESAR == "Possible NON-Carcinogen ") & ADI_CAESAR ==
"moderate reliability" ~ 0.3,
    (.$CMP_CAESAR == "NON-Carcinogen "  | .$CMP_CAESAR == "Possible NON-Carcinogen ") & ADI_CAESAR ==
"good reliability" ~ 0.1,
    (.$CMP_CAESAR == "NON-Carcinogen "  | .$CMP_CAESAR == "Possible NON-Carcinogen ") & ADI_CAESAR ==
"EXPERIMENTAL value" ~ 0.0))

vega_carc_iss <- vega_carc %>% select("ID", contains("ISS")) %>%
  separate("Carcinogenicity model (ISS) - assessment", into =c ("CMP_iss", "ADI_iss"), sep="[(]") %>%
  mutate(ADI_iss = str_replace(ADI_iss, "[)]", "")) %>%
  mutate(vega_carci_iss = case_when(
    (.$CMP_iss == "Carcinogen " | .$CMP_iss == "Possible Carcinogen ")  & ADI_iss == "EXPERIMENTAL value" ~ 1.0,
    (.$CMP_iss == "Carcinogen " | .$CMP_iss == "Possible Carcinogen ")  & ADI_iss == "good reliability" ~ 0.9,
```

```
    (.$CMP_iss == "Carcinogen " | .$CMP_iss == "Possible Carcinogen ")  & ADI_iss == "moderate reliability" ~ 0.7,
    (.$CMP_iss == "Carcinogen " | .$CMP_iss == "Possible Carcinogen ")  & ADI_iss == "low reliability" ~ 0.5,
    (.$CMP_iss == "NON-Carcinogen "  | .$CMP_iss == "Possible NON-Carcinogen ") & ADI_iss == "low reliability" ~
0.5,
    (.$CMP_iss == "NON-Carcinogen "  | .$CMP_iss == "Possible NON-Carcinogen ") & ADI_iss == "moderate reliability"
~ 0.3,
    (.$CMP_iss == "NON-Carcinogen "  | .$CMP_iss == "Possible NON-Carcinogen ") & ADI_iss == "good reliability" ~
0.1,
    (.$CMP_iss == "NON-Carcinogen "  | .$CMP_iss == "Possible NON-Carcinogen ") & ADI_iss == "EXPERIMENTAL
value" ~ 0.0))


vega_carc_antares <- vega_carc %>% select("ID", contains("Antares")) %>%
  separate("Carcinogenicity model (IRFMN/Antares) - assessment", into =c ("CMP_antares", "ADI_antares"), sep="[(]")
%>%
  mutate(ADI_antares = str_replace(ADI_antares, "[)]", "")) %>%
  mutate(vega_carci_antares = case_when(
    (.$CMP_antares == "Carcinogen " | .$CMP_antares == "Possible Carcinogen ")  & ADI_antares == "EXPERIMENTAL
value" ~ 1.0,
    (.$CMP_antares == "Carcinogen " | .$CMP_antares == "Possible Carcinogen ")  & ADI_antares == "good reliability" ~
0.9,
    (.$CMP_antares == "Carcinogen " | .$CMP_antares == "Possible Carcinogen ")  & ADI_antares == "moderate
reliability" ~ 0.7,
    (.$CMP_antares == "Carcinogen " | .$CMP_antares == "Possible Carcinogen ")  & ADI_antares == "low reliability" ~
0.5,
    (.$CMP_antares == "NON-Carcinogen " | .$CMP_antares == "Possible NON-Carcinogen ")  & ADI_antares == "low
reliability" ~ 0.5,
    (.$CMP_antares == "NON-Carcinogen " | .$CMP_antares == "Possible NON-Carcinogen ")  & ADI_antares ==
"moderate reliability" ~ 0.3,
    (.$CMP_antares == "NON-Carcinogen " | .$CMP_antares == "Possible NON-Carcinogen ")  & ADI_antares == "good
reliability" ~ 0.1,
    (.$CMP_antares == "NON-Carcinogen " | .$CMP_antares == "Possible NON-Carcinogen ")  & ADI_antares ==
"EXPERIMENTAL value" ~ 0.0))

vega_carc_cgx <- vega_carc %>% select("ID", contains("IRFMN/ISSCAN-CGX")) %>%
  separate("Carcinogenicity model (IRFMN/ISSCAN-CGX) - assessment", into =c ("CMP_cgx", "ADI_cgx"), sep="[(]")
%>%
  mutate(ADI_cgx = str_replace(ADI_cgx, "[)]", "")) %>%
  mutate(vega_carci_cgx = case_when(
    (.$CMP_cgx == "Carcinogen " | .$CMP_cgx == "Possible Carcinogen ") & ADI_cgx == "EXPERIMENTAL value" ~
1.0,
    (.$CMP_cgx == "Carcinogen " | .$CMP_cgx == "Possible Carcinogen ") & ADI_cgx == "good reliability" ~ 0.9,
    (.$CMP_cgx == "Carcinogen " | .$CMP_cgx == "Possible Carcinogen ") & ADI_cgx == "moderate reliability" ~ 0.7,
    (.$CMP_cgx == "Carcinogen " | .$CMP_cgx == "Possible Carcinogen ") & ADI_cgx == "low reliability" ~ 0.5,
    (.$CMP_cgx == "NON-Carcinogen " | .$CMP_cgx == "Possible NON-Carcinogen ") & ADI_cgx == "low reliability" ~
0.5,
    (.$CMP_cgx == "NON-Carcinogen " | .$CMP_cgx == "Possible NON-Carcinogen ") & ADI_cgx == "moderate
reliability" ~ 0.3,
    (.$CMP_cgx == "NON-Carcinogen " | .$CMP_cgx == "Possible NON-Carcinogen ")  & ADI_cgx == "good reliability"
~ 0.1,
    (.$CMP_cgx == "NON-Carcinogen " | .$CMP_cgx == "Possible NON-Carcinogen ") & ADI_cgx ==
"EXPERIMENTAL value" ~ 0.0))
```

#Summary files

Mutagenicity

```
xlsx::write.xlsx(test_muta, "./Compiled_tox_output.xlsx", sheetName="test_muta", col.names=TRUE, row.names=TRUE,
showNA=FALSE, append=TRUE)
xlsx::write.xlsx(lazar_muta, "./Compiled_tox_output.xlsx", sheetName="lazar_muta", col.names=TRUE,
row.names=TRUE, showNA=FALSE, append=TRUE)
```

```
xlsx::write.xlsx(eq_vega_mut, "./Compiled_tox_output.xlsx", sheetName="eq_vega_mut", col.names=TRUE,
row.names=TRUE, showNA=FALSE, append=TRUE)

test_muta_out_smry <- test_muta %>% select(ID, Compound, CASRN, SMILES, mutagen_test)
lazar_muta_smry <-lazar_muta %>% select(ID, mutagen_lazar)
eq_vega_mut_smry <- eq_vega_mut %>%  select(ID, mutagen_vega)

mutagens <- left_join(test_muta_out_smry, lazar_muta_smry, by="ID")
mutagens <- left_join(mutagens, eq_vega_mut_smry, by="ID")

select_vars <- c("mutagen_test",  "mutagen_lazar", "mutagen_vega")
mutagens <- mutagens %>%
  mutate(mean_muta3 = rowMeans(select(., select_vars)))

xlsx::write.xlsx(mutagens, "./Compiled_tox_output.xlsx", sheetName="mutagens", col.names=TRUE, row.names=TRUE,
showNA=FALSE, append=TRUE)
```

Carcinogenicity

```
xlsx::write.xlsx(lazar_carc_rodent, "./Compiled_tox_output.xlsx", sheetName="lazar_carc_rodent", col.names=TRUE,
row.names=TRUE, showNA=FALSE, append=TRUE)
xlsx::write.xlsx(lazar_carc_rat, "./Compiled_tox_output.xlsx", sheetName="lazar_carc_rat", col.names=TRUE,
row.names=TRUE, showNA=FALSE, append=TRUE)
xlsx::write.xlsx(lazar_carc_mouse, "./Compiled_tox_output.xlsx", sheetName="lazar_carc_mouse", col.names=TRUE,
row.names=TRUE, showNA=FALSE, append=TRUE)

lazar_carc_rodent_smry <- lazar_carc_rodent %>% select(ID, carci_lazar_rod)
lazar_carc_rat_smry <- lazar_carc_rat %>% select(ID, carci_lazar_rat)
lazar_carc_mouse_smry <- lazar_carc_mouse %>% select(ID, carci_lazar_mus)


lazar_carci_smry <- left_join(lazar_carc_rodent_smry, lazar_carc_rat_smry, by="ID")
lazar_carci_smry <- left_join(lazar_carci_smry, lazar_carc_mouse_smry, by="ID")

select_vars <- c("carci_lazar_rod", "carci_lazar_rat",  "carci_lazar_mus")
lazar_carci_smry <- lazar_carci_smry %>%
  mutate(mean_carci_LAZAR3 = rowMeans(select(., select_vars)))

xlsx::write.xlsx(lazar_carci_smry, "./Compiled_tox_output.xlsx", sheetName="lazar_carci_smry", col.names=TRUE,
row.names=TRUE, showNA=FALSE, append=TRUE)
```

```
xlsx::write.xlsx(vega_carc_ceasar, "./Compiled_tox_output.xlsx", sheetName="vega_carc_ceasar", col.names=TRUE,
row.names=TRUE, showNA=FALSE, append=TRUE)
xlsx::write.xlsx(vega_carc_iss, "./Compiled_tox_output.xlsx", sheetName="vega_carc_iss", col.names=TRUE,
row.names=TRUE, showNA=FALSE, append=TRUE)
xlsx::write.xlsx(vega_carc_antares, "./Compiled_tox_output.xlsx", sheetName="vega_carc_antares", col.names=TRUE,
row.names=TRUE, showNA=FALSE, append=TRUE)
xlsx::write.xlsx(vega_carc_cgx, "./Compiled_tox_output.xlsx", sheetName="vega_carc_cgx", col.names=TRUE,
row.names=TRUE, showNA=FALSE, append=TRUE)

vega_carc_ceasar_smry <- vega_carc_ceasar %>% select(ID, vega_carci_caesar)
vega_carc_iss_smry <- vega_carc_iss %>% select(ID, vega_carci_iss)
vega_carc_antares_smry <- vega_carc_antares %>% select(ID, vega_carci_antares)
vega_carc_cgx_smry <- vega_carc_cgx %>% select(ID, vega_carci_cgx)


vega_carci_smry_1 <- left_join(vega_carc_ceasar_smry, vega_carc_iss_smry, by="ID")
vega_carci_smry_2 <- left_join(vega_carc_antares_smry, vega_carc_cgx_smry, by="ID")
vega_carci_smry <- left_join(vega_carci_smry_1, vega_carci_smry_2, by="ID")
```

```
select_vars <- c("vega_carci_caesar", "vega_carci_iss", "vega_carci_antares", "vega_carci_cgx")
vega_carci_smry <- vega_carci_smry %>%
  mutate(mean_carci_vega4 = rowMeans(select(., select_vars)))

xlsx::write.xlsx(vega_carci_smry, "./Compiled_tox_output.xlsx", sheetName="vega_carci_smry", col.names=TRUE,
row.names=TRUE, showNA=FALSE, append=TRUE)
```

```
carci_smry <- left_join(lazar_carci_smry, vega_carci_smry, by="ID")

select_vars <- c("carci_lazar_rod", "carci_lazar_rat",  "carci_lazar_mus", "vega_carci_caesar", "vega_carci_iss",
"vega_carci_antares", "vega_carci_cgx")

carci_smry <- carci_smry %>%
  mutate(mean_carci = rowMeans(select(., select_vars)))

vega_out_sub <- vega_out %>% select(ID, Compound, CASRN, SMILES)
carci_smry <- left_join(vega_out_sub, carci_smry, by="ID")

xlsx::write.xlsx(carci_smry, "./Compiled_tox_output.xlsx", sheetName="carci_smry", col.names=TRUE,
row.names=TRUE, showNA=FALSE, append=TRUE)
```

Plots

Mutagenicity

Barplot [input data example].

ID <fctr>	**Compound** <chr>	**CASRN** <chr>
24	4,4'-Oxydianiline	101-80-4
52	Quinacridone	1047-16-1
33	4,4'-bis(dimethylamino)benzophenone (Michler's ketone)	90-94-8
11	5-Chloro-2-methyl-4-isothiazolin-3-one	26172-55-4
40	Dimethoxyethyl phtalate	117-82-8
48	Pigment Orange 64	72102-84-2
12	Triethylene Glycol	112-27-6
71	4,4'-Bis(diethylamino)benzophenone	90-93-7
13	1,2-Benzisothiazolin-3-one	2634-33-5
29	2,4,6-Trimethylbenzophenone	954-16-5

1-10 of 72 rows | 1-3 of 8 columns

SMILES <chr>	**mutagen_test** <dbl>	**mutagen_lazar** <dbl>	**mutagen_vega** <dbl>
C1=CC(=CC=C1N)OC2=CC=C(C=C2)N	1.00000000	1.0000000	1.00000000
C1=CC=C2C(=C1)C(=O)C3=CC4=C(C=C3N2)C(=O)C5=CC=CC=C5N4	0.80909091	0.9624409	0.85294118
CN(C)C1=CC=C(C=C1)C(=O)C2=CC=C(C=C2)N(C)C	0.35454545	1.0000000	1.00000000

SMILES <chr>	mutagen_test <dbl>	mutagen_lazar <dbl>	mutagen_vega <dbl>
CN1C(=O)C=C(S1)Cl	0.88181818	0.5000000	0.61764706
COCCOC(=O)C1=CC=CC=C1C(=O)OCCOC	0.42727273	0.4433872	1.00000000
CC1=CC2=C(C=C1N=NC3C(=O)NC(=O)NC3=O)NC(=O)N2	0.43636364	0.8077564	0.52941176
C(COCCOCCO)O	0.29090909	0.4231483	1.00000000
CCN(CC)C1=CC=C(C=C1)C(=O)C2=CC=C(C=C2)N(CC)CC	0.14545455	0.7533737	0.76470588
C1=CC=C2C(=C1)C(=O)NS2	0.29090909	1.0000000	0.32352941
CC1=CC(=C(C(=C1)C)C(=O)C2=CC=CC=C2)C	0.50909091	0.6608195	0.32352941

1-10 of 72 rows | 4-7 of 8 columns

mutagen_test <dbl>	mutagen_lazar <dbl>	mutagen_vega <dbl>	mean_muta3 <dbl>
1.00000000	1.0000000	1.00000000	1.000000000
0.80909091	0.9624409	0.85294118	0.874824322
0.35454545	1.0000000	1.00000000	0.784848485
0.88181818	0.5000000	0.61764706	0.666488414
0.42727273	0.4433872	1.00000000	0.623553310
0.43636364	0.8077564	0.52941176	0.591177281
0.29090909	0.4231483	1.00000000	0.571352462
0.14545455	0.7533737	0.76470588	0.554511367
0.29090909	1.0000000	0.32352941	0.538146168
0.50909091	0.6608195	0.32352941	0.497813270

1-10 of 72 rows | 5-8 of 8 columns

```
barplot_muta <- ggplot(muta, aes(x = ID, y = mean_muta3)) +
  geom_bar(stat = "identity") +
  geom_col(aes(fill = mean_muta3)) +
  scale_fill_gradient2(low = "green",
                       high = "red",
                       midpoint = 0.5) +
  theme(axis.text.x=element_text(angle=90,hjust=1,vjust=0.5)) +
  ggtitle("Schematic plot of in silico mutagenicity analysis") +
  xlab("Compound") + ylab("Mutagenic score") +
  theme(legend.position = "none")

barplot_muta
```

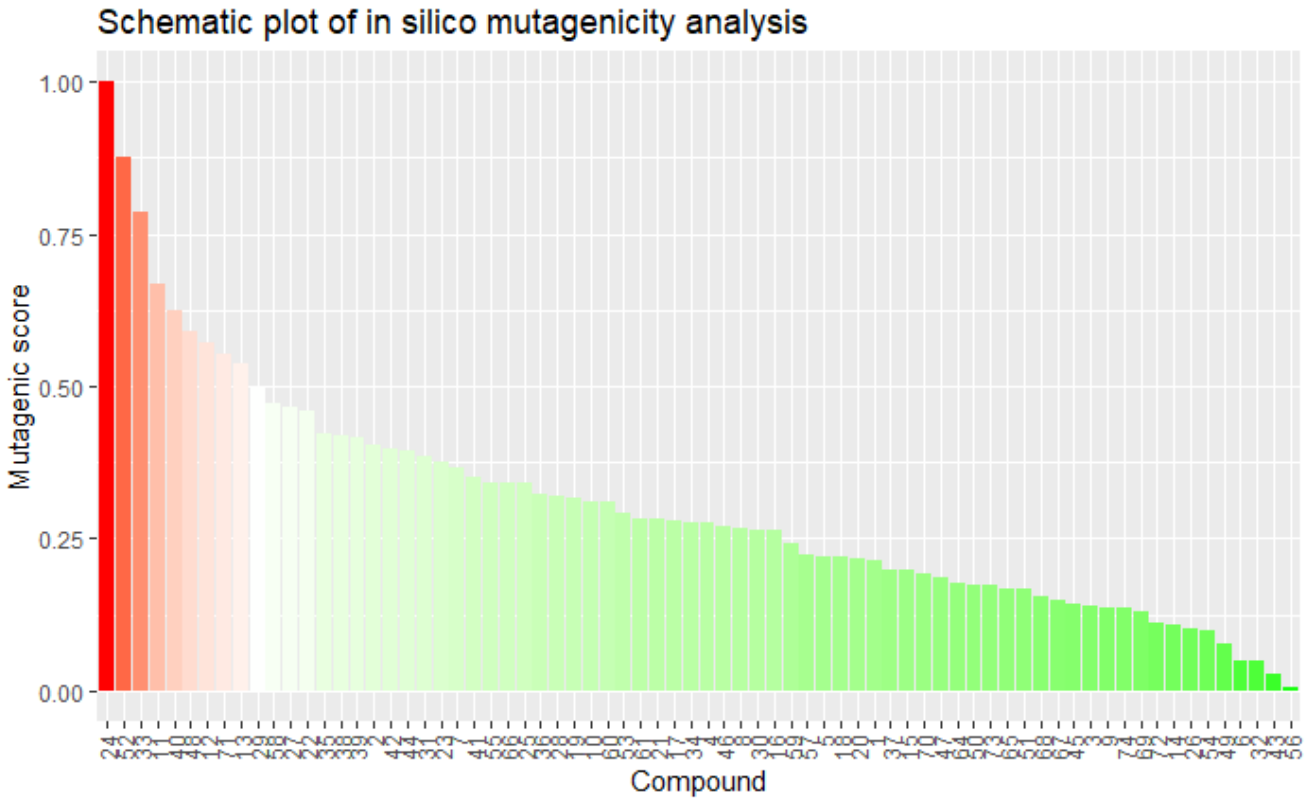

Carcinogenicity

Barplot

```
carc <-
   carci_smry %>%
   arrange(-mean_carci) %>%
   data.table()

carc$ID <-
   factor(
      carc$ID,
      levels = carc$ID
   )
```

```
barplot_carci <- ggplot(carc, aes(x = ID, y = mean_carci)) +
  geom_bar(stat = "identity") +
  geom_col(aes(fill = mean_carci)) +
  scale_fill_gradient2(low = "green",
                       high = "red",
                       midpoint = 0.5) +
  theme(axis.text.x=element_text(angle=90,hjust=1,vjust=0.5)) +
  ggtitle("Schematic plot of in silico carcinogenicity analysis") +
  xlab("Compound") + ylab("Carcinogenic score") +
  theme(legend.position = "none")

barplot_carci
```

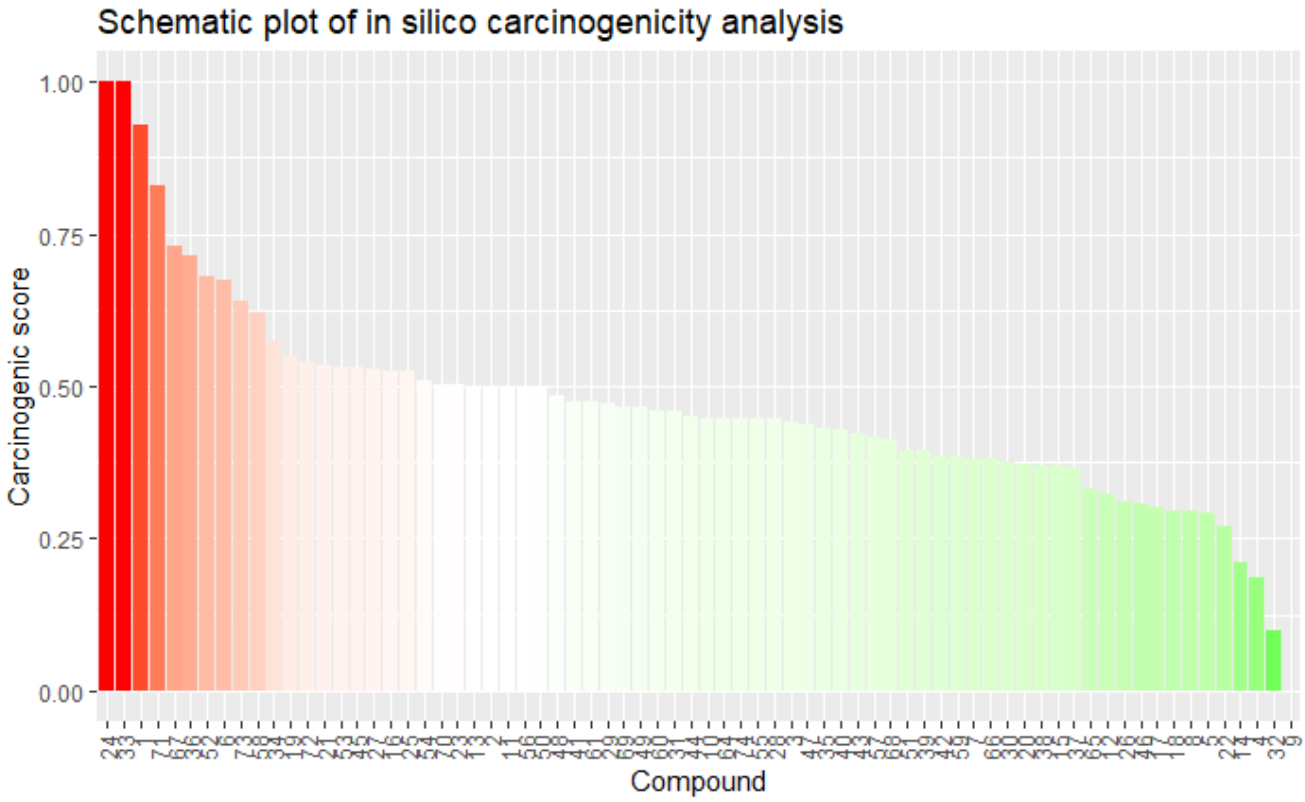
Schematic plot of in silico carcinogenicity analysis
Carcinogenic score
1.00
0.75
0.50
0.25
0.00
Compound

MRM Transitions and Mass Spectrometry Settings.

Analyte	RT(min)	Q1(Da)	Q2(Da)	DP(V)	EP(V)	CE(V)	CXP(V)	Reference
Paraoxon-methyl 1	7.2	248.1	90.1	71	10	37	16	1
Paraoxon-methyl 2	7.2	248.1	202.1	71	10	27	10	1
Paraoxon-ethyl 1	7.7	276.1	220	69	10	19	6	2
Paraoxon-ethyl 2	7.7	276.1	248.1	69	10	13	6	2
Phosmet 1	8.1	318	160	61	10	17	10	2
Phosmet 2	8.1	318	133	61	10	49	11	2
Parathion-methyl 1	8.2	264	125	85	10	25	8	3
Parathion-ethyl 1	9	292	236	80	10	20	7	2
Parathion-ethyl 2	9	292	264	80	10	15	7	2
Coumaphos 1	9.2	363	227	100	10	36	10	2
Coumaphos 2	9.2	363	307	100	10	25	10	2
Tolclofos-methyl 1	9.7	301	268.9	59	10	23	6	2
Tolclofos-methyl 2	9.8	301	175	59	10	35	6	2
Diazinon 1	10	305	169	80	10	27	11	2
Diazinon 2	10	305	153	80	10	28	11	2
Pirimiphos-methyl 1	10.4	306.1	164.1	75	10	29	6	2
Pirimiphos-methyl 2	10.4	306.1	108	75	10	40	6	2
Chlorpyrifos 1	10.8	350	198	82	10	29	9	2
Chlorpyrifos 2	10.8	350	97	82	10	49	9	2

References:

(1) Fillâtre, Y.; Rondeau, D.; Daguin, A.; Jadas-Hecart, A.; Communal, P.-Y. Multiresidue Determination of 256 Pesticides in Lavandin Essential Oil by LC/ESI/SSRM: Advantages and Drawbacks of a Sampling Method Involving Evaporation under Nitrogen. Anal. Bioanal. Chem. 2014, 406 (5), 1541–1550.

(2) Wang, J.; He, Z.; Wang, L.; Xu, Y.; Peng, Y.; Liu, X. Automatic Single-Step Quick, Easy, Cheap, Effective, Rugged and Safe Sample Preparation Devices for Analysis of Pesticide Residues in Foods. J. Chromatogr. A 2017, 1521, 10–18.

(3) Feng, X.; He, Z.; Wang, L.; Peng, Y.; Luo, M.; Liu, X. Multiresidue Analysis of 36 Pesticides in Soil Using a Modified Quick, Easy, Cheap, Effective, Rugged, and Safe Method by Liquid Chromatography with Tandem Quadruple Linear Ion Trap Mass Spectrometry. J. Sep. Sci. 2015, 38 (17), 3047–3054.

PUBLISHED MANUSCRIPTS